Essays on firm's operational flexibility

Cristina Bertolosi

Faculty of Finance

Bayes Business School, City, University of London

This dissertation is submitted for the degree of

Doctor of Philosophy

November 2024

To my beloved Trilly

Declaration

I hereby declare that except where specific reference is made to the work of others, the contents of this dissertation are original and have not been submitted in whole or in part for consideration for any other degree or qualification in this, or any other university. This dissertation is my own work, except for Chapter 3, which has been co-authored with Dr. Francesco Rotondi and for which we claim equal contribution. Whenever any contribution has been provided by others, this is clearly specified in the text or in the Acknowledgements. This dissertation contains fewer than 65,000 words including appendices, bibliography, footnotes, tables and equations and has fewer than 150 figures.

I include the following

Declaration of co-Authorship

I, Dr. Francesco Rotondi, hereby confirm that the content of Chapter 3 in Ms. Cristina Bertolosi's Doctoral thesis, titled Essays on firm's operational flexibility *and finalised in November 2024, is the product of a collaborative effort between Ms. Bertolosi and myself. I fully support the inclusion of our jointly conducted work, to which we contributed equally, in her thesis.*

Dr. Francesco Rotondi
November 2024

[redacted]

Cristina Bertolosi
November 2024

Acknowledgements

I would like to express my deepest gratitude to my supervisors, Prof. Gianluca Fusai and Prof. Ioannis Kyriakou. Their guidance during the writing of this dissertation and their invaluable contributions to my research and personal growth have been profoundly impactful. I have learned an immense amount from both of them, and it has truly been a privilege to work with them.

I am also thankful to Prof. Amir Alizadeh-Masoodian and Prof. Zhenyu Cui for having examined this thesis, providing me with important suggestions and ideas, as well as to Dr. Pietro Millossovich for chairing the Vivavoce examination.

I sincerely thank Dr. Francesco Rotondi for his cooperation in co-authoring the third chapter of this dissertation. Additionally, I am indebted to Dr. Michail Chronopoulos and Prof. Nikos Nomikos for their precious suggestions, which helped improving the first chapter of this thesis. I am grateful to Prof. Giacinta Cestone, Director of the PhD Programme, for her unwavering support and availability. I wish to express my appreciation to Prof. Laura Ballotta, Prof. Giovanni Urga, Prof. Giovanni Cespa and Dr. Malvina Marchese for their inspiring feedback on numerous occasions. I thank City, University of London, for the financial support provided to this research.

I am deeply thankful to the members of the mathematical and statistical groups at the Department of Economics and Business Studies at the University of Eastern Piedmont. Their attentive and thoughtful guidance throughout my academic journey, along with their consistent trust in me, has been profoundly appreciated.

I am also appreciative of Dr. Ruggero Guglielmetti and Dr. Massimo Savastano; their professionalism and empathy helped me navigate truly *breathless* moments. I convey my thanks to all my PhD colleagues at Bayes Business School and friends, who played a key role in making these years part of *a life always committed to renewal and improvement.*

My thanks also go to the *Corpo Musicale "C.&D. Martinetti"*, especially the flute section, for their constant support. I am also deeply grateful to the group of FCI cycling Commissaires from Piemonte and Valle d'Aosta for helping me strengthen my teamwork skills, with special acknowledgement to President Stefano Pavignano, a steadfast example of integrity and fair decision-making, and a treasured friend to whom I will be forever indebted.

Last but not least, this work would not have been possible without the unconditional support, patience, and understanding of my family, especially of my parents Emiliano and Monica, my brother Federico, grandmother Franca, and the affection of my beloved Trilly. To them, I extend my heartfelt gratitude.

Abstract

The primary aim of this thesis is to analyse and provide insights into several critical issues related to the construction, interpretation, and implications of market entry and exit decision models under uncertainty. As discussed by Brennan and Schwartz (1985), Dixit and Pindyck (1994), and Hackbarth and Johnson (2015), operational flexibility refers to the capacity to adjust production in response to market fluctuations with a certain degree of reversibility. In line with this framework, this thesis approaches operational flexibility from three perspectives; each one is examined in a separate chapter and constitutes a different piece of research.

The first chapter explores optimal strategies for managing production projects and the effects of different price models on when to suspend, resume or permanently cease operations. The analysis is conducted calculating the optimal transition barriers, the probabilities of switching between states and the time spent in each. Results suggest that, when dealing with moderately volatile markets, modelling prices by means of simpler processes for ease of use could be acceptable, as this would not significantly impact firms strategic decisions.

The second chapter provides a theoretical basis for understanding the relationship between operational flexibility and the risk-return characteristics of firms equity. Consistently with intuition, more flexible production projects exhibit higher equity

value and lower risk. Implications for risk management and asset pricing pertain a subsequent decrease in the implied volatility of option contracts and in CAPM's β. Importantly, the stochastic nature of the latter is also documented. Moreover, findings are robust across different price diffusion models.

The third chapter investigates the impact of a stochastic convenience yield on flexible projects as a primary scope. The analysis considers a gas-fired turbine for electricity generation that can be switched-off and on at multiple dates in the short term; uncertainty concerns both electricity and gas prices. Findings document that operational flexibility partially offsets the aleatory behaviour of gas' convenience yield, whose impact is, instead, sizeable when flexibility is not available. Bivariate and trivariate trees are used to deal with the model, making this work particularly attractive for use by practitioners.

Table of contents

List of figures

List of tables

List of abbreviations

ABM	Arithmetic Brownian motion
CAPM	Capital Asset Pricing Model
CCGT	Combined cycle gas turbine
DCF	Discounted cash-flows
DPV	Net present value
EEX	European Energy Exchange
EU	European Union
EUR	Euros (currency)
GBM	Geometric Brownian motion
GMR	Geometric mean-reverting process
IC	Information criterion
ICAPM	Intertemporal Capital Asset Pricing Model
ICE	Intercontinental Exchange
IGBM	Inohomogenous geometric Brownian motion
IV	Implied volatility
MR	Mean-reverting
MWh	Mega Watt per hour
OCGT	Open-cycle gas turbines
ODE	Ordinary differential equation

OU	Ornstein-Uhlenbeck process
SDE	Stochastic differential equation
TTF	Title Transfer Facility

Chapter 1

Evaluating operational flexibility under one-dimensional diffusions: impacts on firm policy and valuation

Abstract

We study the optimal operational strategy of production projects. We investigate different underlying price models and determine the optimal barriers of transition to suspension, recovery, or irreversible abandonment of productive activity. We compute probabilities of switching between alternative states and the time spent in each state. Our findings suggest that in moderately volatile markets, different model assumptions lead to minimal variations in project strategy. This insight underscores that adopting sub-optimal choices in the interest of model tractability can be permissible under certain conditions. Our work significantly advances in this direction by demonstrating when and how model simplifications can be made without sacrificing accuracy.

Keywords: Real options; investment; uncertainty; optimal switching

1.1 Introduction

For real options models to be an effective tool in supporting managerial and financial decisions, they should reliably depict the uncertain decision environment. As such, the traditional modelling of underlying state variables through a geometric Brownian motion has been widely disputed. For example, its inadequacy to capture the mean-reverting nature of several variables, such as commodity prices or market demand-supply dynamics has been emphasised.

In this paper, we investigated the impact of the model used for the dynamics of the underlying on the optimal managerial strategy of the project. In particular, we studied not only the effects of variations in the drift coefficient related to the existence of mean-reversion, but also those of changes into the diffusion term. Hence, we compared four models, namely the inhomogeneous geometric Brownian motion (Bhattacharya, 1978; Zhao, 2009), the square root mean-reverting (Cox et al., 1985), the constant elasticity of variance (Cox, 1975) and the usual geometric Brownian motion. Most importantly, we considered a real options model for a production project that can be suspended infinitely many times with partial reversibility or, alternatively, irreversibly abandoned, over an infinite horizon.

The optimal managerial strategy is determined by the values of the underlying variable that triggers the aforementioned switching decisions. Focusing on the relative positions of such boundaries, we were able to numerically verify whether the exercise timing and exercise probability of real options are significantly altered by different underlying models. We document that little differences arise within markets characterised by mutually offsetting mean-reversion and volatility features, subject to an accurate model parametrisation, in contrast with more extreme scenarios for which discrepancies in the project operating strategy are noticeable. Additionally, we report that mean-reverting models seem to be more sensitive to changes in the degree of flexibility of the project. We also find that the value of the project is in general more impacted by the adoption of different models, compared to the project strategy.

Unlike previous works, we did not assume that all the models share the same parameters, but we rather calibrated them to match variance features. In doing this, we mitigated the so called “variance” and “realised price” effects (Metcalf and Hassett, 1995). Additionally, we assumed that, albeit optimal switching boundaries can be derived for different price dynamics, in operational practice they must be applied to observed data; hence, in computing the timing and the probability of options exercise, we attached them to the same reference model. Instead, previous works used to simulate different processes for this purpose.

The remainder of the paper is as follows. In section 1.2 we analyse the main literature in the field. Next, in section 1.3, we present the framework in which our analysis is carried on, introducing our own notation and showing how to find the value of the project and its optimal running strategy. Additionally, we discuss the case of a levered project and we motivate our choice to study an unlevered one, instead. In section 1.4 we provide numerical results, analysing the problem from multiple perspectives. Concluding remarks are given in section 1.5, whereas technical details are relegated to the Appendix.

1.2 Literature Review

The comparative nature of our project inserts it in the field of research that investigates the impact of different dynamics of uncertainty on investment problems. One of the seminal works tackling the comparison between different models in the real options realm is due to Metcalf and Hassett (1995). The Authors studied the problem of irreversibly investing in a production project with stochastic output prices, which can either evolve as a geometric mean reverting process (Dixit and Pindyck, 1994) or as a drift-less geometric Brownian motion. Noticeably, their experimental findings excluded significant differences in terms of cumulative investments when moving from one model to another and led to accept geometric Brownian motion as a good simplifying assumption for investment models under uncertainty. This result was explained in the light of two offsetting effects: the "variance effect" refers to the reduction in the long-run variance associated to auto-regressive dynamics and has a positive effect on investment, as it lowers its trigger price; however, the lower variance of the process also reduces the probability of reaching such critical threshold, having a negative impact on investment - so called "realised price effect".

In contrast, Sarkar (2003) observed that the probability of investing is substantially impacted in either direction by the adoption of mean-reverting dynamics in the input cost process. The reason for this outcome comes from the reduction effect of mean-reversion on systematic risk, termed "risk discounting effect", which was disregarded by Metcalf and Hassett (1995). Tsekrekos (2010) and Tvedt (2022) came to a similar conclusion when revenues are uncertain within the framework of partially reversible entry and exit decisions. Furthermore, it is also shown that the composition of a hypothetical industry undergoes less frequent changes under mean-reversion, compared to the drift-less geometric Brownian motion. The subsequent contribution by Tsekrekos (2013) is likewise relevant to extend these result to a setting with the option to irreversibly exit the market. Additionally, these contributions share the use of the same mean-reverting model, namely the inhomogeneous geometric Brownian motion, meaning they can be compared alongside one another with greater ease.

The higher interest devoted to mean-reverting dynamics, compared to other models, is justified by the fact that, typically, the source of uncertainty underlying real options models is either a price or the demand function of a given good or service and mean-reversion is particularly suitable to describe equilibrium adjustments, as extensively highlighted by Bhattacharya (1978), Kulatilaka (1988), Lund (1993), Bessembinder (1995), Schwartz (1997a), Sarkar and Zapatero (2003), Fama and French (2000) and Ewald and Wang (2010) among the others. Nevertheless, depending on the industry and on the specific features of the project considered, diverse models should be accounted for, either to accommodate different variables or to specifically address particularly attributes. For example, the existence of the *leverage effect* in stock prices showed by Black (1976), or of the *inverse leverage effect* documented in energy markets by Geman and Shih (2008) and Li et al. (2017) among the others, led to the adoption of the constant elasticity of variance process for modelling purposes, as it can be seen in Geman (2005), Čermák (2017), and, in the real options field, in Dias and Nunes (2011).[1]

To the best of our knowledge, a few papers offer a well-structured comparison of many different models for a given investment related problem. Dangerfield et al. (2018) obtained the optimal time of intervention against pests when the level of infection follows a log-normal, a mean-reverting or a logistic SDE, with the last process known to be the most appropriate one according to empirical evidence. The Authors highlighted that, in the worst case scenario, both the geometric Brownian motion and the mean-reverting models prescribe not to intervene, in contrast with the optimal policy found under the benchmark (i. e. the logistic model), which suggest to eradicate the pest within a reasonable amount of time. Moreover, they showed that such a difference is exacerbated when the volatility of the underlying is large. Their setting is comparable to that of getting the optimal investment timing in a financial management framework, hence it is reasonable to presume that similar results are

[1] Recall that the *leverage effect* refers to the negative correlation between asset returns and changes into asset volatilities, whilst *inverse leverage effect* defines a positive correlation among those quantities.

applicable to the financial industry too. To some extent closer to ours, is the work by Dias et al. (2015), who extended Tsekrekos (2010)' analysis to the constant elasticity of variance model, with and without mean-reversion, getting comparable conclusions.

A common feature of the aforementioned works is their focus on a single investment problem at a time, as it can be the decision to enter or to exit the market, either reversibly or irreversibly. Put into practice, decision-makers continuously choose whether to keep their project in its current state or to switch it to the - unique - alternative one. Such kind of framework was originally introduced by Mossin (1968), and the most representative results relate to Brennan and Schwartz (1985), McDonald and Siegel (1986), Dixit (1989), Pindyck (1990), who explicitly promoted reversible switching options as a corporate risk management tool in turbulent markets. In contrast with the full reversible scheme of Brennan and Schwartz (1985), from Dixit (1989) forward it is widely acknowledged that a partially reversible framework with switching costs introduces the so called *hysteresis effect*, which leads firms to bear some losses or to give-up potential profits before suspending or restarting operations, and is more appropriate to represent most productive economic realities.

However, the assumption to reduce the management of a project to the simple comparison between the continuation and a single alternative seems hardly realistic. Indeed, corporate strategies typically include a great variety of options (see, for example, Guthrie, 2009), which might require to compare the value related to continuation with those achievable by undertaking one of multiple alternatives. A simple, yet meaningful example is portrayed in chapter 7 of Dixit and Pindyck (1994), where partially reversible entry and exit options are considered together with the irreversible abandonment of the market within an infinite horizon. The main message from this model is that, depending on the parameters of the price model, irreversible abandonment might overtake reversible options as a result of optimal choices. Far from being a secondary problem, the appropriate parametrisation of the model can become a crucial aspect in determining business operational strategies. As an example, it is worth to mention the ambiguous, non-monotonic, effect of interest rates variations on the timing of investments observed in Gutiérrez (2021), which also highlights the importance of systematically updating the inputs of the model.

In light of the existing results, we contribute to the literature as follows: first, we document that adopting different model specifications for the underlying price process could be not that improper, despite potential changes in the *ex-ante* strategy of the project, in some selected scenarios. Second, in doing this, we try to make the processes under investigation as similar as possible to each other by selecting one of them as a benchmark and carefully calibrating the others against it. Additionally, we address the sensitivity of our results to changes in the degree of flexibility of the project, which we assume to be captured by the costs paid upon switching and by the fixed production costs of the plant. Besides, we discuss that introducing debt into our analysis would not qualitatively affect the validity of our results, at least as long as *second-best* solutions are accounted for. Marginally, we show how to express solutions to the model in terms of confluent hypergeometric functions of the first kind only, aiming at reducing the bias in numerical results due to the use of different special functions.

In Table 1.1 we list the works which are closer to ours, summarising which kind of real options and price models are studied and showing where our paper stands. For the sake of brevity, we adopt the following acronyms: CEV = constant elasticity of variance process; CKLS = mean-reverting CEV (Chan et al., 1992); CIR = square-root mean-reverting diffusion; GBM = drift-less geometric Brownian motion; GMR

= geometric mean-reverting process; IGBM = inohomogenous geometric Brownian motion; OU = Ornstein-Uhlenbeck process (Uhlenbeck and Ornstein, 1930).

Table 1.1 The Table summarises the contributions closer to ours, highlighting which kind of real options and of price models are included, and showing where our article stands.

Reference	Options	Models
Metcalf and Hassett (1995)	irreversible entry	GMR; GBM
Sarkar (2003)	irreversible entry	IGBM; GBM
Tsekrekos (2010)	partially reversible entry and exit	IGBM; GBM
Tsekrekos (2013)	irreversible exit	IGBM; GBM
Tvedt (2022)	partially reversible entry and exit	IGBM; GBM
Dias et al. (2015)	partially reversible entry and exit	IGBM; CIR; OU GBM; CEV; CKLS
This paper	partially reversible entry and exit; irreversible exit	IGBM; CIR; GBM; CEV

1.3 Model and methodology

As for its structure, our model is based on the entry and exit model with scrapping option given in Dixit and Pindyck (1994). In this section, we present its features and we adapt it to our own notation and price models (1.3.1). In particular, we show how to calculate the value of the project, in general as solution of an ordinary differential equation (1.3.2) and, specifically, according to different possible states of production (1.3.3). Last, we state the conditions to satisfy in order to get the optimal managerial strategy of the project (1.3.4).

1.3.1 The framework

We consider an investment project that consists of producing and selling a certain good. We assume that the value of the project is entirely given by the selling price x, determined by the market, net of production costs. Additionally, it is widely accepted in the literature to assume an infinite time-horizon when dealing with long-lived investment projects; we adopt this line of thought. Let $(\Omega, \mathcal{F}, \mathbb{F} = \{\mathcal{F}_t\}_{t\geq 0}, \mathbb{P})$ be a filtered probability space, where $\mathbb{P}$ is a given probability measure. Then, the output price process, $x := \{x_t\}_{t\geq 0}$ solves

$$\mathrm{d}x = \delta(x)\,\mathrm{d}t + \nu(x)\,\mathrm{d}W. \tag{1.1}$$

given the initial condition $x_0 \in \mathbb{R}^+$ and with W being a standard Brownian motion under $\mathbb{P}$. On the other hand, operating costs are constant, strictly non-negative, and equal to $c = v + f$, where v is the variable component, directly related to the production activity, and f represent the fixed cost, which is incurred whether production takes place or not (Dixit and Pindyck, 1994).

Furthermore, managers can partially manage market ups and downs by suspending production; when this happens, then the option to restart activates. Following Dixit (1989), the payment of a lump sum $s_{10} \in \mathbb{R}^+$ (resp. $s_{01} \in \mathbb{R}^+$ is required to switch production from the active (resp. suspended) to the suspended (resp. active) state. Additionally, there exists the option to permanently abandon the project, which can be exercised when production is either active or suspended. In the first case, abandonment is an alternative to suspension, whilst in the second one it comes in place of reactivation. Upon abandonment, all the assets related to the project are liquidated and investors receive a fraction ηI of some initial investment cost $I, \eta \in [0,1], I \in \mathbb{R}^+$, .

Put into practice, every option is instantaneously exercised when the output price hits a critical threshold from above - as it is the case for suspension and abandonment - or from below - considering reactivation. We denote with x_s, x_r, and x_a the price boundaries triggering the suspension, reactivation and abandonment of the project, respectively. We also account for a second project, equivalent to the former one except for the absence of the options to suspend and reactivate production and for which abandonment occurs when the output price drops below $\bar{x}_a$. We call this project "rigid" in contrast with the (former) "flexible" one.

It must be noted that if x_s is lower than x_a the managers of the flexible project behave as if it was rigid and abandonment becomes the only relevant option; in the opposite case, the suspension option is exercised first and the critical level triggering abandonment is pushed-down, compared to the rigid project. Consequently, $\bar{x}_a$ is a cap for x_a.

1.3.2 Underlying dynamics and the value of the project

In this work, we mainly address the implications of adopting different specifications for the process of the underlying variable x, and, in particular, we consider four different processes which satisfy (1.1). Namely, our choice includes the IGBM (Bhattacharya, 1978), the drift-less GBM, the CIR (Cox et al., 1985) and the CEV (Cox, 1975) processes; it is worth mentioning that the CEV model nests a GBM with non-zero drift under the condition $\beta = 0$.

By assumption, the value of the project, denoted by $V(x)$, depends on the cash-flows it generates and on the dynamics of the underlying variable. Applying Itô's Lemma to (1.1) and taking expectation, we get the expected capital gain of the project

$$\frac{\mathbb{E}[dV]}{dt} \approx \frac{\nu^2(x)}{2} V''(x) + \delta(x) V'(x).$$

The risk-free total return of the project, $\frac{rV(x)}{dt}$, must equate the expected capital gain plus the cash-flows $F(x)$ generated per unit of time. Then, multiplying all by dt, defining $\mathcal{A}V(x) := \frac{\nu^2(x)}{2} V''(x) + \delta(x) V'(x)$ and rearranging, we get

$$\mathcal{A}V(x) = rV(x) - F(x). \tag{1.2}$$

We collect the stochastic differential equations for price models, the corresponding expressions for $\mathcal{A}V(x)$, and the related sets of parameters Θ in Table 1.2.

Table 1.2 The Table presents the price models included in this work. The corresponding SDEs, expressions $\mathcal{A}V(x) := \frac{\nu^2(x)}{2}V''(x) + \delta(x)V'(x)$ and sets of parameters Θ are specified.

Model	SDE	$\mathcal{A}V(x)$	Θ
IGBM	$dx = \kappa(\theta - x)dt + \sigma x dW$	$\frac{\sigma^2}{2}x^2V''(x) + \kappa(\theta - x)V'(x)$	κ, θ, σ
CIR	$dx = \kappa(\theta - x)dt + \sigma\sqrt{x}dW$	$\frac{\sigma^2}{2}xV''(x) + \kappa(\theta - x)V'(x)$	κ, θ, σ
CEV	$dx = \mu x dt + \sigma x^{\beta+1}dW$	$\frac{\sigma^2}{2}x^{2\beta+2}V''(x) + \mu x V'(x)$	μ, σ
GBM	$dx = \sigma x dW$	$\frac{\sigma^2}{2}x^2V''(x)$	μ, σ

As usual, the solution to (1.2) is given by the solution of the homogeneous equation $\mathcal{A}V(x) - rV(x) = 0$ plus a particular solution $H(x)$. Specifically, the solution to $\mathcal{A}V(x) - rV(x) = 0$ can be easily obtained in terms of special functions, which, in general, require to be evaluated numerically. Numerical algorithms are available for this purpose, but they potentially exhibit different degrees of accuracy. Given the comparative nature of our study and in order to reduce the computational bias, it is convenient to express all the solutions in terms of the same special function. Then, for the price processes specified in Table 1.2, we have the following

Proposition 1.3.1. *The solution of equation 1.2 is of the form*

$$V(x) = p\Phi(\alpha, \gamma; h(x))\,x^{\xi_1} + q\Phi(1 + \alpha - \gamma, 2 - \gamma; h(x))\,x^{\xi_2} + \psi(x)$$

where $\Phi(\alpha_1, \gamma_1; h(x)) := \sum_{k=0}^{\infty} \frac{(\alpha)_k x^k}{(\gamma)_k k!}, |h(x)| < \infty, \alpha \in \mathbb{C}, \gamma \in \mathbb{C}\setminus\mathbb{Z}^-$ *is a confluent hypergeometric function of the first kind,* $p, q \in \mathbb{R}$ *are constant coefficients to be determined by means of proper boundary conditions, and* $\psi(x)$ *is a properly chosen particular solution.*

Proof. See Appendix A.1. $\square$

1.3.3 The state-contingent valuation problem

It must be remembered that instantaneous cash-flows are contingent to the state of the project. In particular, we have $F(x) = x - c$ when production takes place and $F(x) = -f$ while it is suspended. Consequently, the value of the project differs accordingly. Let $V_1(x)$ and $V_0(x)$ be the value of the project when production is active and suspended, respectively. Then, $V_1(x)$ solves

$$\mathcal{A}V_1(x) = rV_1(x) - (x - c) \tag{1.3}$$

subject to $\lim\limits_{x \to +\infty} V_1(x) < \infty$, whereas $V_0(x)$ is the solution of

$$\mathcal{A}V_0(x) = rV_0(x) + f \tag{1.4}$$

subject to $\lim\limits_{x \to 0^+} V_0(x) < \infty$.

The two conditions prevent the value of the project from exploding as the output price enlarges or approaches zero, respectively. From an economic point of view, it means that the value of the option to suspend (resp. restart) production, which exists while the project is in the active (resp. suspended) state, decreases as the output price grows (resp. converges to zero). When this is the case, the value of the project at time $t = 0$ converges to

$$\psi(x) = \mathbb{E}_0 \left[\int_0^\infty F(x) e^{-ru} du \right].$$

The value-functions of the project can then be easily obtained accounting for the results in Proposition 1.3.1. In particular, we claim that

Proposition 1.3.2. *The value $V_1(x)$ of the project in the active state*

1. *under IGBM is*

$$V_1(x) = q_2 \Phi\left(\alpha_2, \gamma_2; \frac{2\kappa\theta}{\sigma^2 x}\right) x^{\xi_2} + \psi^{MR}(x)$$

with $\{\alpha_1,\gamma_1,\xi_1\}$, $\{\alpha_2,\gamma_2,\xi_2\}$ *as in* (A.14);

2. *under CIR is*

$$V_1(x)=\tilde{q}_2\Phi\left(\alpha_2,\gamma_2;\frac{2\kappa x}{\sigma^2}\right)x^{\xi_2}-\tilde{q}_1\Phi\left(\alpha_1,\gamma_1;\frac{2\kappa x}{\sigma^2}\right)+\psi^{MR}(x)$$

where $\tilde{q}_1=q_2\left(\frac{2k}{\sigma^2}\right)^{1-\gamma_2}\frac{\Gamma(\gamma_2)\Gamma(1-\gamma_2)}{\Gamma(\alpha_2)\Gamma(\gamma_1)}, \tilde{q}_2=q_2\frac{\Gamma(1-\gamma_2)}{\Gamma(\gamma_1)}$ *and* $\{\alpha_1,\gamma_1,\xi_1\}$, $\{\alpha_2,\gamma_2,\xi_2\}$ *as in* (A.15);

3. *under CEV is*

$$V_1(x)=\begin{cases}\left[\tilde{q}_1\Phi\left(\alpha_1,\gamma_1;\frac{\mu}{|\beta|\sigma^2x^{2\beta}}\right)x^{\xi_1}+\tilde{q}_2\Phi\left(\alpha_2,\gamma_2;\frac{\mu}{|\beta|\sigma^2x^{2\beta}}\right)x^{\xi_2}\right]e^{\frac{\mu}{\beta\sigma^2x^{2\beta}}\mathbf{1}_{\{\beta<0\}}}+\\ +\psi(x) \qquad \text{if} \quad \mu\neq 0\\ \left[\tilde{q}_1\Phi\left(\alpha_1,\gamma_1;\frac{2\sqrt{2r}}{|\beta|\sigma x^{\beta}}\right)x^{\xi_1}+\tilde{q}_2\Phi\left(\alpha_2,\gamma_2;\frac{2\sqrt{2r}}{|\beta|\sigma x^{\beta}}\right)x^{\xi_2}\right]e^{\frac{\sqrt{2r}}{|\beta|\sigma x^{\beta}}}+\\ +\psi^{\bar{M}R}(x) \qquad \text{if} \quad \mu=0\end{cases}$$

where

$$\tilde{q}_1=\begin{cases}q_2\frac{\Gamma(1-\gamma_1)}{\Gamma(\alpha_2)} & \text{if} \quad \beta<0;\ \mu\neq 0\\ 0 & \text{if} \quad \beta>0;\ \mu\neq 0\\ q_2\frac{\sqrt{\pi}\Gamma\left(\frac{1}{\beta}\right)}{\Gamma\left(\frac{\beta+1}{2\beta}\right)}\left(-\frac{2\sqrt{2r}}{\sigma\beta}\right)^{-\frac{1}{2\beta}} & \text{if} \quad \beta<0;\ \mu=0\\ q_2\frac{\sqrt{2r}}{2^{\frac{1}{2\beta}}\sigma\beta\Gamma\left(\frac{1}{2\beta}+1\right)} & \text{if} \quad \beta>0;\ \mu=0\end{cases}$$

$$\tilde{q}_2 = \begin{cases} \left(-\dfrac{\mu}{\beta\sigma^2}\right)^{1-\gamma_1} \dfrac{\Gamma(\gamma_1 - 1)}{\Gamma(\alpha_1)} & \text{if} \quad \beta < 0; \mu \neq 0 \\ q_3 \in \mathbb{R} & \text{if} \quad \beta > 0; \mu \neq 0 \\ 0 & \text{if} \quad \beta < 0; \mu = 0 \\ q_2 \dfrac{\Gamma\left(-\dfrac{1}{\beta}\right)}{\Gamma\left(\dfrac{\beta-1}{2\beta}\right)} 2^{-\dfrac{1}{2\beta}} \sqrt{\pi} \left(-\dfrac{\sqrt{2r}}{\sigma\beta}\right)^{\dfrac{1}{2\beta}} & \text{if} \quad \beta > 0; \mu = 0 \end{cases}$$

and $\{\alpha_1, \gamma_1, \xi_1\}$, $\{\alpha_2, \gamma_2, \xi_2\}$ *as in* (A.17), (A.18) *or* (A.21) *depending on the sign of* β *and on* μ*;*

4. *under GBM is*

$$V_1(x) = q_2 x^{\xi_2} + \psi(x)$$

with $\{\alpha_1, \gamma_1, \xi_1\}, \{\alpha_2, \gamma_2, \xi_2\}$ *as in* (A.22).

Across all models, it holds the following

$$\psi(x) = \begin{cases} \dfrac{x}{r+\kappa} + \dfrac{\theta}{r} - \dfrac{\theta}{(r+\kappa)} - \dfrac{c}{r} & \text{if } MR \\ \dfrac{x}{r-\mu} - \dfrac{c}{r} & \text{if not } MR \end{cases} \tag{1.5}$$

which leads to the notation $\psi^{MR}(x)$ *and* $\psi(x)$ *to distinguish between the mean-reverting (MR) and the non-mean-reverting case.*

Proof. See Appendix A.2. □

and

Proposition 1.3.3. *The value* $V_0(x)$ *of the project in the suspended state*

1. *under IGBM is*

$$V_0(x) = p_1 \Phi\left(\alpha_1, \gamma_1; \frac{2\kappa\theta}{\sigma^2 x}\right) x^{\xi_1} + p_2 \Phi\left(\alpha_2, \gamma_2; \frac{2\kappa\theta}{\sigma^2 x}\right) x^{\xi_2} - \frac{f}{r}$$

with $\{\alpha_1, \gamma_1, \xi_1\}$, $\{\alpha_2, \gamma_2, \xi_2\}$ *as in* (A.14)*;*

2. *under CIR is*

$$V_0(x) = p_1 \Phi\left(\alpha_1, \gamma_1; \frac{2\kappa x}{\sigma^2}\right) + p_2 \Phi\left(\alpha_2, \gamma_2; \frac{2\kappa x}{\sigma^2}\right) x^{\xi_2} - \frac{f}{r}$$

with $\{\alpha_1, \gamma_1, \xi_1\}$, $\{\alpha_2, \gamma_2, \xi_2\}$ *as in* (A.15)*;*

3. *under CEV is*

$$V_0(x) = \begin{cases} \left[\tilde{p}_1 \Phi\left(\alpha_1, \gamma_1; \frac{\mu}{|\beta|\sigma^2 x^{2\beta}}\right) x^{\xi_1} + \tilde{p}_2 \Phi\left(\alpha_2, \gamma_2; \frac{\mu}{|\beta|\sigma^2 x^{2\beta}}\right) x^{\xi_2}\right] e^{\frac{\mu}{\beta\sigma^2 x^{2\beta}} 1_{\{\beta<0\}}} + \\ + \psi(x) \qquad \text{if} \quad \mu \neq 0 \\ \left[\tilde{p}_1 \Phi\left(\alpha_1, \gamma_1, \frac{2\sqrt{2r}}{|\beta|\sigma x^{\beta}}\right) x^{\xi_1} + \tilde{p}_2 \Phi\left(\alpha_2, \gamma_2; 2z\right) x^{\xi_2}\right] e^{-\frac{2\sqrt{2r}}{|\beta|\sigma x^{\beta}}} \text{if} \quad \mu = 0 \end{cases}$$

where $\tilde{p}_1 = \left[p_1 \sqrt{\pi} 2^{\frac{1}{2|\beta|}} \frac{\Gamma\left(-\frac{1}{|\beta|}\right)}{\Gamma\left(\frac{1}{2} - \frac{1}{2|\beta|}\right)} + p_2 \frac{1}{2^{\frac{1}{2|\beta|}} \Gamma(\frac{1}{2|\beta|} + 1)}\right] \frac{2\sqrt{2r}}{|\beta|\sigma}$,
$\tilde{p}_2 = p_1 2^{\frac{1}{2|\beta|}} \frac{\Gamma\left(\frac{1}{2|\beta|}\right)}{\Gamma\left(\frac{1}{2} + \frac{1}{2|\beta|}\right)} \frac{2\sqrt{2r}}{|\beta|\sigma x^{\beta}}$ *and* $\{\alpha_1, \gamma_1, \xi_1\}$, $\{\alpha_2, \gamma_2, \xi_2\}$ *as in* (A.17), (A.18) *or* (A.21) *depending on the sign of* β *and on* μ*;*

4. *under GBM is*

$$V_0(x) = p_1 x^{\xi_1} + p_2 x^{\xi_2} - \frac{f}{r}$$

$\{\alpha_1, \gamma_1, \xi_1\}$, $\{\alpha_2, \gamma_2, \xi_2\}$ *as in* (A.22)*;*

Proof. The proof follows the same argument as in Proposition 1.3.2 under the condition $\lim_{x \to 0^+} V_0(x) = 0$ and with $F(x) = -f$. Moreover, $\psi(x) = -\frac{f}{r}$ regardless the model, since, by construction, fixed costs depend on the type of production plant but not on the price process. □

Last, the value of the project at the time of abandonment is equal to the scrap value ηI whatever the dynamics driving the underlying price process.

1.3.4 Optimal switching boundaries

At any instant, managers decide whether to exercise an option, and which one, comparing the continuation value of the project with that achievable through a switching; they choose the running policy that maximises profits. For the purposes of this work, the continuation value is $V_1(x)$ while the project is active and $V_0(x)$ while it is suspended; net of the proper switching cost s_{10} or s_{01}, they are mutually alternative. Additionally, since the abandonment of the project is non-reversible, it can only be an alternative to keeping the project active or suspended. Moreover, the value of the project is driven by the uncertain behaviour of the output price: it turns out that we need to determine three critical values of x - namely, x_s, x_r, x_a ($\bar{x_a}$ for the rigid project) - that trigger switching decisions. Noticeably, in correspondence of such boundaries, managers are indifferent between continuation and switching; hence, the continuation value must be equal to the alternative one, net of switching costs. Consequently, we get the following boundary conditions

$$\begin{aligned} V_1(x_s) &= V_0(x_s) - s_{10} \\ V_0(x_r) &= V_1(x_r) - s_{01} \\ V_0(x_a) &= \eta I. \end{aligned} \tag{1.6}$$

Additionally, for x_s, x_r, x_a to be optimal, smooth-pasting conditions must be satisfied too[2]

$$\begin{aligned} V_1'(x_s) &= V_0'(x_s) \\ V_0'(x_r) &= V_1'(x_r) \\ V_0'(x_a) &= 0. \end{aligned} \tag{1.7}$$

Clearly, when the project is rigid, or whenever it is optimal to immediately exercise abandonment without previously suspending, systems (1.6) and (1.7) reduce to

$$V_1(\bar{x_a}) = \eta I \tag{1.8}$$

and

$$V_1'(\bar{x_a}) = 0. \tag{1.9}$$

Solving (1.6) and (1.7) (resp. equations 1.8 and 1.9) with respect to the constant coefficients and with respect to x_s, x_r, x_a (resp. $\bar{x}_a$), respectively, allows to solve the model. Appendices A.3 and A.4 show how to deal with value-matching and smooth-pasting conditions to get the constant coefficients and the optimal options' boundaries for the IGBM case as an example.

1.3.5 Discussion of the levered case

The model presented in section 1.3 refers to a project entirely financed by equity. In this section, we briefly discuss the case in which debt is present too.

[2]For decision makers' choices to be optimal, both the utility and the marginal utility of staying in the continuation region, evaluated at the optimal stopping point, must be equal to those of switching to (any of) the alternative(s). Such kind of requirements generates boundary conditions that are labelled as "value-matching" and "smooth-pasting" conditions, respectively. A detailed explanation can be found in Dixit and Pindyck (1994), pp: 130-132.

Consider a framework similar to that given in section 1.3 but assume that the project is partially funded by means of a perpetual bond with continuous coupon C; possibly, a tax-shield exists for a constant tax-rate ϑ. Abandoning the project implies the default on debt, with the payment of some recovery value to bondholders and no residual value to equity-holders. The price that optimally triggers default is x_d (project). According to accounting principles, the value of project's assets is the sum of equity an debt values, i. e.

$$V(x) = E(x) + D(x),$$

where $E(x)$ is the value of equity, $D(x)$ it the value of debt and both depend on the instantaneous output price. Hence, they satisfy ordinary differential equations of the kind

$$\mathcal{A}E(x) = rE(x) - F(x) + C(1-\vartheta) \tag{1.10}$$

and

$$\mathcal{A}D(x) = rD(x) - C \tag{1.11}$$

where $F(x)$ is the same cash-flow appearing in (1.2) and $\mathcal{A}E(x)$ and $\mathcal{A}D(x)$ have a form equivalent to that of $\mathcal{A}V(x)$ in Table 1.2. Hence, compared to the basic all-equity case, the only difference for equity-holders is an earning reduction equal to $C(1-\vartheta)$. Conversely, bond-holders receive a constant payment C until default; when this last occurs, the assets of the project are liquidated and they get the value stemming from the sale process as partial reimbursement. We call this value $\omega V(x_d)$, where $V(x_d)$ is the value of an all-equity project for $x = x_d$ and $\omega \in [0,1]$. Hence, equations in (1.11) are solved subject to the boundary conditions

$$\lim_{x\to\infty} D(x) = \mathbb{E}_0\left[\int_0^{+\infty} Ce^{-ru}du\right] = \frac{C}{r}$$
$$D(x_d) = \omega V(x_d).$$

Notice that none of the above conditions is imposed at suspension or resumption boundaries. Additionally, the default boundary is exogenous to bond-holders. Indeed, decision-makers are intended to be equity-holders or managers acting in their interest. Consequently, it can be assumed that operational choices are such that the value of equity - and not that of assets - is maximised. This fact implies to solve equations in (1.10) subject to the systems of value-matching

$$\begin{aligned} E_1(x_s) &= E_0(x_s) - s_{10} \\ E_0(x_r) &= E_1(x_r) - s_{01} \\ E_0(x_d) &= 0 \end{aligned} \tag{1.12}$$

and smooth-pasting

$$\begin{aligned} E_1'(x_s) &= E_0'(x_s) \\ E_0'(x_r) &= E_1'(x_r) \\ E_0'(x_d) &= 0 \end{aligned} \tag{1.13}$$

conditions. Based on the assumptions above, any impact of debt on suspension and restart boundaries can be excluded. This fact depends on the coupon being paid independently from production being active or suspended, and it can be easily verified analytically by solving (1.12) and (1.13).[3] Second, all the other things being equal, the default price of a levered firm is larger than the liquidation price of an unlevered one, because the coupon payment lowers equity cash-flows. In sum, the only effect of introducing debt into the analysis would be a reduction in equity-holders' cash-flows regardless of whether production is ongoing or suspended. However, this effect can be equivalently reached by increasing the level of fixed costs f in the base case all-equity framework.

On the other hand, our assumption of managers maximising equity value gives rise to a *second-best* optimal strategy for the project. Recently, Glover and Hambusch (2016) and Ritchken and Wu (2020) obtained *first-best* solutions for similar problems by maximising over the total asset value under the assumption of output prices evolving as an IGBM and a GBM with drift, respectively. Moreover, they determined the optimal coupon on debt, which we assumed as given in this discussion. Additionally, in presence of the option to relocate investments in foreign Countries, then it would also be interesting to relax the assumption of a constant tax-rate, letting it to be uncertain. In respect of this point, Azevedo et al. (2019) underscored the importance of stable and predictable tax policies in attracting foreign investment and suggested that carefully designed tax holidays can significantly influence investment decisions. This result is presumed to play in role in affecting the optimal level of financial leverage or, equivalently, the amount of debt that a firm can raise.

Indeed, finding the optimal financing strategy of the project is beyond the scope of our work; nevertheless, we signal it as promising area of further research, particularly because of the insightful information about the creditworthiness of firms that can be recovered from the analysis of financial leverage.

[3]Our claim is based on the implicit assumption that debt repayment remains affordable while production is suspended. While this is reasonable for most standard situations, we can not ignore that it is not necessarily true in general. Indeed, cases for which the lack of cash-inflows makes coupon payment unfeasible might exist. A detailed analysis of this point would be beyond the scope of our work; nevertheless we signal it as an interesting topic for future research.

1.4 Results and discussion

In this section, we present the results of our numerical experiments. After the calibration of the parameters of each model against those of a specified benchmark (1.4.1), we investigated numerically how different price models affect the optimal strategy of the project in terms of real options' boundaries (1.4.2), of probabilities that the optimal strategy is implemented within a short-horizon (1.4.3), and of decision timing (1.4.4). Furthermore, we tested the sensitivity of our results to changes in the degree of flexibility of the project (1.4.5). Additionally, we looked for project value implications (1.4.6). Table 1.3 shows the set of parameters, that, unless stated otherwise, were kept constant across the analysis.

Table 1.3 The Table collects and describes the parameters used for the numerical implementation of the model.

Notation	Value	Description
r	0.04	Risk-free rate
v	1.7	Production cost of the project
f	0.1	Fixed cost of the project
I	20	Initial cost of the project
η	0.5	Recovery fraction of I upon project liquidation
s_{10}	0.1	Cost to switch from production to suspension
s_{01}	0.2	Cost to switch from suspension to production

1.4.1 Calibration of the models

The recurrent approach in the literature consists of comparing different models using the same value for parameters that are in common among processes. For example, Sarkar (2003) and Tsekrekos (2010) confronted the results from an IGBM with those from a (drift-less) GBM having the same volatility parameter σ. A rationale for this choice could be found in the low speed of mean-reversion empirically observed in several time-series of data, which led some Authors to simply assume it to be zero. If this could be reasonable to some extent, less easy to understand is the choice of - apparently - keeping the key parameters in Dias et al. (2015) and Dangerfield et al. (2018) the same across different model specifications.

However, an effective comparative analysis should be carried on among models that exhibit similar features. For example, introducing mean-reversion typically reduces the variance of a process for the same volatility parameter. Our reasoning is pretty simple and is based on the fact that parameters values are estimated from data. Within this step, a preliminary analysis of price dynamics can be aimed at fitting a model as consistent as possible with empirical observations; alternatively, a certain process could be assumed *a priori*. Furthermore, even the analyst that captured the correct time-series' dynamics might be willing to substitute them with a process simpler to handle. Nevertheless, they have to calibrate the new process in such a way that the main features of the empirical one are retained.

Hence, we calibrated our models as follows: first, we chose the IGBM model as a benchmark[4] and we assigned it a plausible yet arbitrary set of parameters, assuming it represented a reliable description of some time-series of prices. Next, we estimated the first and second moment for the logarithm of this process and for the k-th model, with $k \in \{\text{CIR, CEV}(\beta), \text{GBM}\}$. Last, we obtained the set of parameters Θ, specified in Table 1.2 for the k-th price model, by solving

$$\min_{\Theta} \sum_{j=1}^{T} (\mu_j(k,\Theta) - \mu_j(\Theta^{\text{IGBM}}))^2 + \frac{1}{4} \sum_{j=1}^{T} (\mu_j^2(k,\Theta) - \mu_j^2(\Theta^{\text{IGBM}}))^2$$

where $j = T_j$ is the j-th time-horizon, $T = 8$, $\mu_j^n(\Theta^{\text{IGBM}}) = \mathbb{E}[\ln(x_j)^n|\mathcal{F}_0]$ if $\{x_t\}_{t\geq 0}$ is an IGBM, and $\mu_j^n(k,\Theta) = \mathbb{E}[\ln(x_j)^n|\mathcal{F}_0]$ if $\{x_t\}_{t\geq 0}$ is the k-th process alternative to IGBM.

[4]We selected the IGBM as benchmark because of its large employment in the literature and of its mean-reverting features, which make it suitable to applications in several markets.

We considered three scenarios that, being based on the opposite effect of the volatility parameter σ and of the speed of mean-reversion κ on the variance of mean-reverting processes, capture a low, an intermediate and a high variance environment. We emphasise that the range of κ (0.07 to 0.30) is significantly larger than that of σ (0.15 to 0.30). By means of this choice, we aimed at focusing on the effect of mean-reversion, capturing two meaningful scenarios: a first one where mean-reversion plays a primary role in shaping firm's characteristics and strategy, and a second framework where mean-reversion is marginal, compared to the turmoil attributable to a larger diffusion coefficient. For the sake of completeness, we recall that the third scenario corresponds the intermediate case. For each case, we implemented the calibration procedure described above. Results are collected in Table 1.4. As expected, little adjustments occurred when moving from IGBM to CIR, whereas a significant reduction in the instantaneous volatility coefficient was necessary to balance the exploding nature of non-mean-reverting processes, particularly when the reversion rate was large in the benchmark case.

1.4.2 Effect on optimal boundaries

Table 1.5, reports the optimal boundaries for the flexible project and, as a benchmark, for its rigid counterpart. Importantly, the last column signals whether reversible suspension is actually included in the optimal strategy of the firm. Apparently, selecting a model different from the IGBM benchmark causes a shift between suspension and abandonment only in few cases. However, the abandonment threshold is much more sensitive to changes in the variance of the price process, compared to the suspension boundary. The reason for that, as highlighted also by Tsekrekos (2013), relies in the irreversible nature of abandonment, which make such decision to be postponed if price variability is high enough to make a recover from losses possible. Instead, the possibility

Table 1.4 The Table displays the parameters for all the analysed models. Acronyms refer to: CEV = constant elasticity of variance process; CIR = square-root mean-reverting diffusion; GBM = drift-less geometric Brownian motion; IGBM = inhomogenous geometric Brownian motion. The IGBM process is taken as benchmark: its parameters have been set arbitrarily, whilst the parameters of all the other models have been calibrated against those of the benchmark following the "moments-matching" procedure described in 1.4.1

	Setting 1				Setting 2				Setting 3			
Model	κ	θ	σ	μ	κ	θ	σ	μ	κ	θ	σ	μ
IGBM	0.3	1.8	0.15		0.15	1.8	0.2	-	0.07	1.8	0.3	-
CIR	0.30699	1.79986	0.20202	-	0.16281	1.79434	0.26551	-	0.10235	1.69053	0.37328	-
GBM	-	-	0.09273	-	-	-	0.11031	-	-	-	0.16758	-
CEV												
$\beta = -0.5$	-	-	0.11075	0.00000	-	-	0.12716	0.00000	-	-	0.19098	0.00000
$\beta = 0$	-	-	0.04227	-0.00524	-	-	0.11032	0.00000	-	-	0.14749	-0.00565
$\beta = 0.5$	-	-	0.03177	-0.00520	-	-	0.05738	-0.00475	-	-	0.12797	0.00001

to switch back again to the previous state makes suspension - and resumption too - less elastic to such variations. Consequently, we observed a sizeable reduction in the abandonment boundary when passing from the low variance scenario depicted in the top panel to the high variance one given in the bottom panel. Most importantly, the distance between the suspension and the abandonment thresholds exhibit a kind of U-shaped behaviour that makes intermediate cases critical. Indeed, when neither the drift nor the diffusion component play a predominant role in the benchmark model, such distance is tiny and makes the occurrence of shifts between the two boundaries more likely and sensitive to model parameters. This is observable for GBM in the mid-panel, where suspension suddenly is included in the strategy of the project in spite of an average variation of about 7% in the relevant thresholds with respect to the IGBM case.

1.4.3 Effect on entry and exit probabilities

We further computed the probability to suspend, restart and abandon production within the short-term, which we quantify in 5 years over a 30-years horizon. The standard approach is to simulate M trajectories for each of the models under investigation and to superimpose to them the corresponding boundaries, then to calculate probabilities by counting the frequency of state transitions. Our method is conceptually similar, but we simulated cash-flows only according to the benchmark process and we attached all the boundaries to it. We believe that our describes better the operational reality of the project.

Results are shown in Table 1.6. Differences among models are sizeable particularly within the two extreme scenarios based on low and high price volatility. Moreover, GBM offers the worst match with respect to the benchmark and it overestimates the probability of multiple transitions between the active and the suspended states;

Table 1.5 The Table shows the optimal abandonment (x_a), suspension (x_s) and resumption (x_r) thresholds of the flexible project next to the abandonment threshold ($\bar{x_a}$) of an otherwise equivalent rigid one. The last column highlights whether the optimal strategy include suspension. Panels **(a)**, **(b)** and **(c)** refer to a scenario of low, medium and high volatility, respectively, identified by different combinations of the IGBM parameters κ and σ. All the other model parameters are as in Table 1.3.

Optimal boundaries, panel **(a)**: $\kappa = 0.30, \sigma = 0.15$.

Model	$\bar{x}_a$	x_a	x_s	x_r	Suspend
IGBM	1.92476	1.92476	1.44852	1.96248	No
CIR	1.95865	1.95865	1.43154	1.95553	No
GBM	1.58730	1.58730	1.53379	1.89496	No
CEV					
$\beta = -0.5$	1.65871	1.65871	1.19290	2.01668	No
$\beta = 0$	1.99913	1.99913	1.60244	1.91355	No
$\beta = 0.5$	1.87485	1.87485	1.60169	1.81494	No

Optimal boundaries, panel **(b)**: $\kappa = 0.15, \sigma = 0.20$.

Model	$\bar{x}_a$	x_a	x_s	x_r	Suspend
IGBM	1.61305	1.61305	1.42419	2.03507	No
CIR	1.67350	1.67350	1.40484	2.01944	No
GBM	1.49308	1.48127	1.51492	1.92030	Yes
CEV					
$\beta = -0.5$	1.58528	1.58517	1.21306	1.97321	No
$\beta = 0$	1.49302	1.48128	1.51511	1.92017	Yes
$\beta = 0.5$	1.66345	1.66345	1.55848	1.87358	No

Optimal boundaries, panel **(c)**: $\kappa = 0.07, \sigma = 0.30$.

Model	$\bar{x}_a$	x_a	x_s	x_r	Suspend
IGBM	1.11047	0.93379	1.36080	2.15801	Yes
CIR	1.28974	1.23948	1.34818	2.11314	Yes
GBM	1.22664	1.11321	1.46148	1.99704	Yes
CEV					
$\beta = -0.5$	1.31758	1.25818	1.33363	1.72098	Yes
$\beta = 0$	1.42044	1.38913	1.48418	1.97782	Yes
$\beta = 0.5$	1.24320	1.14523	1.47271	2.01351	Yes

nevertheless, such error is contained for the intermediate volatility scenario. It is also worth to notice that the rigid project is less sensitive to model changes than the flexible one. In short, the choice of the model substantially impacts the short-term entry and exit probabilities. To understand how much this affects the project strategy as a whole, in the next section we estimate the *time-to-abandonment* of the project.

1.4.4 Effect on the timing of strategic decisions

To fully understand the impact of different models on the project strategy, we calculated its expected *time-to-abandonment*, i. e. the time needed before the abandonment barrier is crossed, causing the liquidation of the project. On top of that, we computed the percentage amount of time spent by the project on the pre-abandonment state over a 30-years horizon; conditional on being alive, we further considered for how long it remained in the active and in the suspended state, respectively. Results are given in Table 1.7. Again, the more significant variations occur for GBM and for the square-root CEV process in the low-variance scenario, confirming they are highly unreliable proxies for the benchmark in such case. In the intermediate and in the high-variance environments, abandonment occurs within 2.5 years of difference between models for the rigid project and 4 years for the flexible one. Although not negligible, these differences are pretty small, compared to the overall horizon. Moreover, the profile of the cumulative time spent in the active and in the suspended state looks very similar in all cases, signalling that little discrepancies in the time to abandonment do not necessarily affect significantly the project strategy as long as it is “alive”. The GBM case in Panel **(b)** is particularly noteworthy: while this is the only case in which suspension in included in the strategy of the project, it is also evident that it acts as a preliminary step towards full abandonment, with the project being kept in this state for less than 4 months in total.

Table 1.6 The Table reports the probabilities to abandon, suspend, and restart production within 5-years. Values have been computed numerically via Monte Carlo simulation, using 100,000 trajectories, a 30-years-long horizon and 250 steps per year. The probability of abandonment is computed conditional on the project being either rigid ($P(\text{A}|\text{rig})$) or flexible ($P(\text{A}|\text{flex})$) whilst $P(\text{S} \geq 1)$ and $P(\text{S} > 1)$ refer to the probability that suspension occurs at least once and more than once, respectively. With analogous interpretation, label "R" denotes restart. Values are expressed in percentage terms.

Entry and exit probabilities, panel **(a)**: $\kappa = 0.30, \sigma = 0.15$.

Model	$P(\text{A}\|\text{rig})$	$P(\text{A}\|\text{flex})$	$P(\text{S} \geq 1)$	$P(\text{S} > 1)$	$P(\text{R} \geq 1)$	$P(\text{R} > 1)$
IGBM	97.708	97.708	0	0	0	0
CIR	98.777	98.777	0	0	0	0
GBM	64.427	64.427	0	0	0	0
CEV						
$\beta = -0.5$	75.276	75.276	0	0	0	0
$\beta = 0$	99.749	99.749	0	0	0	0
$\beta = 0.5$	95.545	95.545	0	0	0	0

Entry and exit probabilities, panel **(b)**: $\kappa = 0.15, \sigma = 0.20$.

Model	$P(\text{A}\|\text{rig})$	$P(\text{A}\|\text{flex})$	$P(\text{S} \geq 1)$	$P(\text{S} > 1)$	$P(\text{R} \geq 1)$	$P(\text{R} > 1)$
IGBM	74.334	74.334	0	0	0	0
CIR	79.864	79.864	0	0	0	0
GBM	62.001	60.640	62.166	2.150	4.738	0.157
CEV						
$\beta = -0.5$	71.587	71.587	0	0	0	0
$\beta = 0$	61.993	60.641	62.227	2.165	4.770	0.161
$\beta = 0.5$	78.935	78.935	0	0	0	0

Entry and exit probabilities, panel **(c)**: $\kappa = 0.07, \sigma = 0.30$.

Model	$P(\text{A}\|\text{rig})$	$P(\text{A}\|\text{flex})$	$P(\text{S} \geq 1)$	$P(\text{S} > 1)$	$P(\text{R} \geq 1)$	$P(\text{R} > 1)$
IGBM	48.053	32.641	67.573	5.211	17.702	0.616
CIR	62.569	58.659	66.712	2.633	7.318	0.199
GBM	57.662	48.267	74.519	14.667	27.125	4.134
CEV						
$\beta = -0.5$	64.553	60.131	65.642	6.129	9.929	0.876
$\beta = 0$	71.777	69.608	75.912	7.170	11.624	1.021
$\beta = 0.5$	58.932	51.031	75.202	14.378	26.240	3.975

Table 1.7 The Table contains the expected time to abandonment of the project($\tau_{x_a}, \tau_{\bar{x}_a}$), the percentage of time spent in the pre-abandonment state in relation to a time horizon of 30 years ($\%\tau_{x>x_a}, \%\tau_{x>\bar{x}_a}$) and the percentage time spent in the active or in the suspended state before abandonment ($\%\tau_{\text{act}}, \%\tau_{\text{sus}}$). Values have been computed numerically via Monte Carlo simulation, using 100,000 trajectories, a 30-years-long horizon and 250 steps per year.

Time description of the project strategy, panel **(a)**: $\kappa = 0.30, \sigma = 0.15$.

Model	$\tau_{\bar{x}_a}$ (years)	$\tau_{x>\bar{x}_a}$ (%)	τ_{x_a} (years)	$\tau_{x>x_a}$ (%)	τ_{act} (%)	τ_{sus} (%)
IGBM	0.64925	2.164	0.64925	2.164	100	0
CIR	0.37887	1.263	0.37887	1.263	100	0
GBM	5.07987	16.933	5.07987	16.933	100	0
CEV						
$\beta = -0.5$	3.73901	12.463	3.73901	12.463	100	0
$\beta = 0$	0.09609	0.320	0.09609	0.320	100	0
$\beta = 0.5$	1.08167	3.606	1.08167	3.606	100	0

Time description of the project strategy, panel **(b)**: $\kappa = 0.15, \sigma = 0.20$.

Model	$\tau_{\bar{x}_a}$ (years)	$\tau_{x>\bar{x}_a}$ (%)	τ_{x_a} (years)	$\tau_{x>x_a}$ (%)	τ_{act} (%)	τ_{sus} (%)
IGBM	4.18030	13.934	4.18030	13.934	100	0
CIR	3.37894	11.263	3.37894	11.263	100	0
GBM	6.02549	20.085	6.23044	20.768	95.406	4.594
CEV						
$\beta = -0.5$	4.57443	15.248	4.57601	15.253	100	0
$\beta = 0$	6.02678	20.089	6.23037	20.768	95.381	4.619
$\beta = 0.5$	3.51263	11.709	3.51263	11.709	100	0

Time description of the project strategy, panel **(c)**: $\kappa = 0.07, \sigma = 0.30$.

Model	$\tau_{\bar{x}_a}$ (years)	$\tau_{x>\bar{x}_a}$ (%)	τ_{x_a} (years)	$\tau_{x>x_a}$ (%)	τ_{act} (%)	τ_{sus} (%)
IGBM	8.80221	29.341	11.73235	39.108	64	36
CIR	6.41350	21.378	7.02868	23.429	88	12
GBM	7.19449	23.982	8.76210	29.207	69.686	30.314
CEV						
$\beta = -0.5$	6.09465	20.315	6.78857	22.629	93	7
$\beta = 0$	4.94099	16.470	5.28362	17.612	88.783	11.217
$\beta = 0.5$	6.98382	23.279	8.29358	27.645	71	29

1.4.5 Sensitivity to flexibility-related costs

Next, we tested the sensitivity of our results to the degree of flexibility of the project. A project is considered to be comparatively more flexible if the costs to move from the active to the suspended state and vice-versa are lower. Similarly, smaller fixed costs increase flexibility by reducing the amount of the negative cash-flows to pay while suspended.

As a preliminary illustration, in Figure 1.1 we plotted the boundaries of the flexible project for the IGBM model and for $s_{10} \in [0, 0.15]$. For simplicity, we assumed that restarting production is as costly as suspending it, i. e. $s_{01} = s_{10}$. It is well-known that, under cost-less reversibility, production is stopped (restarted) as soon as earnings turn negative (positive), hence, $x_s = x_r = v$. Instead, larger transition costs reduce (increase) the level at which suspension (resumption) occurs, progressively widening the spread between the two boundaries. Such mechanism, known in economics as *hysteresis*, is discussed in detail in Dixit (1989) and Dias et al. (2015). We observed that greater variance in the price process exacerbates hysteresis. Furthermore, we noticed a significant asymmetry in the behaviour of the suspension and resumption boundaries. We argue that this is due to the value of the parameters used: when the price process is highly mean-reverting towards a zero-profit long-run scenario (we recall that we set $\theta = v + f$) and has low-variance, the effect on x_s is more pronounced, apparently signalling a preference for production; on the contrary, when the price process exhibit slow mean-reversion and high variance the impact on x_r is stronger than that on x_s. Noticeably, when the values of κ and σ are similar and almost offset in contributing to the variance of the process the asymmetry between boundaries is remarkably reduced. As expected, in response to the decline in the suspension barrier, the abandonment barrier grows moderately.

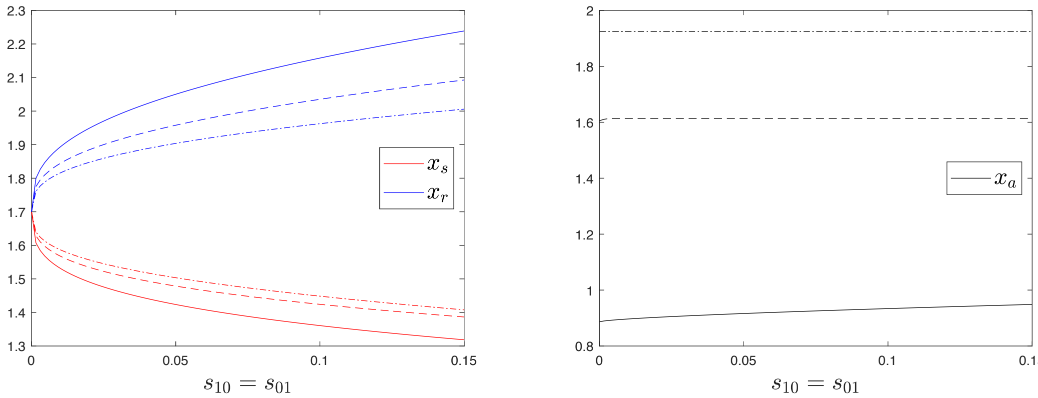

(a) (b)

Fig. 1.1 Panel a displays the suspension and resumption boundaries, x_s and x_r, as functions of the suspension cost s_{10}. In panel (b) the same is done for the abandonment boundary x_a. Low (dashed-dotted lines), intermediate (dashed lines) and high (solid lines) volatility scenarios arise from the couples of parameters $(\kappa = 0.30, \sigma = 0.15), (\kappa = 0.15, \sigma = 0.20), (\kappa = 0.07, \sigma = 0.30)$, respectively. For simplicity, the cost to restart production is assumed equal to that of suspension, i.e. $s_{01} = s_{10}$. .

In contrast, the choice on when to suspend and restart production is insensitive to variations in the fixed costs of the project. In fact, the amount f is paid regardless of whether production takes place. We showed in Figure 1.2 that the earnings reduction due to an increase in this value raises the abandonment barrier of both the flexible and the rigid project.

The reasons behind such behaviours are purely economic, therefore they have to be taken as qualitatively valid for all the price models under exam. Nevertheless, the quantitative sensitivity of each model to changes in the above parameters may vary. Hence, we calculated the variation of each barrier in response to three equidistant changes in the levels of s_{10} and f, respectively. Results, collected in Tables 1.8 and 1.9, document a larger sensitivity of options' exercise boundaries to changes in s_{10} and in f, on average, for IGBM and CIR processes. This fact signals that the operating strategy of the project would be comparatively more affected by changes in the degree of flexibility; this conclusion is attenuated in the case of moderately volatile markets.

Table 1.8 The Table shows the variations in optimal options boundaries attributable to changes in the cost of suspending and restarting production, which are assumed to be equal ($s_{10} = s_{01}$). For each boundary, marginal variations are considered and go under the label $\Delta s(i-1,i)$; the starting point is $s_{10} = 0$. Cumulative variations $\Delta s(0, i_{\max})$ are given in the last three columns. Values are given in percentage terms.

Boundaries variations, panel **(a)**: $\kappa = 0.15, \sigma = 0.20$.

s_{10}	0.03740	0.11210	0.15000	0.03740	0.11210	0.15000	0.03740	0.11210	0.15000			
	$\Delta s(i-1,i)$									$\Delta s(0,i_{\max})$		
Model	x_a			x_s			x_r			x_a	x_s	x_r
IGBM	0	0	0	-10.45359	-4.95496	-1.72654	11.72340	5.20302	1.70482	0	-16.36002	19.54017
CIR	0.04166	0	0	-10.96119	-5.51460	-1.95112	11.44855	4.83792	1.51342	0.04166	-17.51277	18.60862
GBM	0.57559	0.61930	0.25439	-7.06662	-3.17239	-1.10722	7.78099	3.49631	1.15311	1.45590	-11.01116	12.83564
CEV												
$\beta = -0.5$	0	0	0	-28.10698	-0.53254	-0.29214	14.88972	0.58658	0.37358	0	-28.69875	15.99536
$\beta = 0$	0.57559	0.61930	0.25439	-7.06662	-3.17239	-1.10722	7.78099	3.49631	1.15311	1.45590	-11.01116	12.83564
$\beta = 0.5$	16.69973	0	0	-5.49695	-2.35370	-0.77735	6.97530	1.92260	0.96066	16.69973	-8.43860	10.07943

Boundaries variations, panel **(b)**: $\kappa = 0.07, \sigma = 0.30$.

s_{10}	0.03740	0.11210	0.15000	0.03740	0.11210	0.15000	0.03740	0.11210	0.15000			
	$\Delta s(i-1,i)$									$\Delta s(0,i_{\max})$		
Model	x_a			x_s			x_r			x_a	x_s	x_r
IGBM	1.35442	0.94585	2.81756	-13.19776	-5.95605	-2.05406	15.88390	6.95249	2.30076	5.19581	-20.04452	26.79229
CIR	3.11661	3.26459	1.32152	-13.36693	-6.46039	-2.27964	14.67535	6.14198	2.02417	7.89015	-20.81109	24.18249
GBM	0.50658	0.64432	0.26271	-9.17591	-4.13131	-1.38364	10.44989	4.64786	1.53479	1.41991	-14.13289	17.35741
CEV												
$\beta = -0.5$	4.28980	0.56603	0.35265	-3.36204	-18.05428	-1.28403	0.24282	-0.55176	1.36144	0	-21.82616	1.04693
$\beta = 0$	0.73766	0.77788	0.32002	-8.42714	-3.57785	-1.25121	10.93483	3.21423	1.47974	1.84616	-12.80825	16.19484
$\beta = 0.5$	5.89409	0.45740	0.19328	-5.49695	-2.35370	-0.77735	10.75582	5.03267	1.67462	6.58406	-13.48549	18.27787

Table 1.9 The Table shows the variations in optimal options boundaries attributable to changes in the fixed cost of the project, f. For each boundary, marginal variations are considered and go under the label $\Delta f(i-1,i)$; the starting point is $f=0$. Cumulative variations $\Delta f(0,i_{\max})$ are collected in the last three columns. Values are given in percentage terms.

Boundaries variations, panel **(a)**: $\kappa=0.15, \sigma=0.20$.

f	0.03740	0.11210	0.15000	0.03740	0.11210	0.15000		
	$\Delta f(i-1,i)$						$\Delta f(0,i_{\max})$	
Model	$\bar{x}_a$			x_a			$\bar{x}_a$	x_a
IGBM	2.72516	5.18051	2.45069	2.72516	5.18051	2.45069	10.69474	10.69474
CIR	3.15427	6.19868	2.84836	3.15427	6.19868	2.84836	12.66881	12.66881
GBM	1.78993	3.48016	1.72154	2.91156	5.20563	2.31237	7.14571	10.77233
CEV								
$\beta=-0.5$	13.67659	8.01367	2.45705	16.74570	-33.42168	61.85193	8.46294	8.46294
$\beta=0$	1.78993	3.48016	1.72154	2.91156	5.20563	2.31237	7.14571	10.77233
$\beta=0.5$	1.54700	3.03750	1.48661	1.54700	3.03750	1.48661	6.18696	6.18696

Boundaries variations, panel **(b)**: $\kappa=0.07, \sigma=0.30$.

f	0.03740	0.11210	0.15000	0.03740	0.11210	0.15000		
	$\Delta f(i-1,i)$						$\Delta f(0,i_{\max})$	
Model	$\bar{x}_a$			x_a				
IGBM	2.58969	5.00339	2.40093	9.09482	14.55516	5.76519	10.30899	32.17872
CIR	3.47684	6.95151	3.22888	9.64529	15.62389	5.85537	14.24345	34.19936
GBM	1.78167	3.49472	1.71348	4.02777	7.22604	3.21931	7.14361	15.13583
CEV								
$\beta=-0.5$	32.08100	5.90730	2.77681	16.74570	-33.42168	61.85193	9.31622	18.49531
$\beta=0$	1.78098	3.49476	1.71347	3.21738	5.73899	2.57007	7.14292	11.94602
$\beta=0.5$	1.37001	2.65260	1.29626	2.87468	5.20078	2.34471	5.40783	10.76252

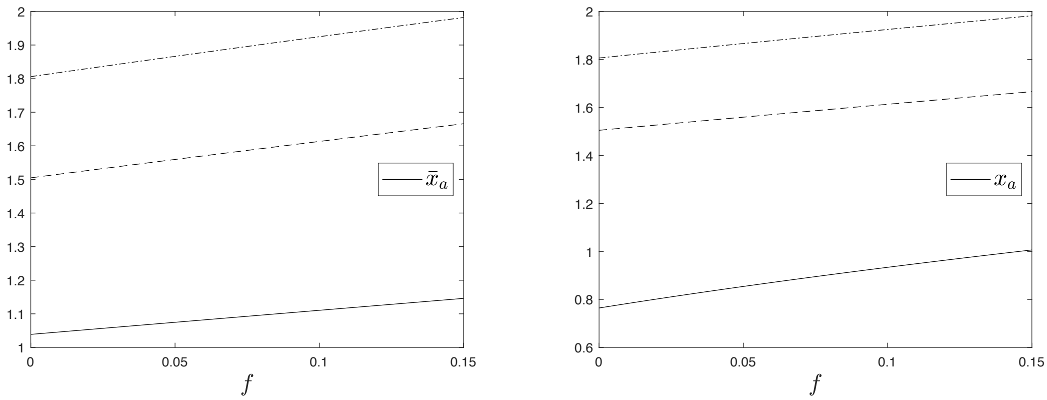

(a) (b)

Fig. 1.2 The Figure displays the abandonment boundaries of the rigid a and of the flexible b project as functions of the fixed cost f. Low (dashed-dotted lines), intermediate (dashed lines) and high (solid lines) volatility scenarios arise from the couples of parameters $(\kappa = 0.30, \sigma = 0.15), (\kappa = 0.15, \sigma = 0.20), (\kappa = 0.07, \sigma = 0.30)$, respectively.

1.4.6 Effect on the value of the firm

We concluded the analysis by measuring how much the value of the project change under alternative price models compared to the IGBM case. Table 1.10 shows that, in terms of direction, the CIR systematically underestimated the value of the project, in contrast to other processes that used to overestimate it. Most importantly, the magnitude of the error appears to be a monotonic increasing function of the degree of volatility in the market if the CIR or the CEV with positive β are considered. The latter, in particular, produced a comparatively highly unreliable estimate of project value in the high-variance scenario. Instead, we observed a sizeable impact of the intermediate volatility case on the error associated to the other CEV and GBM models. Noticeably, zero-β CEV is the one that better accommodates extreme situations of particularly low and high variance of the price process. It is interesting to notice that these last results are almost opposite to those obtained for the strategy of the firm. This fact points out the importance of clearly defining which goal - either valuation of determination of the optimal strategy - has to be pursued when developing a real option model. We did not record remarkably different responses from the rigid and flexible projects.

Table 1.10 This Table shows the variation in the value of an active project when it is computed under the assumption of price processes other than IGBM. The current price level is $x_0 = 2.00$ for all models and scenarios, the value of the active project under IGBM is reported in the first row and is given in monetary terms; variations are given in percentage values.

Setting	$\kappa = 0.30, \sigma = 0.15$		$\kappa = 0.15, \sigma = 0.20$		$\kappa = 0.07, \sigma = 0.30$	
Model	$\Delta V_1^r(x)$	$\Delta V_1^f(x)$	$\Delta V_1^r(x)$	$\Delta V_1^f(x)$	$\Delta V_1^r(x)$	$\Delta V_1^f(x)$
IGBM	10.01708	10.01708	10.58344	10.58344	13.80811	13.99732
CIR	-0.12128	-0.12128	-2.07846	-2.07846	-15.61073	-17.23415
GBM	33.93756	33.93756	37.30910	36.82929	31.38040	31.16004
CEV						
$\beta = -0.5$	23.84919	23.84919	23.93548	23.93547	15.45188	13.73292
$\beta = 0$	-0.17028	-0.17028	37.30910	36.82929	2.14315	0.45043
$\beta = 0.5$	6.19184	6.19184	21.09373	21.09373	50.18965	51.46859

1.5 Conclusion

Most of the real options models are built upon the assumption that the underlying source of uncertainty can be conveniently modelled as a geometric Brownian motion. Such choice is mainly due to the comparatively higher tractability of this model, which allows to get closed-form solution for a variety of managerial decision problems. However, some recent literature disputed this approach, claiming that it superficially ignores some typical features of economic variables, such as mean-reversion or the capability to catch leverage effects. Precisely the effect of mean-reversion has been the subject of careful analysis, which led to the exclusion of its negligibility due to the strong sensitivity of the probability of investment and of the market composition to changes in the reversion parameters.

In this article, we extended the comparison to several different models - the inhomogeneous geometric Brownian motion as a benchmark, then the geometric Brownian motion, the square root mean-reverting and the constant elasticity of variance processes - specifically addressing the issue of determining the optimal management strategy for a project that can be reversibly suspended or irreversibly abandoned. A strength of our study, compared to existing works, is the use of a benchmark model, which we consider representative of the market, and on which we not only calibrated the parameters of the alternative price processes, but we also based the study of the timing and the entry-and-exit probabilities of project real options. In doing this, our goal was to make the comparison as accurate as possible.

We focused on the strategic implications for the operating policy of a flexible and of a rigid project; in particular, for a long-term project, we concentrated on three aspects, namely the determination of the optimal switching price levels (*ex-ante* analysis), the probability of exercising real options within a short time, and the study of the timing at which decisions are made (*ex-post* analysis).

We showed that the differences in project operational strategy due to the adoption of models other than the benchmark are limited for intermediate environments where mean-reversion and variance components mutually offset. Indeed, when this is the case, the adoption of different models may lead to a sub-optimal *ex-ante* strategy, but we observed that *ex-post* effects exhibit small differences compared to the benchmark case, not significantly altering neither the short-term nor the long-term managerial plan of the project. In short, the error is comparatively low and can be neglected with minimal cost. The main implication of this results is the possibility to adopt models simpler to handle than those empirically observed, provided that they are supported by an adequate estimation of the parameters.

However, for extreme cases where the benchmark is meant to capture a highly turbulent market or, alternatively, a strongly mean-reverting one, the above conclusion is no longer valid. In particular, in this last case of the “risk discounting” (Sarkar, 2003) makes definitely not advisable to approximate strongly mean-reverting processes with models without this characteristic.

It is worth noting that such differences, likely, are not without consequences, as spill-over effects could arise either in the same market or in several related markets. Moreover, the analysis of the interplay between the aspects above and the uncertainty that pertains to some important macroeconomic variables, in the market or in several related markets. The analysis of these aspects, not touched on in this article, could be a promising starting point for further research.

Chapter 2

Operational flexibility and firm risk: a real options perspective

Abstract

This paper aims at providing a theoretical foundation to explain the relation between operational flexibility and the risk-return characteristics of firms equity. We focus on the implied volatility of option contracts and on CAPM's β as measures of risk and on the distribution of firms values and returns at future horizons. We obtain the optimal running policy of production firms characterised by different degrees of operational flexibility, represented as real options, and we get equity values at both current time and future maturities, stressing the path-dependent nature of the algorithm. As a main result, we document a remarkable reduction in the IV curve and in the cost of equity, together with an increase in equity values and returns due to the introduction of an exit option; interestingly, the value added by further optionalities is marginal. Additionally, we prove the stochastic nature of CAPM's β. Moreover, our results are robust to different price model specifications.

Keywords: Operational flexibility; implied volatility; cost of equity; uncertainty

2.1 Introduction

Amidst economic unpredictability, the capability of businesses to reshape their production lines with fluctuating market conditions becomes a pivotal corporate risk management tool (Triantis, 2000). In this work, we explored the relationship between this form of operational flexibility and the riskiness of companies. In particular, we investigated the impact of exit options on two key risk metrics: the implied volatility of equity option contracts and the systematic risk coefficient of the Capital Asset Pricing Model (Sharpe, 1964). Our main findings reveal a sizeable risk reduction related to the introduction of a single disinvestment opportunity with respect to the absence of optionalities, whilst the effect of adding further stopping options is marginal.

Most of the literature on operational flexibility aims at understanding the value that such a characteristic adds to projects, the role it plays in determining the optimal running policy of firms, and the interplay between these aspects and the enrichment of traditional models with more realistic features (Bengtsson, 1999; Carmona and Ludkovski, 2008; Fontes, 2008; Guthrie, 2009; Triantis and Hodder, 1990; Yash P. Gupta, 1989). On top of that, a flourishing stream of literature relates to industry specific applications; lots of examples can be found in the commodity sector, spanning from the agricultural field to the energy environment (Abadie, 2015; Bastian-Pinto and Brandão, 2016; Brennan and Schwartz, 1985; Geman, 2005; Liu et al., 2019).

In finance, attention was paid to the complex interplay between production flexibility and the capital structure of firms (Chod and Zhou, 2014; Goldstein et al., 2001; Hackbarth and Mauer, 2012; Leland, 1994; Lin, 2009; Mackay, 1999; Mauer and Ott, 1995; Mauer and Sarkar, 2005; Reinartz and Schmid, 2016). For example, Sarkar

(2014) used a contingent-claim model to study corporate structure choices when there is uncertainty over the selling price because of a stochastic demand curve. The work concluded that the presence of product-market flexibility is potentially crucial in determining optimal capital structure decisions, unless the firm is already operating at full capacity when financing choices are made. Also, Iancu et al. (2017) and Li et al. (2020) pointed out that flexibility might even induce the rise of inefficiencies, because the risk-shifting mechanism it generates promotes agency conflicts.

Gu et al. (2018) showed that in presence of contraction and expansion options, the risk level of a firm is subject to changes, being mitigated by the exercise of the first option and comparatively enhanced by that of the latter. Furthermore, they noted that the level of risk rises with operating leverage for firms lacking flexibility, whereas it diminishes for those characterised by flexibility.

El Ghoul et al. (2023) empirically investigated the relation between flexibility and the cost of equity, finding evidence of higher *risk premia* required by equity-holders of less flexible firm. As a sample, they collected corporate financial data from 1989 to 2018 for manufacturing firms from over 60 countries. Moreover, no significant changes occurred to their results neither when the measure of flexibility was adapted to account for potential changes of such metrics over time, nor when alternative measures of the cost of capital were considered. Their conclusion was thus consistent with the hypothesis of an inverse relation between the degree of flexibility and the riskiness of a company.

Considering the recognised influence of firms' characteristics on stock returns, the question arises as to whether business policies and structural features are also reflected in the price of financial options. Toft and Prucyk (1997) delved into the complexities of option pricing in leveraged firms, proposing a model that integrates leverage effects into the Black and Scholes (1973) framework. Geske et al. (2016) explored how a firm's capital structure influences the pricing of equity call options. They demonstrated that changes in leverage can significantly impact option prices due to shifts in the volatility of firm's assets. Through mathematical modelling, they showed that the relationship between leverage and option prices is nonlinear and can vary depending on factors such as the firm's risk level and market conditions. Recently, Chen et al. (2023) investigated how firm fundamentals influence the implied volatility (IV) in the option market, finding a remarkable effect of factors like leverage and firm size on shaping the IV curve. Specifically, they observed that firms with riskier financial profiles exhibit, on average, higher implied volatility, while those with higher liquidity and larger size may have a flatter IV curve.

Closer to our study, Gamba and Saretto (2022) related equity option price formation to a structural model for a production economy where contraction and expansion options are available. They observed that option prices resulted endogenously from the running policy that managers made optimally to maximise firm value. It is particularly relevant to notice that such mechanism empirically fits market data, stressing the goodness of their approach and how promising this line of research is to understand the relations between the productive economy and financial markets.

In this work, we focused on the relation between operational flexibility and firms risk-return characteristics as measured by options contracts' implied volatility and by the systematic risk - "beta" - coefficient. We first build an artificial economy with three firms, of which one without real options and the others provided the possibility to leave the market and temporarily suspend production activity, according to an increasing degree of operational flexibility in light of Brennan and Schwartz (1985), Dixit and Pindyck (1994) and Hackbarth and Johnson (2015).

We conducted our analysis as an inside-out exploration. First, we focused on the effects of operational flexibility on firm value and its empirical distribution to different future horizons; we established that introducing a single option is much more relevant than increasing the level of flexibility when some optionality is already in place. In detail, the reduction of variability in cash-flows and in the corresponding equity returns associated with the inclusion of options has been identified as the cause of a significant impact on the implied volatility curve. Furthermore, making reference to the CAPM, we derived the relation between the "beta" of the underlying price of firms' output and that of firms' equity. We emphasised that this last quantity is itself stochastic regardless the presence of real options: in fact, it directly depends on the current level of the production output price. Most importantly, when real options are available, it takes values strictly contingent to the state of the firm. Further, we carried our analysis according to different specifications for the output price dynamics, thus enhancing the robustness of our findings. We believe that our investigation could provide a fruitful starting point for future empirical works aimed at understanding the complex relations between real options and asset prices.

The remainder of the paper is as follows: in the next Section we present the basic setting and the assumptions behind the model; Section 2.3 numerically illustrates our results, presenting, separately, the effect of flexibility on the firms valuation, the impact on the returns distribution and on options' implied volatility, and the link with equity *risk premia*. Last, Section 2.4 concludes.

2.2 Basic setting and assumptions

We consider an economy within which we take the position of three manufacturing firms that face uncertainty over the selling price of their output. Firms are price-taker and two of them have some flexibility in the form of real options. Our goal is to investigate the effect of optionalitites on firms' risk-return profile. In the next paragraphs we provide details of the market hypotheses and model construction.

2.2.1 The market model

Our first assumption relates to the market structure, which we assume to be perfectly competitive. When this is the case, market participants are price-taker, that is, they have no power on setting the selling price, which results from market equilibrium. Consequently, market price comes as a primary source of uncertainty to drive firms policies. In this work, we assume that the market price $x := \{x_t\}_{t\geq 0}$ at which the product is sold is described by an SDE of the kind

$$\mathrm{d}x_t = a(x_t)\,\mathrm{d}t + b(x_t)\,\mathrm{d}W_t. \tag{2.1}$$

for a given filtered probability space $(\Omega, \mathcal{F}, \mathbb{F} = \{\mathcal{F}_t\}_{t\geq 0}, \mathbb{P})$; W is a Wiener process and the initial condition $x_0 \in \mathbb{R}^+$ is set. Furthermore, we assume that operations take place over a virtually infinite horizon. Also, firms cash-flows depend on production variable and fixed costs, denoted by v and f, respectively. For notation compactness, we define $c := v + f$. Differently from the output price, production costs are assumed to be constant throughout time.

Firms' characteristics

We postulate the existence of three kinds of equity-financed firms within the market. A first firm is committed to continuously producing whatever it happens on the market; we refer to this entity as to the "rigid" firm. The second company holds the real option to permanently exit the market in return for a scrap value from assets liquidation when prices fall below a certain threshold; this is what we call "semi-rigid". Last, in light of Dixit and Pindyck (1994), the third business has both the options to irreversibly and reversibly exit; this firm is called "flexible" and it is characterised by the payment of a lump switching, non-negative, cost s whenever production is either stopped or resumed. Importantly, fixed costs f continue to be paid also when production is suspended. Moreover, real options are immediately exercised when the output price hits some specific thresholds. If only abandonment is available, then there is a unique boundary called $\bar{x}_a$. Instead, in the case of the "flexible" firm, three boundaries exist: x_s triggers suspension, x_r determines resumption, and x_a leads to abandonment. The values of such thresholds are determined endogenously by each firm. In light of Dixit and Pindyck (1994), getting the optimal options' boundaries entails the solution of a system of value-matching and smooth-pasting conditions[1] that have to be imposed over the value function of the firm; in particular, for the "flexible" firm, one has

$$E_C(x_j) = E_A(x_j) - s \quad j \in \{s, r, a\} \tag{2.2}$$

and

$$E'_C(x_j) = E'_A(x_j) \quad j \in \{s, r, a\} \tag{2.3}$$

where $E_C(x)$ (resp. $E_A(x)$) is the value of the firm in the current (resp. alternative) state. Specifically, the current state of production is either "active" or "suspended" and both states also represent mutual alternatives, while the "abandoned" state, by virtue of its irreversibility, comes only as an alternative. The reasoning behind the "semi-rigid" is conceptually the same, but the current state can only be "active" and abandonment is the unique alternative available.

Figure 2.1 depicts the above framework. In the top-left panel, we plotted a simulated path for the price process x over a period of 30 years and we assume this was the market

[1]Being well-known in the optimal stopping literature particularly because of its applications to American options (McKean Jr., 1965; Merton, 1973; Samuelson, 1965), the methodology we adopt is extensively used in the real options literature to find the optimal boundaries that trigger the switching between mutually alternative operational states. See Dixit and Pindyck (1994); Sødal (1998) for a detailed explanation.

situation faced by firms. On the same graph, we reported the optimal suspension, resumption and abandonment barriers of the flexible and semi-rigid firms and we noticed that these are crossed several times by the price process. Based on this picture, we obtained the cash-flows for each kind of firm and we plotted the results in the remaining panels.

The amount and the size of losses incurred by the rigid firm (top-right panel) are remarkable; moreover, we observe that the company generates losses for about the half of the simulation period and no recoveries occur in the last 18 years, during which they become even heavier.

By contrast, the cash-flows pattern of the semi-rigid firm (bottom-left panel) stresses the exercise of the abandonment option, which occurs as prices fall below $\bar{x}_a$: in correspondence of this point, a unique positive cash-flow (i. e. the scrap value) is gained and no further cash-flows are generated since then on.

Last, the options to suspend and restart allow the flexible firm (bottom-right panel) to mitigate losses in all its life stages. Importantly, by containing the amount of negative earnings, this company is able to defer its abandonment, which in fact occurs later in time compared to the semi-rigid firm as a consequence of a comparatively lower abandonment threshold x_a.

Valuation of firms equity

The equity value of each firm can be decomposed into two components, namely the expected discounted present value (DPV) of future cash-flows, as per the standard DCF analysis, and the value of real options. Also, from a differential calculus perspective, the value of equity can be expressed as the solution of a second order ODE, with the value of the options component, denoted by $h(x_t)$, as general solution and the DPV

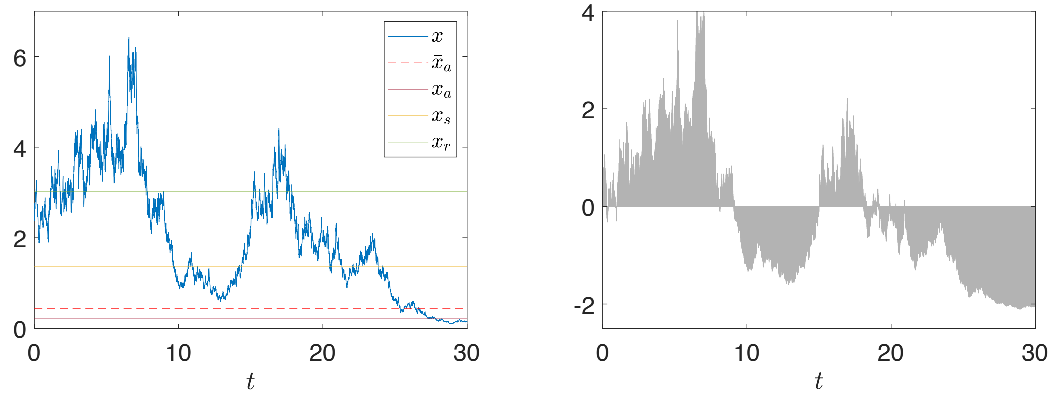

(a) A simulated trajectory for x (b) Cash-flows - rigid firm

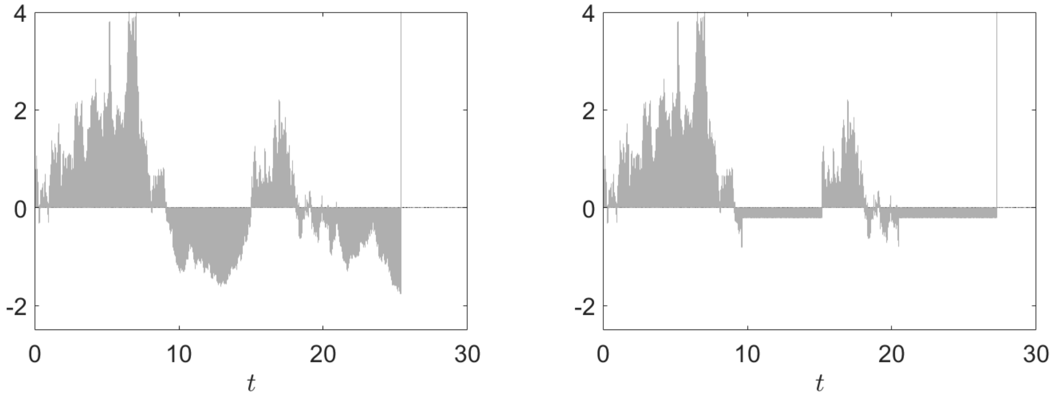

(c) Cash-flows - semi-rigid firm (d) Cash-flows - flexible firm

Fig. 2.1 The Figure shows the cash-flows of the 3 different companies (rigid, semi-rigid and flexible in panel (b), (c) and (d), respectively) given by a simulated trajectory of the underlying price x (a) and by the optimal suspension (x_s), resumption (x_r) and abandonment (x_a : flexible; $\bar{x}_a$: semi-rigid) barriers.

part as particular solution, i. e. we can write

$$E(x_t) = \mathrm{DPV}(x_t) + h(x_t)$$

regardless the kind of firm.

By definition, the value of the DPV component is calculated as

$$\mathrm{DPV}(x_t) = \mathbb{E}_t\left[\int_t^{\infty}(x_u - c)e^{-\delta u}\mathrm{d}u\right]$$

given a discount rate δ. In practice, given that cash-flows are discounted at the same rate for all the kinds of firms included in our analysis, we will adopt the risk-free rate r as discount rate without loss, i. e. we set $\delta \equiv r$. We incorporate Merton's ICAPM (Merton, 1973) into the model; in doing this, we define $\tilde{a}(x) := a(x) - \lambda\rho\sigma x$, with $\lambda = \frac{\mathbb{E}[r_m]-r}{\sigma(r_m)}$ being the market price of risk and $\rho \in [-1,1]$ representing the correlation of changes in x with the market portfolio. Then, the value of the option component solves a differential equation of the kind

$$\frac{b^2(x)}{2}h''(x) + \tilde{a}(x)h'(x) - rh(x) = 0, \tag{2.4}$$

whose general solution takes the form

$$h(x) = pH_1(x,\Theta_1) + qH_2(x,\Theta_2)$$

where $H_1(x,\Theta_1)$ and $H_2(x,\Theta_2)$ are an increasing and a decreasing function of x and of the set of parameters Θ_1 and Θ_2, respectively. Moreover, they constitute linearly independent solutions of (2.4).

We can exploit the above results to provide a general expression for the equity value of the firm, which is

$$E(x_t) = \mathbb{E}_t\left[\int_t^{\infty}(x_u - c)e^{-ru}\mathrm{d}u\right] + pH_1(x,\Theta_1) + qH_2(x,\Theta_2). \tag{2.5}$$

Notice that $p, q \in \mathbb{R}$ are constant parameters that, in general, need to be determined by boundary conditions. It is crucial to note that boundary conditions are firm specific and state-contingent; for the semi-rigid and the flexible firms, they coincide with the value-matching conditions in (2.2). Furthermore, the rigid firm holds no options, hence its equity value constitutes a special case for which $p = q = 0$. For this reason, the equity value of the rigid firm at time t, denoted by $E^R(x_t)$, is simply given by

$$E^R(x_t) = \mathbb{E}_t \left[\int_t^\infty (x_u - c) e^{-ru} \mathrm{d}u \right].$$

When production takes place and a stopping option is available, it should be intuitively clear that if earnings are particularly high no company would consider it profitable to stop productive activity. Consequently, both the semi-rigid and the flexible active firm read the condition

$$\lim_{x \to \infty} h(x) = 0,$$

which imposes the coefficient of the increasing function in (2.2.1) to be equal to zero. Given this framework, we can now provide the expressions for the equity value of the semi-rigid and of the flexible firm, denoted by $E^{SR}(x_t)$ and $E^F(x_t)$, respectively; these are

$$E^{SR}(x_t) = \begin{cases} \mathbb{E}_t \left[\int_t^\infty (x_u - c) e^{-ru} \mathrm{d}u \right] + d_2 H_2(x, \Theta_2) & \text{if active} \\ \text{Scrap Value} & \text{if abandoned} \end{cases}$$

and

$$E^F(x_t) = \begin{cases} \mathbb{E}_t \left[\int_t^\infty (x_u - c) e^{-ru} \mathrm{d}u \right] + q_2 H_2(x, \Theta_2) & \text{if active} \\ -\dfrac{f}{r} + p_1 H_1(x, \Theta_1) + p_2 H_2(x, \Theta_2) & \text{if suspended} \\ \text{Scrap Value} & \text{if abandoned.} \end{cases}$$

Coefficients $d_2, q_2, p_1, p_2 \in \mathbb{R}$ have the same meaning as p and q in (2.5) and replaced them in terms of notation to emphasise that their numerically differ across firms and states of production.

Last, it is worth to mention that, in all cases when the firm is active, the actual form of the DPV component is conditioned to the dynamics of x. Instead, the same computation is trivial if the flexible firm is in the suspended state, as the results reduces to the present value of the perpetual stream of flows $-f$, i. e. to $-\frac{f}{r}$.

2.2.2 Flexibility and options' implied volatility

Our first goal is to understand whether the value of flexibility is reflected in financial options' prices. In doing this, we take the perspective of a given firm and we assume that European call option contracts have been written on its equity value; for illustrative purposes, we consider three option maturities, namely 3, 6 and 12 months. The main challenge in pricing these options, unless the fully rigid firm is considered, is to determine the state of production at maturity. Indeed, the equity value will depend on the state of the firm at the option maturity. We also have to consider the probability that the firm has abandoned. For this reason, flexibility introduces some path-dependency that must be recognised in pricing the apparently standard plain vanilla European option. In practice, we need to know the value of firm's underlying, i. e. x, and to put it in relation with the exercise boundaries of the real options retained by the company. Also, it is crucial to keep track of the entire trajectory followed by x in the interval between the time of assessment t_0 and the reference maturity. In fact, this recording allows us to identify at every moment in which state of production the company is in and, consequently, to determine its correct value. In the following, we detail the procedure we adopted.

Equity valuation and option pricing

Consider a time interval $[t_0, T]$, where T denotes the maturity of the option contract and $t_0 = 0$ is the current time. At t_0 real options' boundaries, the current value x_0 of the output price and, so, the state of the firm are known: in practice, we assume that all the firms are currently producing; for this hypothesis to be consistent, we set x_0 to be higher than the suspension threshold. Further, we recall that the payoff at maturity is

$$C_T = (x_T - K)^+,$$

where K is the strike of the option, and that the option price is obtained by calculating

$$c_0 = e^{-rT}\mathbb{E}_0[(x_T - K)^+]. \tag{2.6}$$

In practice, we need to make use of Monte Carlo simulation techniques. We simulate M trajectories for the underlying price process at dates $t \in (t_0, T]$ and we superimpose them to real options' boundaries. Let $x_t^{(j)}$ be the value of x_t on trajectory $j, j \in \{1, 2, \ldots, M\}$; getting the value of the semi-rigid firm only requires to verify that $x_t^{(j)} > \bar{x_a}$ and no abandonment occurred up to time t. If abandonment occurs at time $t_k \in (t_0, T), k \geq 1$, then a single cash-flow, stemming from the liquidation of firm's assets, is obtained immediately; from that point forward, there will be no other flows generated. Following the path of the flexible firm is less immediate: indeed, production is active at time t_k if it was active also at t_{k-1} and $x_{t_k}^{(j)} > x_s$ (continuation) or if it was suspended at t_{k-1} but $x_{t_k}^{(j)} \geq x_r$ (switching). Similarly, production is suspended if it was active at t_{k-1} but $x_{t_k}^{(j)} \leq x_s$ (switching) or if it was suspended at t_{k-1} and $x_a < x_{t_k}^{(j)} < x_r$ (continuation). The implication of abandonment, i. e. of $x_{t_k}^{(j)}$ falling below x_a is the same as in the semi-rigid firm. In other words, the step-by-step simulation of the equity price must account for the current state of the firm (active, suspended, or abandoned).

Finally, at T we are able to observe the equity value of the firm for each trajectory, namely $E(x_T^{(j)})$. A preliminary analysis allows us to appreciate the impact of increasing operational flexibility on the equity value of the firm as well as on its returns distribution.

Most importantly, known the strike price K, we can calculate payoff of a call option contract for each j-th path, i. e.

$$C_T^{(j)}(x_T^{(j)}, K) = \left(x_T^{(j)} - K\right)^+$$

and the we estimate the related option price averaging across the M paths

$$\hat{c}_0(T, K) = e^{-rT} \frac{1}{M} \sum_{j=1}^{M} \left(x_T^{(j)} - K\right)^+ .$$

Last, implied volatilities are obtained from Black-Scholes (1973); specifically, one gets the volatility $\sigma(K, T)$, which, if substituted into the Black-Scholes formula

$$\mathrm{BS}(K, T, \sigma) = x_0 \Phi(d_1) - K e^{-rT_i} \Phi(d_2),$$

where

$$\begin{aligned} d_1 &= \frac{\ln(x_0/K) + \left(r + \frac{\sigma^2}{2}\right) T}{\sigma\sqrt{T}} \\ d_2 &= d_1 - \sigma\sqrt{T}, \end{aligned}$$

returns the theoretical price $\hat{c}_0(K, T)$ given the maturity T.

2.2.3 Flexibility and the cost of equity

Consider the price of a certain good following (2.1). Further, consider the equity value of a firm whose profits depend on the underlying x. Then, by Ito's Lemma,

$$\mathrm{d}E = \left[\frac{b^2(x)}{2} E''(x) + \tilde{a}(x) E'(x)\right] \mathrm{d}t + b(x) E'(x) \mathrm{d}W. \tag{2.7}$$

Let r_x and r_E be the return on x and on E within the period dt given the current levels of the two processes. Then, CAPM's equation allows to express the cost of equity for a generic i-th asset as

$$\mathbb{E}[r_i] = r + \beta_i \left(\mathbb{E}[r_m] - r\right) \tag{2.8}$$

where $(\mathbb{E}[r_m] - r)$ is the expected excess return of the market portfolio with respect to r and the coefficient $\beta_i := \frac{Cov(r_i, r_m)}{Var(r_m)}$ is a measure of systematic risk. Assuming the same reference market portfolio for both the value of equity and its underlying, it can be noticed that the quantity driving their expected excess returns over r is the coefficient β_i. Let us call β_x and β_E, respectively, the coefficients for the ouput price and for the equity value of the firm. Then, it is easy to get the link between them. Recalling that

$$\begin{aligned}
\beta x :&= \frac{\mathrm{Cov}\left(r_x, r_m\right)}{\mathrm{Var}\left(r_m\right)} \\
&= \frac{\mathrm{Cov}\left(\frac{\mathrm{d}x_t}{x_t}, r_m\right)}{\mathrm{Var}\left(r_m\right)} \\
&= \frac{\mathrm{Cov}\left(\frac{b(x_t)\mathrm{d}W_t}{x_t}, r_m\right)}{\mathrm{Var}\left(r_m\right)} \\
&= \frac{\mathrm{Cov}\left(b(x_t)\mathrm{d}W_t, r_m\right)}{x_t \, \mathrm{Var}\left(r_m\right)}
\end{aligned} \tag{2.9}$$

we have

$$
\begin{aligned}
\beta_E\left(x_t\right) &:= \frac{\operatorname{Cov}\left(r_E, r_m\right)}{\operatorname{Var}\left(r_m\right)} \\
&= \frac{\operatorname{Cov}\left(\frac{\mathrm{d}E(x_t)}{E(x_t)}, r_m\right)}{\operatorname{Var}\left(r_m\right)} \\
&= \frac{\operatorname{Cov}\left(\frac{b(x_t)E'(x_t)\mathrm{d}W_t}{E(x_t)}, r_m\right)}{\operatorname{Var}\left(r_m\right)} \\
&= \frac{\frac{E'(x_t)}{E(x_t)} \operatorname{Cov}\left(b\left(x_t\right)\mathrm{d}W_t, r_m\right)}{\operatorname{Var}\left(r_m\right)} \\
&= x_t \frac{E'\left(x_t\right)}{E\left(x_t\right)} \beta_x .
\end{aligned} \tag{2.10}
$$

Notice that, in (2.9) and in (2.10), $\mathrm{d}x_t$ and $\mathrm{d}E(x_t)$ have been replaced with their own expressions as per equations (2.1) and (2.7), respectively, from which we considered only the non-zero term. Further, to ease notation, we define $\beta_E := \beta_E(x_t)$. We exploit the relation in (2.10) to observe the variation of the ratio $\frac{\beta_E}{\beta_x}$ as a function of the degree of flexibility of the firm, remembering that firms' equity value is also a function of the switching cost s. Specifically, we perform a sensitivity analysis by computing the values of $E(x_t)$ and $E'(x_t)$ at different levels of the switching cost and we next scale-up the result obtained by x_t.

Notice that even though the value of β_x is constant over time, that of β_E is stochastic due to the dependence on x_t, which, in fact, varies stochastically.

Analysis under the GBM case

By way of example, we derive the relations of the previous paragraphs in the case of the geometric Brownian motion, which is distinguished by the particular tractability. In particular, we have

$$
\mathrm{d}x_t = \mu x_t \mathrm{d}t + \sigma x_t \mathrm{d}W_t
$$

that leads to

$$E(x_t) = Ax_t^{\gamma_1} + Bx_t^{\gamma_2} + \mathrm{cf}(x_t),$$
$$E'(x_t) = \gamma_1 Ax_t^{\gamma_1 - 1} + \gamma_2 Bx_t^{\gamma_2 - 1} + \mathrm{cf}'(x_t)$$

and

$$\beta_E = x_t \beta_x \frac{\gamma_1 Ax_t^{\gamma_1 - 1} + \gamma_2 Bx_t^{\gamma_2 - 1} + \mathrm{cf}'(x_t)}{Ax_t^{\gamma_1} + Bx_t^{\gamma_2} + \mathrm{cf}(x_t)}$$

where $A, B \in \mathbb{R}$ are constant coefficients to be determined by boundary conditions as in (2.2) and will be different according to the kind (i. e. rigid, semi-rigid or flexible) of the firm; $\mathrm{cf}(x_t) = \frac{x_t}{r - \mu + \lambda\rho\sigma} - \frac{c}{r}$; $\gamma_{1,2}, \gamma_1 > 1, \gamma_2 < 0$, are the roots of the characteristic equation $\frac{\sigma^2}{2}\gamma(\gamma - 1) + (r - \mu + \lambda\rho\sigma)\gamma - r = 0$.

Furthermore, the simplest case of a rigid firm is particularly suitable to illustrate what happens to β_E. We recall that the equity value of the rigid firm equals $\mathrm{cf}(x_t)$, hence, under GBM,

$$E(x_t) = \frac{x_t}{r - \mu + \lambda\rho\sigma} - \frac{c}{r},$$
$$E'(x_t) = \frac{1}{r - \mu + \lambda\rho\sigma}.$$

Consequently,

$$\beta_E = \frac{rx_t}{rx_t + c(\mu - r - \lambda\rho\sigma)}\beta_x. \tag{2.11}$$

In Figure 2.2 we illustrate how the empirical distribution of β_E might look like. After simulating 20,000 paths for the output price x_t and plotting its empirical distribution (panel a), we used the values of x_t to recover the corresponding β_E following (2.11) and choosing $\beta_x = 1$. While the first one clearly matches a lognormal distribution by definition of GBM, the latter does not. Moreover, we performed the same steps using different GBM parameters ($\mu = 0.15, \sigma = 0.55$ in panel b and $\mu = 0.30, \sigma = 0.35$ in panel c), finding significantly different shapes. Additionally, we explored the relation between β_x and β_E for both the couples of GBM parameters as well as for the couples ($\mu = 0.15, \sigma = 0.35$) and ($\mu = 0.30, \sigma = 0.55$) to visualise differences entirely due to changes in μ or in σ. Interestingly, β_E converges to β_x in all cases; nevertheless, parameters determine whether this happens from the above or from the below (panel d). It is worth to mention that, given μ, lower volatility levels make the firm comparatively less risky; on the contrary, lower levels of the drift parameter increase β_E for a given value of σ. Overall, these results are proving that not only β_E is stochastic, but that it is also strictly contingent to model parameters.

2.3 Numerical illustration

In this section, we show the results of some numerical experiments we run to understand how operational flexibility relates to the value and riskiness of firms. To incorporate more possibilities in the analysis, we often made use of three specifications for the price process given in (2.1): we assumed this takes the form of a geometric Brownian motion (GBM), of an inhomogeneous geometric Brownian motion (IGBM) and of a square root mean-reverting process (CIR), whose SDEs are as follows:

$$\mathrm{d}x = \mu x \mathrm{d}t + \sigma x \mathrm{d}W \qquad \text{(GBM)}$$

$$\mathrm{d}x = \kappa(\theta - x)\mathrm{d}t + \sigma x \mathrm{d}W \qquad \text{(IGBM)}$$

$$\mathrm{d}x = \kappa(\theta - x)\mathrm{d}t + \sigma \sqrt{x} \mathrm{d}W \qquad \text{(CIR).}$$

These processes have been chosen as they are widely used in computational finance to describe the dynamics of many variables, such as the prices of equity and commodities or interest rates fluctuations (Bhattacharya, 1978; Brennan and Schwartz, 1979; Brigo

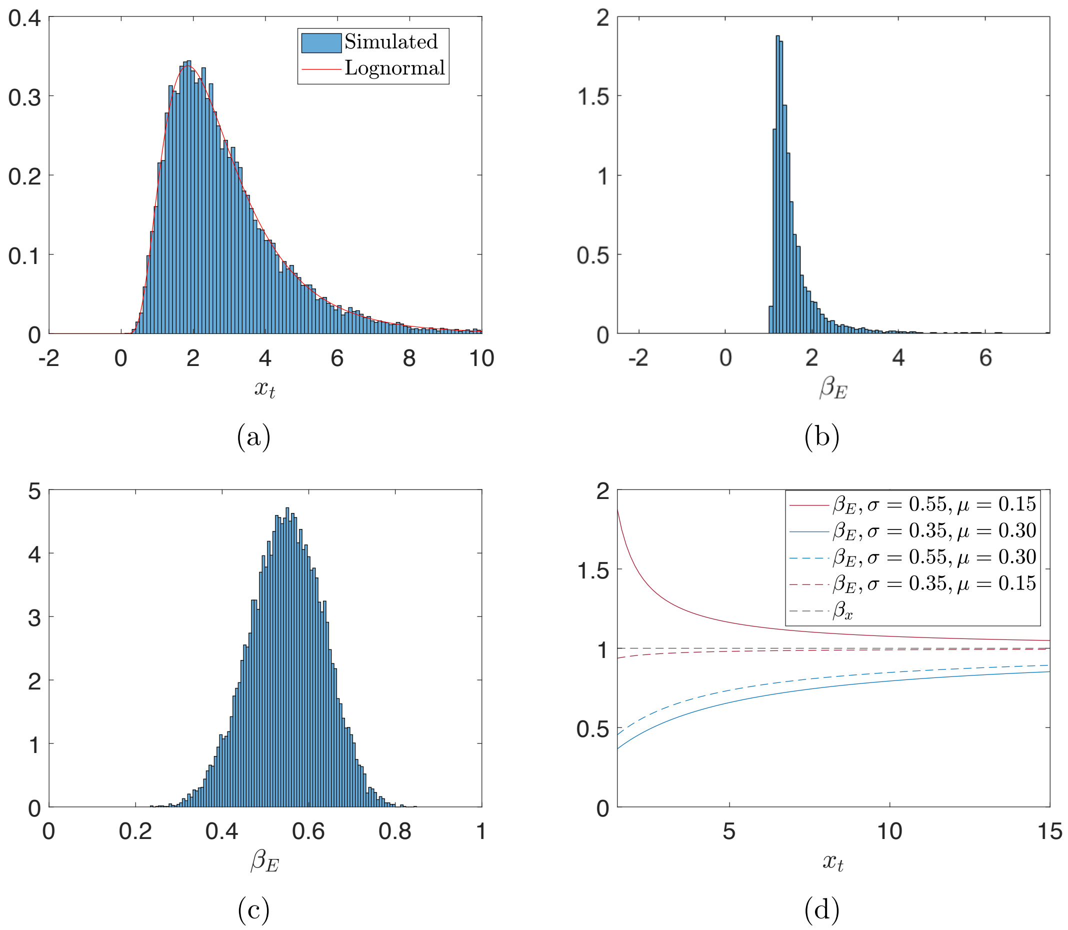

Fig. 2.2 The Figure shows the distribution of the output price x_t when it follows a GBM with $\mu = 0.15, \sigma = 0.55$ (panel a) together with that of the coefficient β_E calculated from the same values of x_t (panel b). Panel c displays the distribution of β_E when the GBM parameters are changed to $\mu = 0.30, \sigma = 0.35$. Last, panel d shows the relationship between β_x and β_E as a function of x_t for specified GBM parameters.

and Mercurio, 2007; Hull, 2018). Our aim was to exclusively compare different levels of flexibility within each model, hence we disregarded cross-comparisons between them. For this reason, we chose an arbitrary main set of parameters, given in Table 2.1. For simulations, we resorted to standard methodologies, looking for a compromise between accuracy and computational time: for GBM, we made use of simulated increments of

Table 2.1 The table collects the parameters used in the computation of firms' equity values and subsequent option contracts' prices.

Notation	GBM	IGBM	CIR	Description
μ	0.01	-	-	Drift parameter
σ	0.35	0.55	0.55	Volatility parameter
κ	-	0.02	0.02	Speed of mean-reversion
θ	-	2	2	Long-run price level
r	0.06	0.06	0.06	Risk-less rate of return
x_0	2.50	2.50	2.50	Current price
s	0	0	0	Switching cost
v	1	1	1	Production cost
f	0.05	0.05	0.05	Fixed cost
SV	9	9	9	Scrap value from assets liquidation
λ	0.20	0.20	0.20	Market price of risk
ρ	0.20	0.20	0.20	Correlation of changes in x with the market portfolio

ABM and then we took the exponential; we adopted the Euler–Maruyama method for IGBM and the Gaussian approximation for CIR[2].

We divided our study in three parts: following the procedure described in section 2.2.2, we first focused on the implications of flexibility for valuation purposes by investigating how firms' equity value at current and future times is affected by the introduction of flexibility; we put this in relation with the time spent by flexible firms in each production state. Second, we studied subsequent implications for the equity returns of firms and, moreover, for the implied volatility embedded in financial option contracts. Third and last, we turned our attention to the impact of flexibility on the cost of equity, focusing on the effect that abandonment, suspension and resumption options have on CAPM's β of equity.

2.3.1 Flexibility and equity value: a primer

The most intuitive impact of operational flexibility is on equity value. Theory suggests that companies with greater operational flexibility have greater value, other things

[2]See Tubikanec et al. (2022) and Ballotta and Fusai (2018) for a detailed discussion on simulation methods for IGBM and CIR, respectively.

being equal. The reasoning behind this statement is easily understood from what is seen in equations (2.2.1)-(2.2.1). Indeed, there are two channels of transmission: on the one hand, the increase in the value of the optional component at the same cash-flow; on the other hand, a change in cash-flows themselves, aimed at reducing the negative amounts. Our findings are consistent with this argument and, most interestingly, highlight that introducing some form of flexibility over its total absence returns a more pronounced effect, compared to adding further options, in terms of both point valuation at t_0 and distributional features at future horizons. This is clearly visible in Table 2.2, where we reported the current equity values for the three firms and estimates for such quantities at short and mid-term maturities, and in Figure 2.3, in which we showed how the distribution of equity values changes with longer horizons.

The growth over time of the variability of the underlying increases the probability of exercising any available options and determines a shift to the right of the distribution of the equity value, in contrast to the shift to the left of the equity value of the rigid company, which faces extreme values of losses and profits with increasing probability. In particular, the value of the semi-rigid company and that of the flexible one tend to concentrate around the scrap-value to indicate the permanent abandonment of the productive activity. The difference, even if minimal, observed between these two types of company is entirely explained by the presence of the suspension option, which mitigates the effect of the uncertainty delaying the abandonment of the market. These considerations are consistent with the increase in the time spent by the flexible firm in the state of suspension as the reference time horizon increases (Figure 2.4). Furthermore, they are valid regardless of the model that describes the dynamics of the underlying. However, it is important to stress the fact that our findings are contingent to parameters' values; for example, different operational costs would change the level of the optimal switching thresholds and this fact would ultimately affect both the probability of exercising the available real options and the time spent within each operational cost. The same argument holds for different price model parameters.

Table 2.2 The Table displays the current equity value of the firm - $E_0(x)$ - as well as an estimate for such quantity at given maturities - $\hat{E}_{T_i}(x)$, for $T_i = 3$, 6, 12 months and 10 years - with 95% confidence intervals. Each panel refers to a given model for the underlying price process, as specified.

Panel **(a)**: GBM

	$E_0(x)$	$\hat{E}_{3m}(x)$	$\hat{E}_{6m}(x)$	$\hat{E}_{12m}(x)$	$\hat{E}_{10y}(x)$
Rigid	21.5625	21.6546 ± 0.0484	21.7303 ± 0.0691	21.7287 ± 0.0997	24.9272 ± 0.4634
Semi-rigid	28.9350	29.1221 ± 0.0431	29.2961 ± 0.0616	29.5151 ± 0.0892	35.8642 ± 0.4409
Flexible	29.0569	29.2456± 0.0430	29.4213 ± 0.0615	29.6438 ± 0.0890	36.1430 ± 0.4405

Panel **(b)**: IGBM

	$E_0(x)$	$\hat{E}_{3m}(x)$	$\hat{E}_{6m}(x)$	$\hat{E}_{12m}(x)$	$\hat{E}_{10y}(x)$
Rigid	13.5458	13.4778 ± 0.0478	13.5268 ± 0.0696	13.6080 ± 0.1032	12.6975 ± 0.6216
Semi-rigid	23.0751	23.1395 ± 0.0430	23.3138 ± 0.0629	23.6544 ± 0.0940	25.0072 ± 0.6107
Flexible	23.3331	23.4011 ± 0.0428	23.5786 ± 0.0627	23.9234 ± 0.0937	25.6196 ± 0.6111

Panel **(c)**: CIR

	$E_0(x)$	$\hat{E}_{3m}(x)$	$\hat{E}_{6m}(x)$	$\hat{E}_{12m}(x)$	$\hat{E}_{10y}(x)$
Rigid	13.5458	13.5085 ± 0.0302	13.5124 ± 0.0431	13.5204 ± 0.0601	12.6767 ± 0.1715
Semi-rigid	21.0176	21.0719 ± 0.0246	21.1636 ± 0.0351	21.3428 ± 0.0488	22.6651 ± 0.1419
Flexible	21.2081	21.2673 ± 0.0244	21.3613 ± 0.0349	21.5443 ± 0.0486	23.0733 ± 0.1413

Digging deeper into GBM, we analysed the impact of different values of the drift parameter μ. The increased volatility of the underlying process linked to higher values of μ favours the reduction of the abandonment barrier; this fact promotes a higher percentage of time spent in the state of suspension by the flexible company, given a reference time horizon (Figure 2.5). At the same time, a minimal reduction in the value of the suspension option is accompanied by a significant increase in the present value of cash flows, with a net effect showing a remarkable growth in the expected equity value (Figure 2.6). In particular, comparatively higher values of μ lead the output price to exhibit a positive trend that favours the generation of profits through

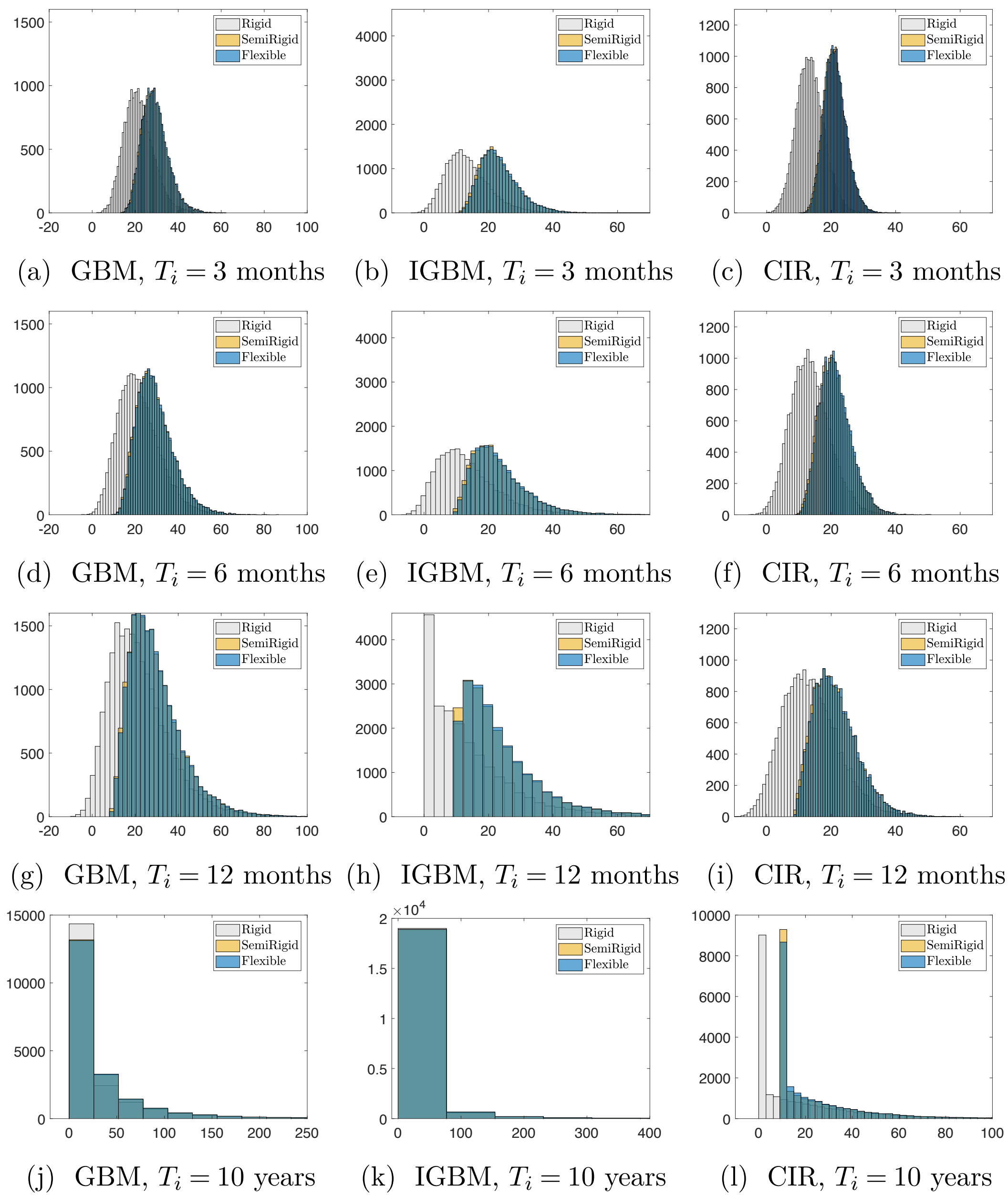

(a) GBM, $T_i = 3$ months (b) IGBM, $T_i = 3$ months (c) CIR, $T_i = 3$ months

(d) GBM, $T_i = 6$ months (e) IGBM, $T_i = 6$ months (f) CIR, $T_i = 6$ months

(g) GBM, $T_i = 12$ months (h) IGBM, $T_i = 12$ months (i) CIR, $T_i = 12$ months

(j) GBM, $T_i = 10$ years (k) IGBM, $T_i = 10$ years (l) CIR, $T_i = 10$ years

Fig. 2.3 The Figure shows the distribution of firms' equity values at four different time horizons - namely 3, 6, 12 months and 10 years - labelled by T_i. For the flexible firm, switching costs are set to 0. All the other model parameters are as in Table 2.1 and the models for the underlying output price x are GBM, IGBM and CIR.

productive activity. It is therefore reasonable to observe fewer differences between the three types of company, depending on the reduced use of any real option.

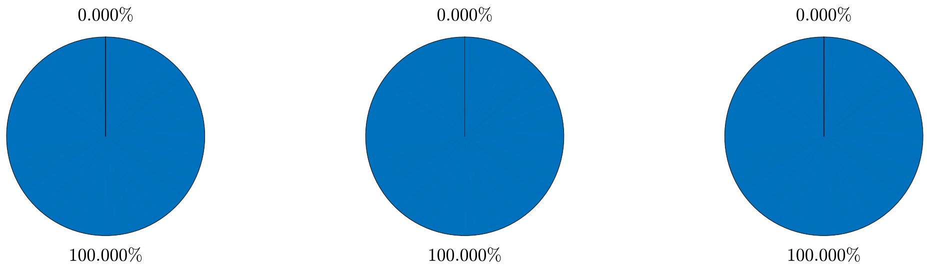

(a) GBM, $T_i = 3$ months (b) IGBM, $T_i = 3$ months (c) CIR, $T_i = 3$ months

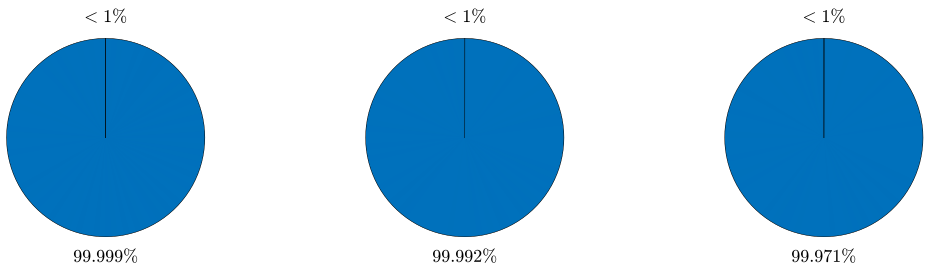

(d) GBM, $T_i = 6$ months (e) IGBM, $T_i = 6$ months (f) CIR, $T_i = 6$ months

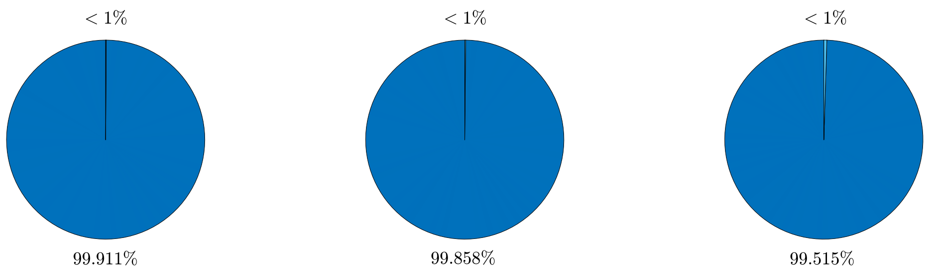

(g) GBM, $T_i = 12$ months (h) IGBM, $T_i = 12$ months (i) CIR, $T_i = 12$ months

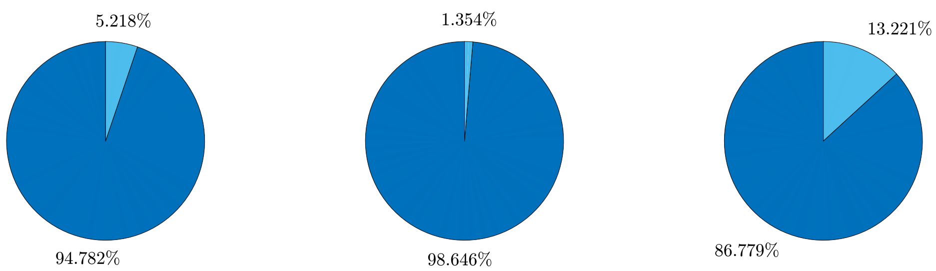

(j) GBM, $T_i = 10$ years (k) IGBM, $T_i = 10$ years (l) CIR, $T_i = 10$ years

Fig. 2.4 The Figure graphically represents the percentage amount of time spent in the active or suspended state of production out of specified horizons T_i. For the flexible firm, switching costs are set to 0. All the other model parameters are as in Table 2.1 and the models for the underlying output price x are GBM, IGBM and CIR.

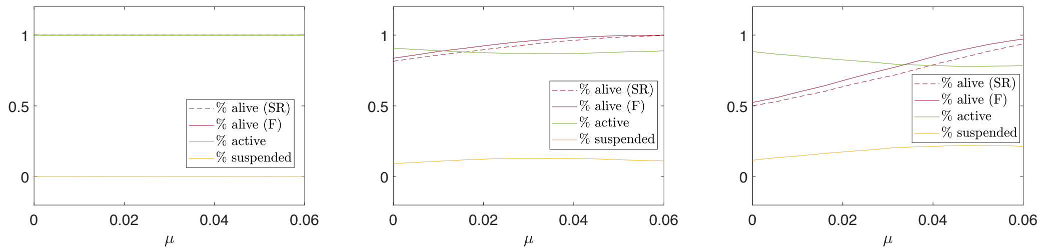

(a) $T_i = 1$ year (b) $T_i = 10$ years (c) $T_i = 30$ years

Fig. 2.5 The Figure displays the percentage amount spent each possible production state by the the semi-rigid and flexible firms at different horizons, labelled by T_i, as a function of the GBM drift coefficient μ. All the other model parameters are as in Table 2.1.

2.3.2 Flexibility and options' implied volatility

In this section, we studied the returns distributions of the three companies focusing on the usual four time horizons of 3, 6, 12 months and 10 years. Results, reported in Table 2.3, show that the impact of operational flexibility on the growth in the average levels of simple returns is increasingly pronounced as the horizon enlarges. In particular, the recurrent change of sign in the value of the expected average return as we move from the rigid to the semi-rigid is emblematic of the added value provided by real options. Additionally, increasing asymmetry and marked leptokurtosis have been observed for higher maturities; this is motivated by a higher probability of generating losses (rigid firm) and to exercise suspension and abandonment options (flexible and semi-rigid companies, respectively).

In light of this, it is not surprising to observe a remarkable decrease in standard deviation already in the very short term, in accordance with greater operational flexibility and despite the enlargement in the overall variability. It is reasonable to expect a similar outcome when analysing the implied volatility of options. Indeed, Figure 2.7 documents an important gap between the implied volatility of a call option written on the equity value of a rigid firm compared to the same measure calculated for comparatively more flexible firms. For at-the-money options, we note that implied

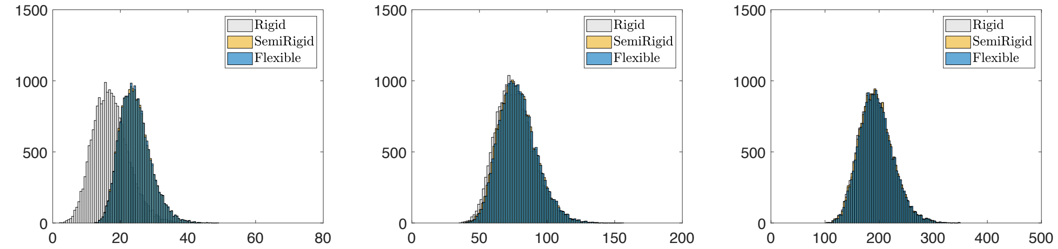

(a) $\mu = 0.00\%, T_i = 3$ months (b) $\mu = 4.50\%, T_i = 3$ months (c) $\mu = 6.00\%, T_i = 3$ months

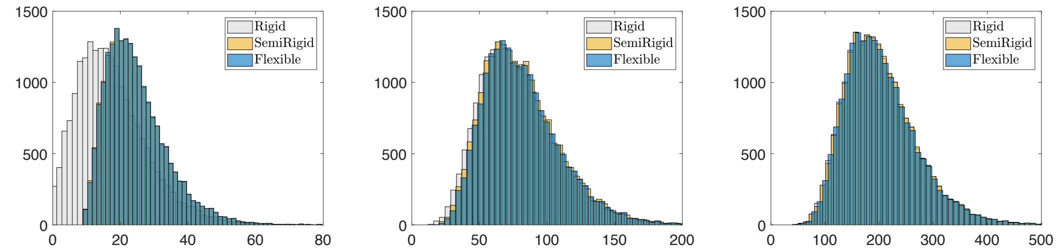

(d) $\mu = 0.00\%, T_i = 1$ year (e) $\mu = 4.50\%, T_i = 1$ year (f) $\mu = 6.00\%, T_i = 1$ year

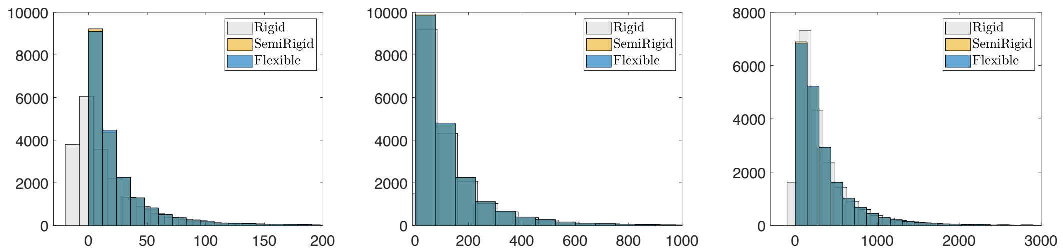

(g) $\mu = 0.00\%, T_i = 10$ years (h) $\mu = 4.50\%, T_i = 10$ years (i) $\mu = 6.00\%, T_i = 10$ years

Fig. 2.6 The Figure shows the distribution of firms' equity values at four different time horizons, labelled by T_i. The models for the underlying price process are three GBM which differ in the drift coefficient μ. In particular, given $\sigma = 0.30$, the value of the parameter μ has been chosen such that the drift of the return process $\mathrm{d}\ln(x_t/x_0)$ is, respectively, negative, null and positive. For the flexible firm, switching costs are set to 0. All the other model parameters are as in Table 2.1.

volatility is almost halved in the best case scenario and is reduced by about 20% in the worst case; no significant variations are found for different moneyness levels. In addition, this result is maintained regardless the maturity of the option. Noticeably, no relevant changes have been detected between the semi-rigid and the flexible firm, once again signalling that adding the suspension option to that of abandonment has only a marginal effect.

Furthermore, it is worth noting that, in contrast to what we observed for simple equity returns, the presence of mean-reversion in the output price process leads to an overall reduction in the level of implied volatility. This result is contingent on the values of the parameters used and, in particular, is due to a trend in prices towards a lower value than the initial x_0. This fact negatively affects the value of equity and, therefore, the average payoff at maturity and the price of the option. Also, within the context of GBM, Figure 2.8 emphasises that the previous results are significantly dampened as the drift parameter increases, in line with the observations made in the previous section.

Moreover, we turned our attention to a different risk metric as is the β coefficient of CAPM's equation. As a very first step, we calculated the ratio $\frac{\beta_E}{\beta_x}$ based on the current level of the production output price; we immediately noticed that adding some form of optionality remarkably decreases the risk coefficient and that, again, the effect of adding further options is marginal regardless the underlying model adopted (Table 2.4). We stressed these results by computing the same quantity as a function of the switching cost s and according to different levels of the initial price. Although it involves a variation in levels, using different values of the starting price does not alter the conclusions obtained so far. Similarly, the ratio between the betas is almost insensitive to changes in switching costs. This result is absolutely consistent with the minimal differences found between the semi-rigid and the flexible company (Figure 2.9).

Last, equation (2.10) highlights that the risk coefficient of equity is a function of the production output price and, indirectly, of the options available to the firm. Hence, its value fluctuates stochastically and, second, is contingent to the state of production. We provide a graphic illustration in Figure 2.10, where one can appreciate, on the

Table 2.3 The Table collects sample summary statistics - namely, mean, standard deviation and quartiles - for the distribution of firm's equity returns at 3, 6, 12 months and 10 years horizons. Each panel refers to a given model for the underlying price process, as specified.

Panel **(a)**: GBM

		$\hat{\mu}(R)$	$\hat{\sigma}(R)$	$\hat{q}_{0.25}$	$\hat{q}_{0.5}$	$\hat{q}_{0.75}$
$T_i = 3$ m	Rigid	0.0043	0.3175	-0.2184	-0.0204	0.1966
	Semi-rigid	0.0065	0.2106	-0.1426	-0.0135	0.1314
	Flexible	0.0065	0.2093	-0.1417	-0.0134	0.1306
$T_i = 6$ m	Rigid	0.0078	0.4534	-0.3152	-0.0455	0.2741
	Semi-rigid	0.0125	0.3012	-0.2044	-0.0301	0.1839
	Flexible	0.0125	0.2994	-0.2031	-0.0299	0.1828
$T_i = 12$ m	Rigid	0.0077	0.6538	-0.4603	-0.0991	0.3561
	Semi-rigid	0.0200	0.4359	-0.2948	-0.0652	0.2397
	Flexible	0.0202	0.4332	-0.2928	-0.0648	0.2383
$T_i = 10$ y	Rigid	0.1560	3.0395	-1.3114	-0.7520	0.4323
	Semi-rigid	0.2395	2.1547	-0.6890	-0.4988	0.2822
	Flexible	0.2439	2.1439	-0.6903	-0.4809	0.2849

Panel **(b)**: IGBM

		$\hat{\mu}(R)$	$\hat{\sigma}(R)$	$\hat{q}_{0.25}$	$\hat{q}_{0.5}$	$\hat{q}_{0.75}$
$T_i = 3$ m	Rigid	-0.0050	0.4993	-0.3602	-0.0721	0.2809
	Semi-rigid	0.0028	0.2634	-0.1860	-0.0378	0.1493
	Flexible	0.0029	0.2597	-0.1833	-0.0372	0.1472
$T_i = 6$ m	Rigid	-0.0014	0.7269	-0.5185	-0.1370	0.3709
	Semi-rigid	0.0103	0.3852	-0.2649	-0.0716	0.1976
	Flexible	0.0105	0.3799	-0.2609	-0.0705	0.1949
$T_i = 12$ m	Rigid	0.0046	1.0772	-0.7302	-0.2505	0.4569
	Semi-rigid	0.0251	0.5758	-0.3664	-0.1302	0.2441
	Flexible	0.0253	0.5681	-0.3607	-0.1283	0.2408
$T_i = 10$ y	Rigid	-0.0626	6.4894	-1.5968	-1.3010	-0.4302
	Semi-rigid	0.0837	3.7429	-0.6100	-0.6100	-0.3496
	Flexible	0.0980	3.7040	-0.6143	-0.6143	-0.2828

Panel **(c)**: CIR

		$\hat{\mu}(R)$	$\hat{\sigma}(R)$	$\hat{q}_{0.25}$	$\hat{q}_{0.5}$	$\hat{q}_{0.75}$
$T_i = 3$ m	Rigid	-0.0027	0.3149	-0.2213	-0.0176	0.1983
	Semi-rigid	0.0026	0.1655	-0.1143	-0.0093	0.1058
	Flexible	0.0026	0.1630	-0.1125	-0.0091	0.1043
$T_i = 6$ m	Rigid	-0.0025	0.4495	-0.3190	-0.0330	0.2810
	Semi-rigid	0.0069	0.2360	-0.1632	-0.0173	0.1507
	Flexible	0.0071	0.2325	-0.1606	-0.0171	0.1485
$T_i = 12$ m	Rigid	-0.0019	0.6277	-0.4558	-0.0550	0.3896
	Semi-rigid	0.0154	0.3286	-0.2298	-0.0288	0.2103
	Flexible	0.0157	0.3238	-0.2261	-0.0284	0.2073
$T_i = 10$ y	Rigid	-0.0642	1.7905	-1.4449	-0.5795	0.7764
	Semi-rigid	0.0784	0.9549	-0.5718	-0.3565	0.4044
	Flexible	0.0878	0.9423	-0.5757	-0.3166	0.4111

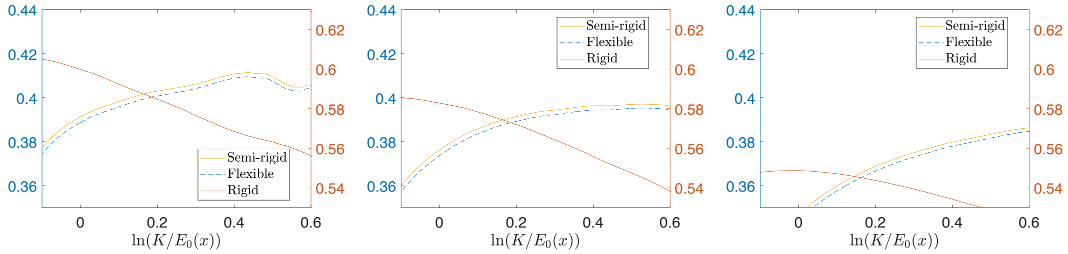

(a) GBM, $T_i = 3$ months (b) GBM, $T_i = 6$ months (c) GBM, $T_i = 12$ months

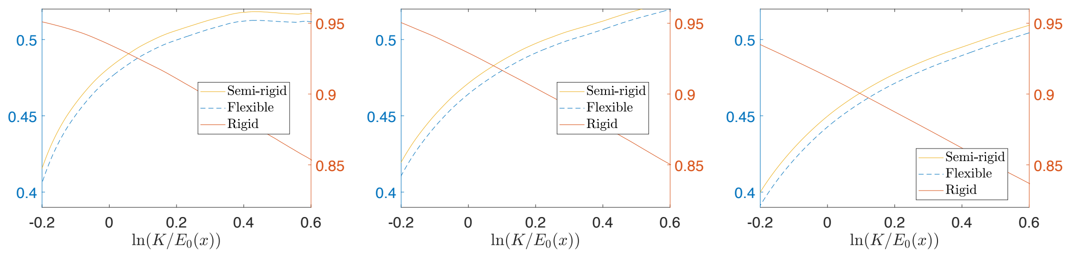

(d) IGBM, $T_i = 3$ months (e) IGBM, $T_i = 6$ months (f) IGBM, $T_i = 12$ months

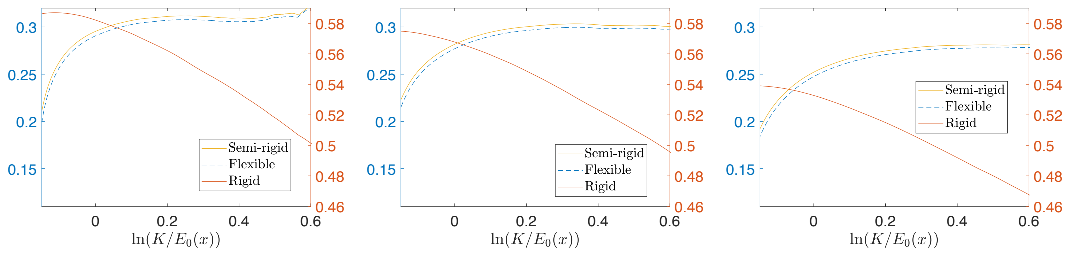

(g) CIR, $T_i = 3$ months (h) CIR, $T_i = 6$ months (i) CIR, $T_i = 12$ months

Fig. 2.7 The Figure displays the implied volatility for a set of European call options written on the value of firms' equity. Different maturities, labelled by T_i, have been considered for option contracts. Black, yellow and blue lines refer to the rigid, semi-rigid and flexible firm, respectively. For the flexible firm, switching costs are set to 0. All the other model parameters are as in Table 2.1 and the models for the underlying output price x are GBM, IGBM and CIR.

left-hand-side, few simulated trajectories for the price process x and the related options exercise boundaries, and, on the right, as many corresponding trajectories of the $\frac{\beta_E}{\beta_x}$ ratio. Additionally, we considered the expected value of such variable, averaging across all the simulated paths, and we noticed a decreasing trend over time. This fact once again highlights that operational flexibility contributes to reduce the riskiness of the firm by means of its impact on the volatility of cash-flows. In fact, the longer the horizon the higher the probability to exercise suspension and abandonment options,

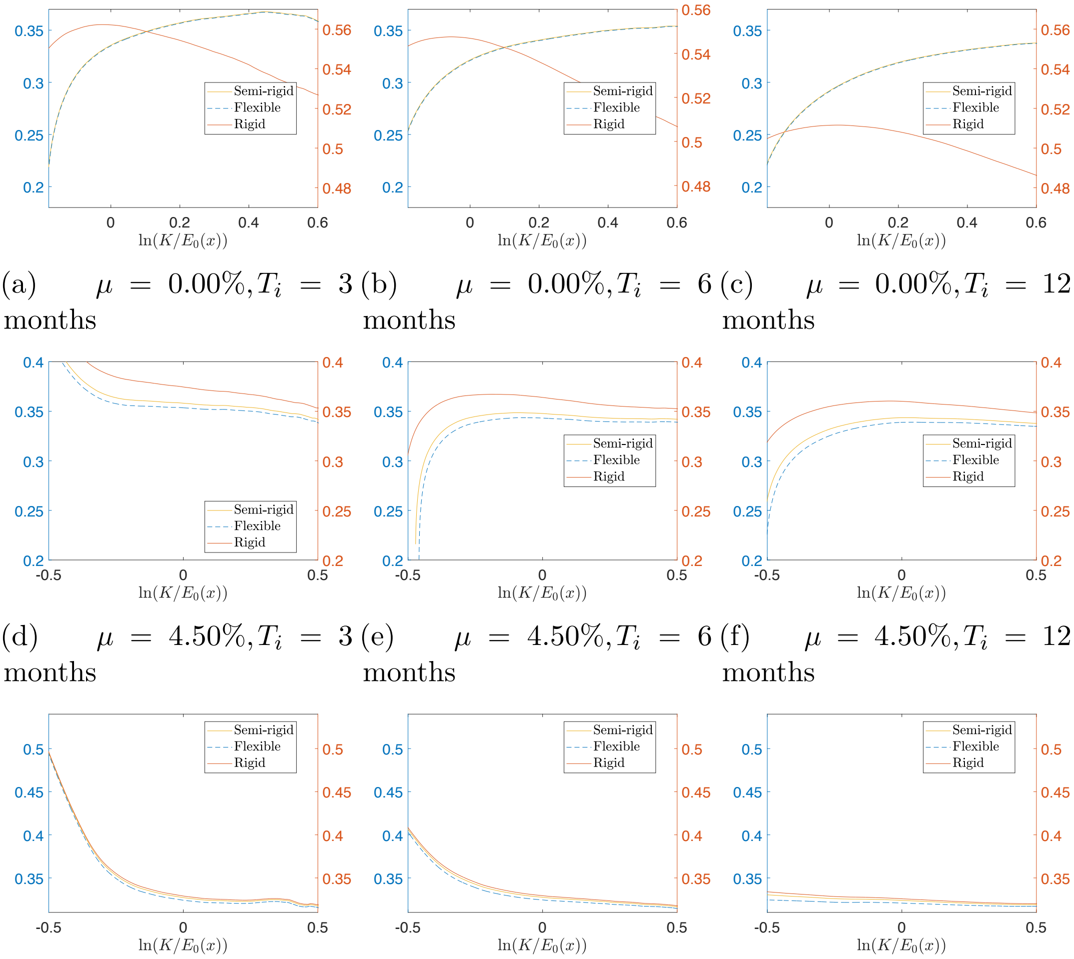

(a) $\mu = 0.00\%, T_i = 3$ months (b) $\mu = 0.00\%, T_i = 6$ months (c) $\mu = 0.00\%, T_i = 12$ months

(d) $\mu = 4.50\%, T_i = 3$ months (e) $\mu = 4.50\%, T_i = 6$ months (f) $\mu = 4.50\%, T_i = 12$ months

(g) $\mu = 6.00\%, T_i = 3$ months (h) $\mu = 6.00\%, T_i = 6$ months (i) $\mu = 6.00\%, T_i = 12$ months

Fig. 2.8 The Figure displays the implied volatility for a set of European call options written on the value of firms' equity. Different maturities, labelled by T_i, have been considered for option contracts. The models for the underlying price process are three GBM which differ for the drift coefficient μ. In particular, given $\sigma = 0.30$, the value of the parameter μ has been chosen such that the drift of the return process is, respectively, negative, null and positive. For the flexible firm, switching costs are set to 0. All the other model parameters are as in Table 2.1.

with a remarkable effect on the uncertainty about earnings, which is reduced; on average, this makes investing in the firm less risky.

Table 2.4 The Table reports the value of the ratio β_E/β_x for each kind of firm according to different models for the output price process x.

	GBM	IGBM	CIR
Rigid	1.8116	1.8094	1.8094
Semi-rigid	1.1993	0.9514	0.9519
Flexible	1.1918	0.8917	0.9377

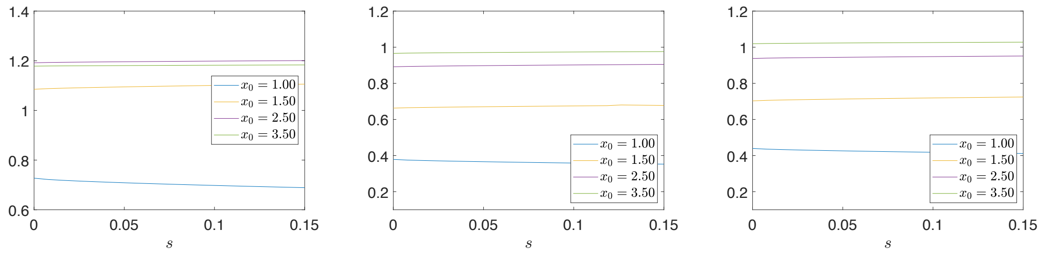

(a) GBM (b) IGBM (c) CIR

Fig. 2.9 The Figure shows the ratio β_E/β_x as a function of the switching cost s given different levels of the current price x_0. All the other model parameters are as in Table 2.1.

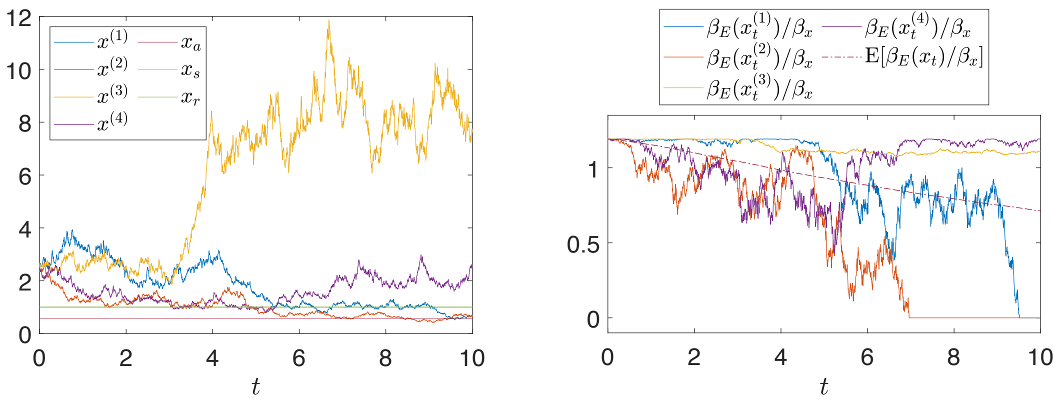

(a) (b)

Fig. 2.10 The Figure links stochastic price realisations to the β_E/β_x ratio. The left-hand-side panel displays four simulated paths for the price process x together with the optimal real options exercise boundaries. The panel on the right shows the corresponding trajectories of β_E/β_X, calculated from equation (2.10) as well as their expected value obtained by averaging across 20,000 paths.

2.4 Final remarks and future research directions

In this work, we adopted a real options model to show how operational flexibility affects both the value and the riskiness of firms. We considered three kinds of firms, moving from the absence of optionalities, passing through the opportunity of irreversibly abandon the market, and introducing a further level of flexibility by means of reversible suspension and resumption options. We found that the introduction of flexibility in the form of real options has an unambiguously positive impact on both raising the value of companies and on reducing their riskiness.

The effects of flexibility on firms' value and risk that we observed are explained by the reduction in the variability of firms' cash-flows achievable through the strategic exercise of stopping opportunities. In practice, the aforementioned outcomes are observable in a remarkable reduction in the implied volatility curve obtained for European equity call options, whatever the moneyness level, and in the cost of equity. Making reference to the latter point, we highlighted how the beta coefficient in the CAPM equation for equity returns, traditionally considered constant, actually has a stochastic nature. In fact, it turns out to be a function of firms' output price, uncertain by assumption. In addition, it also depends on the current state of production of the company, which is the channel through which the effect of the exercise of any real options propagates.

Our work aims at enriching the literature on corporate risk, traditionally dominated by studies on default risk, by offering a further perspective that links a structural feature like operational flexibility to key financial risk indicators such as options' implied volatility and CAPM's β. Most important, we consider our study to offer a promising foundation for future empirical research endeavours seeking to unravel the intricate connections between real options and asset prices.

Moreover, directions for further research include the possibility to expand our model by accounting for more firm characteristics. First, the existence of corporate debt is disregarded in our setting. As it is established in the literature, operational flexibility might give rise to agency costs related to the different goals pursued by managers and debt-holders; these impact negatively the returns and risk of firms. Including this component to the model would likely shed additional light on the analysis. Second, we assumed that all the three kinds of firms share the same model parameters, i. e. they operate at the same costs; also, the semi-rigid and the flexible firm would obtain the same scrap value from asset liquidation. It could be realistic to assume that the technology adopted by such companies is different and related to their degree of flexibility. Hence, a variety of different model parameters could be used. Even though we do not expect that this changes would significantly alter our conclusions, their magnitude could be modified. In particular, it is possible that larger difference will raise between the semi-rigid and the rigid firm. Finally, particularly when referring to mid and long-term horizons, changes in the level of flexibility could be introduced to account for the acquisition of new and more efficient production technologies.

Chapter 3

Flexibility and uncertainty: the optimal management of a gas-fired turbine

Abstract

In this paper we propose a real options model for the valuation of a gas-fired power-generating turbine that can be switched off-and-on many times according to the time-varying profitability of energy production over the short-term. In this framework, we study the effect of including several correlated sources of uncertainty - the spot prices of both electricity and natural gas as well as the latter's convenience yield - on the value of operational flexibility, investigating also its determinants and the optimal production decisions. Interestingly, flexibility turns out to mitigate the effect of the uncertainty around gas' convenience yield, whilst this last aspect is crucial in the evaluation of non flexible projects. From a methodological point of view, we exploit lattice-based valuation techniques, deriving bivariate and trivariate binomial trees for the underlying processes calibrating the proposed models to the current European

energy market conditions.

Keywords: Real options; gas-fired turbine; flexibility value; stochastic convenience yield; trivariate lattice.

3.1 Introduction

An inspection of the mix of resources used for electricity generation in 2022 in the European Union reveals that, on average, fossil fuels cover the 38.6% of production needs, with natural gas being the most used input source. Instead, a 40% share is attributable to renewable sources; moreover, such a percentage is more than doubled in the last 20 years and is expected to grow as European countries committed to reach climate neutrality by 2050.[1] As a consequence, traditional power plants, in which gas injection feeds a combustion and compression process that allows to produce electricity through the activation of a turbine, are assumed to suffer further demand uncertainty. This fact, together with rapidly changing macroeconomic and geopolitical scenarios, motivates the need for flexible facilities that allow to efficiently adjust production as market conditions change (Glensk and Madlener, 2019; Gonzalez-Salazar et al., 2018).

In this work, we propose a real options model for a flexible gas-fired power-generating plant that has the option to stop and resume production at multiple dates within a finite short-term horizon. Stopping and resumption decisions are driven by the stochastic behaviour of the input and output prices, whose difference contributes to the so called *spark spread*. Furthermore, we account for the inventory problem implicit in storable commodities and that is reflected in uncertainty over convenience yields; as a consequence, we recognise and model the convenience yield of natural gas as stochastic too.

[1] Data from the European Council report available here.

We document that operational flexibility has a significant impact on the value of the turbine, with substantial variations against a non-flexible benchmark. Moreover, we find that ignoring the uncertainty over commodity's convenience yield leads to systematically underestimate project values. Additionally, we document the relevance of the cross-correlations between the underlying state variables, which is sizeable if compared to the usual impact observed in financial derivatives pricing. Our analysis highlights the importance of modelling the variability of both the input and the output in this kind of production problems.

Put into a practical perspective, these results are drawn by means of a real options framework trying to improve over some of their most renowned critical points. Indeed, despite several decades of research in real options, related techniques are still not much used by practitioners; potentially, this is due to the significant degree of simplifying assumptions on which models rely on: while needed to keep a satisfying tractability of the model, such hypotheses can be seen as hardly realistic, determining the refuse of models themselves. Also, the methodologies adopted, such as continuous-time analytical solutions and Monte Carlo methods, might be perceived as "black boxes" by managers (Lambrecht, 2017). Hence, on the one hand, we consider a model that incorporates multiple sources of uncertainty: the input and the output prices and the convenience yield of the input commodity. On the other hand, we make use of intuitive lattice based techniques that allow to retain tractability being also transparent and easy to understand.

Our work is not the first one accounting for three different sources of uncertainty (see, for example, Abadie, 2015; Elias et al., 2016), and the first contributions on a stochastic convenience yield dates back to Gibson and Schwartz (1990). However, to the best of our knowledge, this is one of the first attempts to merge the two points together, thus facing the problem of simultaneously handling not only correlated processes, but also nested ones.

Analogously, lattice based techniques are commonly used when dealing with real options valuations. Nevertheless, we exploit here their full potential to derive not only the overall value of the project but also to visualise the underlying optimal strategy. In particular, we summarise in a simple graph the optimal actions the manager should take given the current level of state variables.

Summing up, we contribute to the literature in several ways: first, we shed light on the valuation and of the optimal running policy of a gas-fired turbine for electricity generation accounting for multiple realistic sources of uncertainty; second, we document the value of operational flexibility in this environment by means of advanced lattice based evaluation techniques; third, whilst most of the existing real options models are related to infinite time-horizons or to long-term projects, we restrict our analysis to a short-term maturity, looking at infra-annual decisions.

The remainder of the paper is as follows. The next section briefly reviews the existing literature; an overview of the energy system is provided in Section 3.3, while the model and the methodology we used are described in Section **??**; Section 3.4 presents the numerical analysis; Section 3.5 summarises the results and concludes; last, minor technicalities are deferred to the Appendix.

3.2 Literature Review

Our work is related to several branches of the literature. Structurally, it belongs to decision models under operational flexibility and to the research investigating the impact of alternative stochastic models for underlying variables; it also touches the point of choosing a proper time-horizon for investment decisions; methodologically, it relates to the literature on lattice based algorithms and, in particular, to their applications to the energy industry. In the following paragraphs we briefly revise the most relevant contributions within each of these fields.

Corporate investments implicitly includes several kinds of flexibility (Cortazar and Casassus, 1998; McDonald and Siegel, 1986; Pindyck, 1990). In particular, operational flexibility is the possibility to switch between alternative states and, starting from Brennan and Schwartz (1985), it is widely described throughout the whole commodity literature. For example, the option to reversibly change the input commodity of an electricity or of a bio-diesel production plant is the core foundation of Abadie and Chamorro (2008) and of Brandão et al. (2013), respectively. Equivalent models can be designed for alternative outputs, as in Bastian-Pinto et al. (2009), Dockendorf and Paxson (2013), Dong et al. (2014) and in Detemple and Kitapbayev (2020).

Being particularly relevant as a risk management tool in presence of uncertain cash-flows, operational flexibility requires a careful modelling of the underlying drivers of uncertainty. For many commodity prices, mean-reversion is known to exist (Nomikos and Andriosopoulos, 2012; Schwartz, 1997b) and to impact investment related decisions (Sarkar, 2003; Tsekrekos, 2010). Furthermore, factor models can be used to disentangle the effects of short-term shocks and long-run equilibrium, as in Schwartz and Smith (2000); the Authors also consider the implications for managerial problems and they highlight that short-term maturity projects are significantly sensitive to short-run variations. If read in the spotlight of Gibson and Schwartz (1990), then this result relates to the role played by a stochastic convenience yield.

Tsekrekos et al. (2012) finds that ignoring the stochastic behaviour of the commodity convenience yield leads to significantly underestimate the value of a project with shut-down and resumption options. Also, Tsekrekos and Yannacopoulos (2016) analyse the impact of fast mean-reverting stochastic volatility within a similar framework, finding that it induce a non-negligible effect on the switching frequency and on the preference of decision makers for keeping production in the active state. All these findings are in favour of proposing models that investigate deeper not only the impact of multiple, but also of nested sources of uncertainty.

Choosing the proper horizon for investment-related decision making processes is a non-trivial problem. A large part of the existing real options literature focuses on infinite time-horizons. Such a choice is motivated by the desire of getting closed-form or semi closed-form solutions and it is not in contrast with long-term investments (see Dixit and Pindyck, 1994 and Trigeorgis, 1996 for an introduction to the topic). However, for short living projects a similar assumption is potentially misleading. Carmona and Ludkovski (2008) present a numerical scheme with operational constraints to evaluate the flexibility of switching between multiple operating regimes in the context of a gas fired power plant; most importantly, they focus on finite and fixed expiry dates (e. g. 2 years). We make a similar reasoning here, noting that oftentimes strategic decisions shall cover periods no longer than one year. Furthermore, we restrict our attention to a predetermined set of monitoring dates (e. g. twice a month), assuming that decisions are made on a regular basis rather than being taken continuously.

From a computational point of view, lattice algorithms are a powerful tool to deal with finite life projects and can be adapted to complex valuations of both financial derivatives (see, for example, Gambaro et al., 2020) and real options. The simplest approaches resort to the recombining binomial model of Cox et al. (1979), which, however, is not suitable for approximating the behaviour of mean-reverting economic variables such as most energy prices. This obstacle is overcome by Hahn and Dyer (2008), who develop a method based on Nelson and Ramaswamy (1990) to obtain recombining lattices for homoskedastic mean-reverting stochastic processes. Hahn and

Dyer (2011) further improve over their previous contribution showing how to represent two-factor models, also finding a good computational efficiency. Moreover, lattice algorithms are seen as more “transparent” than simulation-regression based approaches and can be easily linked to decision trees (Brandão et al., 2005; Brandão and Dyer, 2005; Guthrie, 2009), thus potentially meeting the favour of managers.

Recombining trees are widely used in the energy sector to manage up to three sources of uncertainty. Elias et al. (2016) consider a model where all the *clean spark spread* components (namely, electricity, gas and carbon prices) exhibit a stochastic though correlated behaviour. They contribute to determine the value of the option to switch among different turbines in a gas-fired power plant within a very short horizon of about 90 days. Abadie et al. (2011) and Abadie et al. (2013) also consider as stochastic the prices of the input commodities and that of the electricity to evaluate the option to abandon coal-fired stations in Europe and the flexibility embedded in long-term investments, respectively. We adopt three drivers of uncertainty as well. However, we differentiate from the existing works because one of our variables - the convenience yield - is nested into another one - the price of natural gas.

Overall, we contribute to the literature by solving the switching problem of a gas-fired turbine through a trivariate lattice algorithm that accommodates three sources of uncertainties of which one is nested. We further differentiate from the majority of the existing works as we emphasise the value of flexibility within a short-term horizon decision process. Our approach offers a robust, yet easy to handle, tool to deal with complex and more realistic problems embedded in the world of energy.

3.3 A glimpse into the energy system

In this section we first describe the system of production and distribution of electricity (Subsection 3.3.1); next, we focus on gas turbines, providing a scheme about the way electricity is generated (Subsection 3.3.2). Our aim is to give the reader the taste of the environment we are working in, capturing its main features and being conscious that, to construct our model, we will certainly need to rely on some simplifying assumptions over many technical aspects.

3.3.1 The electricity grid

Electricity grid is the name given to the complex network that, from generators, allows to reach final electricity consumers by means of power transmission lines. In the first stage, generators produce electricity out of a given fuel. Electricity is then passed to a first transmission station, where its voltage is increased; this step is required to counteract the dissipation of energy due to physical frictions and allow the transmission of electricity to hundreds of kilometres away. However, high-voltage power is not directly usable neither for industrial nor for domestic purposes, thus, before reaching the final consumer, a certain number of transmission substation is required to reduce voltage, making it consistent with consumers' needs.

Observing the transmission network more closely, we find that the amount of electricity within the network is called load; the terms *base load* and *peak load* refer, respectively, to the minimum, stable, amount of electricity demanded over the 24 hours and to sudden, shorter, demand spikes. Peaks are typically related to certain periods of the day, like working hours, or to weather conditions. To prevent grid breaks, the amount of energy demanded by consumers and that produced by generators needs to be in equilibrium at any time instant. This fact clearly imposes restrictions on the type of energy plants that can satisfy either base load or peak load demand. In particular, base load plants must be able to provide the system with a continuous amount of energy: this is the case, for example, of nuclear plants, particularly expensive and slow to shut-down but very efficient while producing. On the other side of the coin, natural gas power plants typically require lower costs to be shut-down and restarted; their intrinsic higher flexibility makes them suitable for peak load management too.

3.3.2 Gas-fired turbines

Gas-fired turbines are made of three main chambers: a compressor, a combustion chamber and the turbine itself. Each one of these components plays a specific role within a four-steps cycle. Specifically, the air is injected into the compressor and, from there, fed into the combustion chamber, where it meets the gas. The oxidation reaction of natural gas has as main products carbon dioxide and high temperature steam. Hot air then expands into the turbine producing work, which is then converted into electricity by means of a generator. The cycle ends with a cooling process. By virtue of its non-storage capacity, the electricity produced is immediately sent to the electricity grid according to the scheme described in the previous section. The residual fluid is then wasted in open-cycle gas turbines (OCGT), whilst it is employed as an input for a second turbine in more efficient plants known as combined cycle gas turbines (CCGT). Beside the difference in efficiency, which makes CCGT more desirable for base load production, one should also account for the lower upfront costs required by OCGTs, which make them more suitable for small, regional grids and for peak load energy production. Furthermore, we recall that natural gas is a mixture of hydrocarbons within which the largest share (on average, the 97%) is given by methane (CH_4) and ethane (C_2H_6), which, however, represents less than 1% of the components. Other hydrocarbons are typically present in variable but smaller percentages and, from a chemical point of view, would absorb part of the thermal energy from oxidation. On the one hand, this would have an impact on the amount of fuel required to produced 1MWh of electricity. On the other hand, differences in gas composition are normally that low that they can safely be ignored from a modelling point of view; in particular, by focusing on a short time horizon as may be a year, we intend to minimise the likelihood that the energy producer will change its supply source, a fact that could increase the differences in the quality of the gas itself.

In our analysis, we do not take a position with respect to the type of turbine used. A case study based on real data should account for the specific costs linked to the technical characteristics of the plant and the specific market in which it operates. Our study aims to be more oriented to the development of a basic model that, however, can be extended taking into account specific constraints of a technical, economic or regulatory nature with relative ease.

3.3.3 The European market for gas and electricity

The European gas and electricity markets are complex and interdependent. Imports are a key feature of Europe's gas market; the primary regions of origin are Russia, Norway, North Africa, and, increasingly, the United States via liquefied natural gas (LNG). Gas is then distributed throughout pipelines and storage facilities. Gas' prices are heavily dependent on supply and demand dynamics, geopolitical influences, and energy policies. As such, they experienced significant volatility over the last four years, mainly because of geopolitical tensions and of the shifts in demand due to the COVID-19 pandemic.

On the other hand, Europe's electricity market recently transitioned from national monopolies to competitive markets in which wholesale prices are determined mainly by demand and supply mechanisms and are affected by fuel prices and related generation costs. As such, we expect to observe a positive correlation between time series of gas

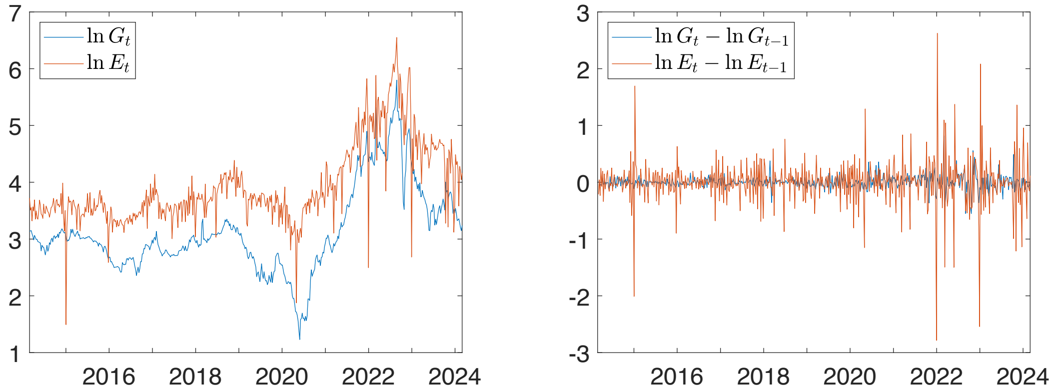

(a) (b)

Fig. 3.1 The Figure displays the time series of weekly log-spot prices for gas and electricity (panel 3.1a) and of their first differences (panel 3.1b) over a 10 years period (March 2014 - March 2024). Gas prices are labelled by G_t, whilst E_t refers to electricity.

and electricity prices.

In order to get a preliminary analysis of the price processes relevant to our study, we observed the prices of gas and electricity over the last 10 years, i. e. from March 2014 to March 2024. We proxied spot prices with one-day ahead prices. Moreover, our ultimate goal is the valuation of turbines and the determination of their optimal running strategy, which we assume to happen at low frequency within the year. For this reason, we focused on weekly time series. Gas' data refer to the one day-ahead contract for the Dutch TTF and have been downloaded from the Intercontinental Exchange's website; electricity prices refer to the average 24-hour ahead base load daily price provided by the European Energy Exchange. We plotted the times series for the level of log-prices and for their first differences in Figure 3.1.

We immediately notice that the levels time series shows a period of disruption attributable to the effects of the COVID-19 pandemic as well as a sudden spike with persistent effect due to the Russian-Ukrainian conflict. Furthermore, neither of the two time series appears to be stationary, contrary to what appears to their prime differences (Figure 3.1b). Graphic intuition is in line with the results of the Augmented Dickey-Fuller (Said and Dickey, 1984) and of the Kwiatkowski-Phillips-Schmidt-Shin (Kwiatkowski et al., 1992) tests, which both suggest the presence of a unit root in the series of log-prices and the stationarity of first differences (see Table 3.1).

Table 3.1 The Table presents the results of the Augmented Dickey-Fuller (ADF) and Kwiatkowski-Phillips-Schmidt-Shin (KPSS) test conducted on the time series of log-prices for gas and electricity as well as on their first differnces. We recall that the ADF test reads the presence of a unit root as null hypothesis, whilst the KPSS test works on a trend-stationary null hypothesis. The header "c-value" refers to the "critical value" of the test.

	ADF test			KPSS test		
	p-value	Test statistic	c-value	p-value	Test statistic	c-value
$\ln G_t$	0.516	-0.371	-1.941	0.010	4.910	0.146
$\ln E_t$	0.239	-1.126	-1.941	0.010	2.681	0.146
$\ln G_t - \ln G_{t-1}$	0.001	-21.459	-1.941	0.100	0.075	0.146
$\ln E_t - \ln E_{t-1}$	0.001	-36.304	-1.941	0.100	0.004	0.146

In the remainder of this work, we are going to assume that the price dynamics of both gas and electricity can be modelled by means of a geometric Brownian motion. Despite our assumption being in line with most of the existing literature, we wonder how realistic it is compared to empirical evidence. A first critical point regards the presence of a seasonal component in energy prices, which is widely documented in the literature. However, accounting from the observations given in Figure 3.1, it seems that seasonality is not much pronounced for low frequency data such as weekly ones; additionally, neglecting intra-daily variations, the behaviour of electricity and gas prices are qualitatively similar, suggesting that treating both series as if they were de-seasonalised ones is reasonable. Last, we claim we can "safely" omit to include the seasonal component in our models as long as we work under the pricing measure, as we will recall in Remark 3.3.3. However, a limitation of our study consists in not including jump components, which are a renowned stylised feature of energy prices. Indeed, the sample statistics computed for the four time series of interest and collected in Table 3.2 suggest a departure of market data from normality. Nevertheless, values are not particularly pronounced; we therefore believe that the error of not including jumps is not too significant and we propose to incorporate them to refine the model in future research.

Table 3.2 The Table shows the sample mean, standard deviation (Std), skewness and kurtosis for the levels of log-prices of gas and electricity and for their first differences. The kurtosis of the normal distribution is 3.

	Mean	Std	Skewness	Kurtosis
$\ln G_t$	3.1311	0.7500	0.8976	4.0125
$\ln E_t$	3.9334	0.7019	1.0840	4.3535
$\ln G_t - \ln G_{t-1}$	0.0002	0.1159	0.5171	12.5177
$\ln E_t - \ln E_{t-1}$	0.0008	0.4104	-0.4873	15.8799

3.3.4 The market model

We present below the dynamics of the input (the natural gas) and of the output (the electricity) of our production problem. As already discussed in the introduction and in the literature review of our work, a careful modelling of the input's convenience yield[2] is needed for appropriate investment decisions. Therefore, we first review the role of the convenience yield within the no-arbitrage analysis of a commodities market model (Subsection 3.3.4), then we describe a bivariate model with a constant convenience yield for the gas price process (Subsection 3.3.4) and finally we extend this to a trivariate model with a stochastic convenience yield (Subsection 3.3.4).

[2]Notice that the output of our production problem is electricity which is hardly storable. Therefore, we can safely assume that there is no convenience yield in the output's price process. On the contrary, there is strong evidence (see, e.g., Volmer, 2011 and Martínez and Torró, 2023) of the need of a convenience yield in the natural gas price process.

Convenience yield in the modelling of commodities

In the modelling of commodities price processes, the convenience yield represents the advantage or disadvantage that comes from holding physical inventories of the commodity[3] rather than holding a financial instrument that represents the ownership to that commodity. The (possibly stochastic) net flow of these contributions per unit of time and commodity is termed convenience yield, labelled by δ (or δ_t).

Since the convenience yield captures extra gains (or losses) coming from the direct ownership of the underlying, it is standard in the literature to treat it as a dividend yield (Pindyck, 1993). We briefly review below the risk-neutral adjustment that is needed if a commodity price process features a convenience yield.

Let $X = \{X_t\}_{t\geq 0}$ be the spot price process of a generic commodity and assume that under the physical (or historical) measure $\mathbb{P}$ the dynamics of X is defined by

$$\frac{\mathrm{d}X_t}{X_t} = \mu_t \mathrm{d}t + \sigma_t \mathrm{d}W_t^{\mathbb{P}} \tag{3.1}$$

with $S_0 \in \mathbb{R}^+$ and where $W^{\mathbb{P}} = \{W_t^{\mathbb{P}}\}_{t\geq 0}$ is a standard $\mathbb{P}$-Brownian motion, μ_t is a deterministic function of time and of the current level of X possibly capturing the mean reversion and/or the seasonality of the commodity spot price and σ_t is a strictly positive deterministic function (of time and of the current level of X). For sake of simplicity assume that the risk-free rate r is constant[4] and let $B = \{B_t\}_{t\geq 0}$ with $B_t = e^{rt}$ be the money market account that will serve as a numéraire. Recalling that the (possibly stochastic) convenience yield δ_t represents the proportional benefit, or cost, of holding one unit of the commodity, the discounted total gain of holding one unit of X over an

[3]As such, the convenience yield was originally introduced as the price of storage according to a demand-supply equilibrium model (Kaldor, 1939).

[4]As noted by Schwartz (1997b), the variability of the short-term interest rate r_t is usually an order of magnitude smaller than the one of the convenience yield δ_t, when stochastic.

infinitesimal period of time $\mathrm{d}t$ reads

$$\mathrm{d}\left(\frac{X_t}{B_t}\right)+\delta_t\frac{X_t}{B_t}\mathrm{d}t=\frac{X_t}{B_t}\sigma_t\left(\frac{\mu_t-(r-\delta_t)}{\sigma_t}\mathrm{d}t+\mathrm{d}W_t^{\mathbb{P}}\right).$$

Under an equivalent martingale measure $\mathbb{Q}$ this discounted gain must be a martingale; therefore, under mild integrability assumptions on μ_t, σ_t and δ_t, Girsanov's Theorem allows us to define a $\mathbb{Q}$-standard Brownian motion $W=\{W_t\}_{t\geq 0}$ setting

$$\mathrm{d}W_t=\lambda_t\mathrm{d}t+\mathrm{d}W_t^{\mathbb{P}}$$

where $\lambda_t:=\frac{\mu_t-(r-\delta_t)}{\sigma_t}$ is the possibly time-dependent and state-contingent market price of risk per unit of X. Therefore, under the physical measure $\mathbb{P}$ we can also rewrite the dynamics of X as

$$\frac{\mathrm{d}X_t}{X_t}=(r-\delta_t+\lambda_t\sigma_t)\mathrm{d}t+\sigma_t\mathrm{d}W_t^{\mathbb{P}} \tag{3.2}$$

while under the equivalent martingale measure introduced before we have

$$\frac{\mathrm{d}X_t}{X_t}=(r-\delta_t)\mathrm{d}t+\sigma_t\mathrm{d}W_t. \tag{3.3}$$

Notice that, by construction, we have that $\{X_te^{-(r-\delta_t)}\}_{t\geq 0}$ is a $\mathbb{Q}$-martingale.

Finally, by a standard no-arbitrage argument, the T-forward[5] price of X at time t, with $T\geq t$, is equal to

$$F(t,T)=\mathbb{E}^{\mathbb{Q}}\left[X_T|\mathcal{F}_t\right], \tag{3.4}$$

where $\mathbb{F}=\{\mathcal{F}_t\}_{t\geq 0}$ is the filtration generated by (X,δ).

[5]As detailed in Chapter 29 of Björk (2009), if the risk-free interest rate is deterministic, forward prices and futures prices/quotes coincide.

It is important to stress the fact that convenience yields are not directly observable on the market, hence their values must be proxied. Writing equation (3.4) explicitly as

$$F(t,T) = X_t e^{(r_t-\delta_t)(T-t)}$$

and following Gibson and Schwartz (1990) and Rotondi (2024), we can obtain an estimate for the instantaneous convenience yield $\hat{\delta}_t$ by computing

$$\hat{\delta}_t = r_t - \frac{1}{t^+ - t} \ln \frac{F\left(t,t^+\right)}{X_t}, \tag{3.5}$$

where $F\left(t,t^+\right)$ is the price of the futures contract whose maturity is the closest to t. For example, if we consider the gas spot price at December 1, 2023, i. e. $X_0 = 43.940$ EUR and the futures contract with maturity date December 30, 2023, i. e. $F(0, 0.08\text{years}) =$ 43.496 EUR, and a risk-free rate r_t equal to 3.5%, we obtain $\hat{\delta}_t = 16.20\%$, significantly different from zero[6].

Remark 3.3.1. *We highlight here that due to the peculiar change of the probability which is needed to obtain an equivalent martingale measure, the diffusive coefficient σ_t in (3.2), under $\mathbb{P}$, and in (3.3), under $\mathbb{Q}$, stays the same.*

Remark 3.3.2. *Even[7] when σ_t is constant, say $\sigma_t \equiv \sigma_X \in \mathbb{R}^+$, a different choice of the drift term in (3.1) generates different dynamics for X and different parameters σ_X. For example, if we decide to model a commodity spot price process X with a precise μ'_t and $\sigma'_t \equiv \sigma'_X$ and then we consider another model for X with $\mu''_t \neq \mu'_t$ and $\sigma''_t \equiv \sigma''_X$, it must be $\sigma'_X \neq \sigma''_X$.*

[6]See Rotondi (2024) to appreciate a 14-years-long time series of convenience yields empirically obtained following equation (3.5).

[7]We thank an anonymous Referee for pointing out this crucial issue.

Deterministic convenience yield

We first assume that the convenience yield of our input, namely the gas, is constant.

Let $(\Omega, \mathcal{F}, \mathbb{F} = \{\mathcal{F}_t\}_{t\geq 0}, \mathbb{Q})$ be a filtered probability space, where $\mathbb{Q}$ is a pricing measure. Under $\mathbb{Q}$, the (spot) price processes of the gas, $G := \{G_t\}_{t\geq 0}$ and of the electricity, $E := \{E_t\}_{t\geq 0}$ solve

$$\begin{cases} \mathrm{d}G_t = (r-\delta)\, G_t \mathrm{d}t + \sigma_G^{bi} G_t \mathrm{d}W_t^G \\ \mathrm{d}E_t = r E_t \mathrm{d}t + \sigma_E E_t \mathrm{d}W_t^E \end{cases} \tag{3.6}$$

with two initial conditions $G_0, E_0 \in \mathbb{R}^+$ and where $r \in \mathbb{R}$ is the riskless short-term interest rate, $\delta \in \mathbb{R}$ is the constant convenience yield of the input, $\sigma_G^{bi} \in \mathbb{R}^+$ and $\sigma_E \in \mathbb{R}^+$ are the volatilities of the two prices and $\{W_t^G\}_{t\geq 0}$ and $\{W_t^E\}_{t\geq 0}$ are two standard Brownian motions under $\mathbb{Q}$ with instantaneous correlation equal to $\rho_{GE} \in (-1,1)$. In words, we assume that under $\mathbb{Q}$, G and E are two correlated geometric Brownian motions.

Remark 3.3.3. *Working with spot prices under an equivalent martingale measure spares us from taking a stand on the seasonality and on the mean-reversion properties*[8] *the price processes would exhibit under the historical measure*[9]. *Indeed, since under* $\mathbb{Q}$ *both* $\{G_t e^{(\delta-r)t}\}_{t\geq 0}$ *and* $\{E_t e^{-rt}\}_{t\geq 0}$ *must be martingales, their precise drifts under the historical measure are irrelevant.*
Finally, it is worth to acknowledge that our models neglect jump components that would be there even under a risk-neutral specification; however, the lattice-based valuation techniques we will exploit can be extended to jump-diffusive settings following Amin (1993).

[8]See, e.g., Geman (2008); Geman and Shih (2008); Lucia and Schwartz (2002); Roncoroni et al. (2015).

[9]When considering forward or futures prices instead, Latini et al. (2019) and Benth et al. (2019) show how to account for mean-reversion even under a pricing measure.

Definition of spark spread

When switched on, our turbine produces electricity out of gas. The company's theoretical gross margin from selling one unit of electricity produced by the turbine is called *spark spread*, that we label by $S := \{S_t\}_{t\geq 0}$. At each point in time, this quantity is defined as

$$S_t := E_t - \frac{G_t}{\eta_E}. \tag{3.7}$$

Notice that since the linear combination of geometric Brownian motions is not a geometric Brownian motion itself, the dynamics followed by S is not a standard one. The parameter $\eta_E \in (0,1)$, typically called *thermal efficiency*, measures the amount of fuel needed to generate a certain amount of work, and, consequently, of electricity (usually, 1 MWh).

From a strictly technical viewpoint, turbines' actual efficiency is related to the general features of the plant - for example, a CCGT would be more efficient than an OCGT - as well as to the materials used in its construction and to the chemical composition of gas. As such, thermal efficiency could be regarded as a time-varying quantity. However, in spark spreads' market quotations, η_E has much an economic than a physical meaning; indeed, it is a Country specific constant. Data from ICE (Intercontinental Exchange) show that the reference value of η_E is set 50% for Dutch, German and Italian spark spreads and to 49.13% for the UK. In what follows, we will adopt this line keeping η_E fixed across the whole analysis; nevertheless, should it be desired, time-dependency is affordable, as it will be pointed out in Remark 3.3.6.

Finally, we acknowledge that some value is potentially dismissed when a turbine that has been stopped for a while needs to be restarted because the inertial benefit of residual heat is wasted: we will let this loss to be conveyed into the so called switching cost.

Stochastic convenience yield

We now extend the input-output model described in the previous subsection removing the assumption of a constant convenience yield in the input price process. Following the seminal works of Gibson and Schwartz (1990) and Casassus and Collin-Dufresne (2005) we assume that under $\mathbb{Q}$ the convenience yield $\delta := \{\delta_t\}_{t\geq 0}$ follows a mean reverting Ornstein-Uhlenbeck process. Therefore, the stochastic differential equations driving this extended market models read

$$\begin{cases} \mathrm{d}G_t = (r-\delta_t)\,G_t\mathrm{d}t + \sigma_G^{tri} G_t \mathrm{d}W_t^G \\ \mathrm{d}\delta_t = \alpha\left(\bar{\delta}-\delta_t\right)\mathrm{d}t + \sigma_\delta \mathrm{d}W_t^\delta \\ \mathrm{d}E_t = rE_t\mathrm{d}t + \sigma_E E_t \mathrm{d}W_t^E \end{cases} \tag{3.8}$$

with an extra initial condition $\delta_0 \in \mathbb{R}$. The meaning of the parameters for G and E remains unchanged from the previous subsection while $\alpha \in \mathbb{R}^+$ represents the speed of mean reversion of the stochastic convenience yield towards its long-run mean $\bar{\delta} \in \mathbb{R}$ and $\sigma_\delta \in \mathbb{R}^+$ is its volatility. Moreover, we assume that the instantaneous correlation between W^δ and W^G (resp. W^E) is equal to $\rho_{G\delta} \in (-1,1)$ (resp. $\rho_{\delta E} \in (-1,1)$).

We point out here that, according to Remark 3.3.2, the volatility parameter of G in this augmented model, σ_G^{tri}, differs from the one in the previous simplified model, σ_G^{bi}. In particular, in this augmented model part of the observed variability of G is due to the variability of δ_t, which impacts G's drift term. On the contrary, according to the previous version of the model, the constant δ contributes in no way to the variability of G. Following this consideration, if G and δ have a positive correlation, we expect data to support $\sigma_G^{bi} > \sigma_G^{tri}$.

3.3.5 The valuation problem

The optimal production problem faced by the manager of the turbine is a one-dimensional optimal switching problem. In particular, the manager has to decide when let the turbine operate balancing the costs of the input (the natural gas) and the output (the electricity) and the fixed costs that she bears when the turbine is operating and when it is not.

Fix a time horizon T. Inspired by the notation of Bayraktar and Egami (2010) let $I := \{I_t\}_{t\in[0,T]} \in \{0,1\}$ be a right-continuous switching process defined by[10]

$$I_t = J_0 + \sum_{n\in\mathbb{N}_0} J_n 1\left(\tau_n \leq t < \tau_{n+1}\right) \tag{3.9}$$

where $\{J_n\}_{n\in\mathbb{N}} \in \{0,1\}$ is a discrete time stochastic process such that $J_{n+1} = 1 - J_n$ for all $n \in \mathbb{N}$ and $\tau := \{\tau_n\}_{n\in\mathbb{N}}$ is an increasing sequence of (controlled) $\mathbb{F}$-stopping times on $[0,T]$. Here, process I represents the status of the turbine at time t: if $I_t = 1$ the turbine is operating at time t if $I_t = 0$ it is not; process J represents the status of the turbine right after the n^{th} switching decision; the sequence of stopping times τ represents the switching times decided by the manager of the turbine.

The operating cash-flow $X(S_t, I_t)$ generated by the turbine is equal to

$$X(S_t, I_t) := \begin{cases} (S_t - c_{11}) & \text{if } I_t = 1 \\ (-c_{00}) & \text{if } I_t = 0 \end{cases} \tag{3.10}$$

where $c_{11} \in \mathbb{R}^+$ (resp. $c_{00} \in \mathbb{R}^+$) is the fixed cost of the turbine if operating (resp. suspended).

[10] $1(A)$ denotes the indicator function of the event A.

The immediate switching costs $H(J_n, J_{n-1})$ are equal to

$$H\left(J_n, J_{n-1}\right) := \begin{cases} c_{10} & \text{if } J_n - J_{n-1} = -1 \\ c_{01} & \text{if } J_n - J_{n-1} = 1 \end{cases} \tag{3.11}$$

where $c_{10} \in \mathbb{R}^+$ (resp. $c_{01} \in \mathbb{R}^+$) is the switching cost of turning off (resp. on) the turbine, moving from $J_{n-1} = 1$ to $J_n = 0$ (resp. from $J_{n-1} = 0$ to $J_n = 1$).

Given the initial value of the spark spread S_0 and the initial status of the turbine $J_0 = I_0$, the optimal value of the turbine (possibly) operating from time zero to time T is

$$\sup_{\tau} \mathbb{E}\left[\int_0^T e^{-rt} X(S_t, I_t) \mathrm{d}t - \sum_{n \in \mathbb{N}_0} e^{-r\tau_n} H\left(J_n, J_{n-1}\right) \middle| S_0, J_0 \right] \tag{3.12}$$

where functions X and H, defined in (3.10) and (3.11), depend on the state variable S, defined in (3.7), and on the τ-controlled processes I and J, defined in (3.9).

Finding the optimal value of the problem in (3.12) where the state variable (which is here the spark spread S) is not a "standard" process (like a generalised/geometric Brownian motion) is quite challenging. Moreover, it is not realistic to assume that the manager can/will switch the turbine's status infinitely many times over a fixed time horizon $[0, T]$. On the contrary, it might be reasonable to assume that the manager decides on the turbine's status on a regular basis, like at the beginning of each week/month, observing the evolution of the prices of the natural gas and of electricity. Following this realistic approach to the optimal switching problem in (3.12), we restrict the possible switching times to a set of monitoring dates and we solve the resulting problem by dynamic programming.

Given the time interval $[0,T]$, consider its uniform partition $\Upsilon := \{t_i\}_{i=0,\dots,m}$, with $t_i := i\Delta t$ and where $m \in \mathbb{N}$ is the number of time steps and $\Delta t := \frac{T}{m}$. Restrict now the sequence of stopping times τ to Υ, namely consider $\tilde{\tau} := \{\tau_n\}_{n\leq m}$, an increasing sequence of (controlled) $\mathbb{F}$-stopping times on Υ. As a consequence of this restriction, the manager can change the status of the turbine only at the beginning of each period: if $I_{t_i} = 1$ (resp. $I_{t_i} = 0$), with $t_i \in \Upsilon$, the turbine will operate (resp. will not operate) over the interval $[t_i, t_{i+1}[$. Accounting for this restriction, the optimal value of the turbine reads

$$\sup_{\tilde{\tau}} \mathbb{E}\left[\sum_{t_i \in \Upsilon \setminus \{T\}} e^{-rt_i} \Big(X(S_{t_i}, I_{t_i})\Delta t - c_{01} 1(I_{t_i} - I_{t_{i-1}} = 1) - c_{10} 1(I_t - I_{t_{i-1}} = -1) \Big) \Bigg| S_0, I_0 \right]. \tag{3.13}$$

Remark 3.3.4. *While it is straightforward to account for instantaneous switching costs c_{10} and c_{01} when moving from the continuous time problem (3.12) to its discretised counterpart in (3.13), it is less so for operating cash-flows X. Given the uniform partition Υ of $[0,T]$, we can write $\int_0^T e^{-rt} X(S_t, I_t)\mathrm{d}t = \sum_{i=0}^{m-1} \int_{t_i}^{t_{i+1}} e^{-rt} X(S_t, I_t)\mathrm{d}t$. Then, it is necessary to proxy each continuous integral $\int_{t_i}^{t_{i+1}} e^{-rt} X(S_t, I_t)\mathrm{d}t$. We decide to do this in a simple way and we approximate each integral by $e^{-rt_i} X(S_{t_i}, I_{t_i})\Delta t$, which implies an accounting of the profit/loss that is going to be generated from t_i to t_{i+1} as of the market values of input/output at time t_i. While the input must be purchased at the beginning of the production period at the t_i-price, the output is likely to be sold at the end of it at the t_{i+1}-price. However, given also the relatively small Δt we consider, we assume here that the output is sold forward at the t_i-price. Numerical tests in Appendix C.2 show that a slightly more sophisticated approximation rule for $\int_{t_i}^{t_{i+1}} e^{-rt} X(S_t, I_t)\mathrm{d}t$, like a trapezoidal rule, delivers almost identical results while being a little less straightforward to justify at an economic level.*

We acknowledge that the optimal value of (3.13) converges to the one of (3.12) only as $\Delta t \to 0$ *and that any choice of a finite* Δt *delivers a discretisation bias. However, our goal here is to evaluate the turbine assuming a realistic finite set of switching dates and not to find the best numerical approximation to the continuous time problem in (3.12). Anyway, the numerical experiments collected in Appendix C.2 show that the optimal values of (3.13) are quite stable after a relatively small number of monitoring dates* m*; moreover, they also show that in the only case in which (3.12) can be evaluated almost perfectly (which happens for static turbine when the convenience yield of natural gas is assumed to be constant, see below) the approximated value we get solving (3.13) is comparable even using a relative small number of steps.*

One of the main goal of this study is to asses whether *flexibility* has a relevant (economic) value in this production problem. Here we define "flexibility" as the possibility of switching on/off the turbine.

The manager of a *flexible turbine* can switch it on-and-off timely, sticking to the optimisation problem in (3.13). The manager of a *static turbine* can not intervene on its status, which is assumed to be always operating, even when generating a loss (namely, when the net spark spread is negative).

The value of a static turbine reduces to

$$V_0^S(S_0,1) = \mathbb{E}\left[\sum_{t_i \in \Upsilon \setminus \{T\}} e^{-rt_i} X(S_{t_i},1)\Delta t\right] = \sum_{t_i \in \Upsilon \setminus \{T\}} e^{-rt_i} \Delta t \mathbb{E}\left[S_{t_i} - c_{11}\right]. \tag{3.14}$$

If the convenience yield of the gas price process is constant (namely, if we consider the bivariate model described in Subsection 3.3.4), the expected value at time t_i of the spark spread can be computed explicitly and we get

$$V_0^{S,bi}(S_0,1) = \sum_{t_i \in \Upsilon \setminus \{T\}} e^{-rt_i} \Delta t \left(E_0 e^{rt_i} - \frac{G_0 e^{(r-\delta)t_i}}{\eta_E} - c_{11}\right). \tag{3.15}$$

If the convenience yield of the gas price process is stochastic (namely, if we consider the trivariate model described in Subsection 3.3.4), the expected value at time t_i can not be computed explicitly but $V_0^S(S_0,1)$ in (3.14) can be computed by standard Monte Carlo techniques.

The valuation of a flexible turbine is more challenging and relies on dynamic programming techniques.

3.3.6 The dynamic programming algorithm

We solve the problem in (3.13) by backward induction. For all $t_i \in \Upsilon$ let $V_{t_i}(S_{t_i}, I_{t_i})$ denote the optimal (i.e. the one obtained sticking to the optimal switching policy) value of the turbine whose current status is I_{t_i} and when the spark spread is equal to S_{t_i}.

At $T = m\Delta t$ there is no decision to take nor any profit to account for.

At $T-\Delta t$ the manager decides whether to let the turbine operate between dates $T-\Delta t$ and T based on the turbine's status at time $T-\Delta t$. If the turbine is already producing ($I_{T-\Delta t} = 1$), the manager compares the cash-flow (evaluated at the $T-\Delta t$-prices) from keeping the production on ($(S_{T-\Delta t} - c_{11})\Delta t$) to the cash-flow from the switching and leaving the turbine off ($-c_{10} - c_{00}$). On the contrary, if the turbine is not producing already ($I_{T-\Delta t} = 0$), the manager compares what she would get switching the turbine on and paying the related operating and switching costs ($(S_{T-\Delta t} - c_{11})\Delta t - c_{01}$) to what she would get leaving the turbine off ($-c_{00}$). In formulae, we have:

$$V_{T-\Delta t}(S_{T-\Delta t}, I_{T-\Delta t}) = \begin{cases} \max\{(S_{T-\Delta t} - c_{11})\Delta t, -c_{00} - c_{10}\} & \text{if } I_{T-\Delta t} = 1 \\ \max\{(S_{T-\Delta t} - c_{11})\Delta t - c_{01}, -c_{00}\} & \text{if } I_{T-\Delta t} = 0 \end{cases} \tag{3.16}$$

At each other monitoring date t_i, depending on the status of the turbine at t_i, the manager decides whether to let the turbine operate between dates t_i and t_{i+1}. She does so accounting on the one hand for the immediate profit/loss of this action as of the market values of input/output at time t_i and on the other hand for the discounted expected value of the optimally run turbine given the status in which it will be left at t_{i+1}. The recursive relationship (i.e. the Bellman equation) between the value functions at two generic dates t_i and t_{i+1}, $i=0,...,m-2$, reads

$$V_{t_i}(S_{t_i},I_{t_i})=\begin{cases}\max\Big\{(S_{t_i}-c_{11})\Delta t+e^{-r\Delta t}\mathbb{E}\left[V_{t_{i+1}}(S_{t_{i+1}},1)\Big|\mathcal{F}_{t_i}\right], \\ \qquad\qquad -c_{00}-c_{10}+e^{-r\Delta t}\mathbb{E}\left[V_{t_{i+1}}(S_{t_{i+1}},0)\Big|\mathcal{F}_{t_i}\right]\Big\} & \text{if } I_{t_i}=1 \\ \max\Big\{(S_{t_i}-c_{11})\Delta t-c_{01}+e^{-r\Delta t}\mathbb{E}\left[V_{t_{i+1}}(S_{t_{i+1}},1)\Big|\mathcal{F}_{t_i}\right], \\ \qquad\qquad -c_{00}+e^{-r\Delta t}\mathbb{E}\left[V_{t_{i+1}}(S_{t_{i+1}},0)\Big|\mathcal{F}_{t_i}\right]\Big\} & \text{if } I_{t_i}=0\end{cases} \tag{3.17}$$

where

$$S_{t_{i+1}}=E_{t_i}\exp\left(\left(r-\frac{\sigma_E^2}{2}\right)\Delta t+\sigma_E\left(W^E_{t_{i+1}}-W^E_{t_i}\right)\right)+ \\ -\frac{G_{t_i}}{\eta_E}\exp\left(\left(r-\frac{\sigma_G^2}{2}\right)\Delta t-\int_{t_i}^{t_{i+1}}\delta_t\mathrm{d}t+\sigma_G\left(W^G_{t_{i+1}}-W^G_{t_i}\right)\right).$$

Remark 3.3.5. *Several constraints can be added to the original problems in (3.12) and (3.13). For example, conditional on a given set of values of the state variables, the manager of the turbine could be forced to always produce electricity (even if facing a negative spark spread) to satisfy a large demand. This or other restrictions to the switching policy can be implemented in the recursive step in (3.17) and would yield a value of the turbine lower than the one obtained sticking to an optimal unconstrained policy.*

From a practical point of view, we implement the backward recursion described in (3.17) along a bivariate (resp. trivariate) lattice discretisation of the market model described in Subsection 3.3.4 (resp. 3.3.4). As the dynamics of the spark spread (defined by 3.7) is not standard, we first discretise the primary processes E and G (and δ) and then we compute the values of S, node by node.

The lattice discretisations we use are derived following Hahn and Dyer (2008) that extend the lattice approximation of diffusions described by Nelson and Ramaswamy (1990) to the bivariate case. All the related formulae and technical details are deferred to Appendix C.1.

Remark 3.3.6. *One of the many advantages of our lattice-based valuation approach is that it allows for a straightforward extension to time-dependent and state-contingent parameters. Since the valuation algorithm works backward, node by node, all the parameters (like the thermal efficiency η_E or the fixed/switching costs c_{ij}, $i, j = 0, 1$) could also depend on the current time and/or the current value of the state variables. This would neither complicate nor slow down the valuation algorithm.*

3.4 Numerical Illustration

In the following, we first calibrate our market models to current market conditions (Subsection 3.4.1), then, using realistic parameters, we compute a benchmark value of the turbines (Subsection 3.4.2); we then proceed with an extensive analysis of the sensitivity of our benchmark values to changes: in the level (Subsection 3.4.3) of the convenience yield and of its uncertainty (Subsection 3.4.4); in the market parameters (Subsection 3.4.5) and, in particular, in the correlations between state variables (Subsection 3.4.6). Finally, we inspect the optimal switching policy (Subsection 3.4.7).

Across our study, we always compute the quantity

$$\frac{V^{k,tri}}{V^{k,bi}} - 1, \tag{3.18}$$

with $k \in \{S, F\}$, to measure how much the value of the projects varies when accounting for the uncertainty over the convenience yield (trivariate model, tri) compared to the case when it is constant (bivariate model, bi). We recall that the static firm ($k = S$) is committed to operate all time, whereas the flexible ($k = F$) can switch production off and resume it when convenient.

3.4.1 Estimation of the models

In order to get realistic parameters for our numerical investigations and to understand which specification of the convenience yield for the natural has works better, we perform a simple but effective calibration of the models in Subsection 3.3.4 to current market data. In particular we calibrate the models as of $t_0 =$ December 1, 2023.

First of all, we need to identify a reliable proxy for the spot price processes of the natural gas G and of electricity E within the European energy market. For both these commodities we decide to proxy spot prices by one-day ahead prices. As our ultimate goal is to value a static/flexible turbine, we neglect infra-day movements and consider only daily settlement prices. As far as the natural gas is concerned, we consider the one day-ahead contract for the Dutch TTF[11] as provided by ICE (Intercontinental Exchange). For electricity, we consider the average 24-hour ahead base load daily price provided by EEX (European Energy Exchange). As of $t_0 =$ December 1, 2023, we have $G_0 = 43.94$ EUR/MWh and $E_0 = 116.41$ EUR/MWh.

Since the convenience yield of natural gas is not directly observable, we have to retrieve it from futures prices using (3.4). Therefore, we collect also the settlement price of futures contracts on natural gas (as provided by ICE) with residual maturity less than one year (which is our investment horizon).

[11]The TTF (Title Transfer Facility) is a virtual trading point for natural gas in the Netherlands, which has become one of the most important hubs for natural gas trading in Europe.

Calibration of the deterministic convenience yield model

Since spot prices are observed under the physical measure $\mathbb{P}$, we first have to map the risk-neutral expression of the deterministic convenience yield model in Subsection 3.3.4 to its physical counterpart. Following the arguments in Subsection 3.3.4, the risk-neutral SDEs in (3.6) become

$$\begin{cases} \mathrm{d}G_t = \left(r - \delta + \lambda^G \sigma_G^{bi}\right) G_t \mathrm{d}t + \sigma_G^{bi} G_t \mathrm{d}W_t^{\mathbb{P},G} \\ \mathrm{d}E_t = \left(r + \lambda^E \sigma_E\right) E_t \mathrm{d}t + \sigma_E E_t \mathrm{d}W_t^{\mathbb{P},E} \end{cases} \tag{3.19}$$

where λ^G and λ^E are the constant market prices of risk of natural gas and electricity. For any given Δt, the t-conditional log solutions of these SDEs read

$$\begin{cases} \ln \dfrac{G_{t+\Delta t}}{G_t} = \left(r - \delta + \lambda^G \sigma_G^{bi} - \dfrac{(\sigma_G^{bi})^2}{2}\right) \Delta t + \sigma_G^{bi} \left(W_{t+\Delta t}^{\mathbb{P},G} - W_t^{\mathbb{P},G}\right) \\ \ln \dfrac{E_{t+\Delta t}}{E_t} = \left(r + \lambda^E \sigma_E - \dfrac{\sigma_E^2}{2}\right) \Delta t + \sigma_E \left(W_{t+\Delta t}^{\mathbb{P},E} - W_t^{\mathbb{P},G}\right) \end{cases}$$

where $r_t^G := \ln \frac{G_{t+\Delta t}}{G_t}$ and $r_t^E := \ln \frac{E_{t+\Delta t}}{E_t}$ are the log returns of G and E. This implies that we can estimate σ_G^{bi}, σ_E and ρ_{EG} as

$$\begin{aligned} \hat{\sigma}_G^{bi} &= \sqrt{\hat{V}\left[r_t^G\right] \Delta t} \\ \hat{\sigma}_E &= \sqrt{\hat{V}\left[r_t^E\right] \Delta t} \\ \hat{\rho}_{EG} &= \hat{Corr}\left[r_t^E, r_t^G\right] \end{aligned}$$

where $\hat{V}[\cdot]$ and $\hat{Corr}[\cdot]$ are the sample variance and the sample correlation. As highlighted in Remark 3.3.1, the volatility coefficients of G and E are formally the same under $\mathbb{P}$ and under $\mathbb{Q}$ and, therefore, in our numerical experiments, we are going to rely on the sample estimates described above. We acknowledge that we could also consider implied volatilities. However, this alternative approach would require an analysis of the natural gas/electricity option markets, which is out of the scope of the present work[12].

Using the last four[13] years of data we obtain $\hat{\sigma}_G^{bi} = 1.1044$, $\hat{\sigma}_E = 1.9689$ and $\hat{\rho}_{EG} = 0.4015$. As expected the natural gas and the electricity markets are extremely volatile and exhibit a positive correlation.

Unfortunately, it is impossible to identify δ and λ^G from the sample mean of r_t^G. Therefore, in order to estimate δ, we rely on futures prices. When the convenience yield is deterministic, futures prices in (3.4) simplify to

$$F(t,T) = G_t e^{(r-\delta)(T-t)}.$$

Once a proxy for the risk-less rate r is chosen, we can retrieve an estimate of δ minimising the mean squared pricing error, namely setting

$$\hat{\delta} = \arg\min_{\delta \in \mathbb{R}} \sum_i \left(F^{mkt}(0,T_i) - G_0 e^{(r-\delta)T_i} \right)^2 \tag{3.20}$$

where $\{T_i\}_i$ is the set of maturities of the futures contracts of interest and $\{F^{mkt}(0,T_i)\}_i$ are their t_0-market prices. Setting $r = 0.0350$, computed as the average spot rate of the AAA-rated European Government bonds with maturity less than one year, and considering the twelve monthly future contracts with delivery dates from January 2024 to December 2024 we get $\hat{\delta} = 0.0571$. The residual mean squared pricing error is equal to 38.31. Considering that this calibration exercise involves twelve futures prices, only one parameter (δ) and that the variance of the squared residual pricing errors is equal

[12] Moreover, unless there exists a derivative written on both G and E that would allow to retrieve an estimate of implied ρ_{EG}, we should always rely on an historical estimate for the correlation between the two spot price processes.

[13] We opted for a lengthy time series to mitigate to some extent the significant disruption caused by the unprecedented turmoil in the energy markets stemming from the Ukraine-Russia war that began in 2022.

to 55.66, the classical information criteria for this model are equal to: 4.19 (Akaike IC), 4.43 (Schwarz Bayesian IC), 4.17 (Hannan-Quinn IC).

Calibration of the stochastic convenience yield model

If the convenience yield is stochastic, working out the log solution for G under the physical measure $\mathbb{P}$ is of no help. Indeed, following what we did in the previous subsection, we get

$$\ln \frac{G_{t+\Delta t}}{G_t} = \left(r + \lambda^G \sigma_G^{tri} - \frac{(\sigma_G^{tri})^2}{2} \right) \Delta t - \int_t^{t+\Delta t} \delta_s \mathrm{d}s + \sigma_G^{tri} \left(W_{t+\Delta t}^{\mathbb{P},G} - W_t^{\mathbb{P},G} \right)$$

and the sample variance of r_t^G is not an estimator for σ_G^{tri} anymore. Indeed, the theoretical (t-conditional) variance of r_t^G now reads

$$V \left[\ln \frac{G_{t+\Delta t}}{G_t} \right] = V \left[\int_t^{t+\Delta t} \delta_s \mathrm{d}s \right] + \left(\sigma_G^{tri} \right)^2 \Delta t + \\ +2\sigma_G^{tri} Cov \left[\int_t^{t+\Delta t} \delta_s \mathrm{d}s, W_{t+\Delta t}^{\mathbb{P},G} - W_t^{\mathbb{P},G} \right]$$

since, as already pointed out in Remark 3.3.2, the variability of G is now partially due to the variability of δ_t. Nevertheless, we can retrieve σ_G^{tri} (along with the parameters of δ_t) from futures prices. When the convenience yield is stochastic, the expected value in (3.4) rewrites as

$$F(0,T) = G_0 \mathbb{E} \left[\exp \left(\left(r - \frac{(\sigma_G^{tri})^2}{2} \right) T - \int_0^T \delta_s \mathrm{d}s + \sigma_G^{tri} W_T^{\mathbb{P},G} \right) \right] \tag{3.21}$$

and if δ_t follows an Ornstein-Uhlenbeck we can adapt the computations in Schwartz and Smith (2000) and obtain

$$F(0,T) = G_0 e^{rT + A(T) - B(T)\delta_0}$$

where

$$
\begin{aligned}
B(T) &= \frac{1}{\alpha}\left(1-e^{-\alpha T}\right) \\
A(T) &= \frac{\alpha\bar{\delta}+\sigma_G^{tri}\sigma_\delta\rho_{G\delta}}{\alpha^2}\left(1-e^{-\alpha T}-\alpha T\right)+\frac{\sigma_\delta^2}{\alpha^3}\left(2\alpha T-3+4e^{-\alpha T}-e^{-2\alpha T}\right).
\end{aligned}
$$

Fitting the market futures curve with (3.21), we can retrieve an estimate of the parameters $\Theta = \{\sigma_G^{tri}, \rho_{G\delta}, \delta_0, \bar{\delta}, \alpha, \sigma_\delta\}$ as

$$
\hat{\Theta} = \arg\min_{\Theta\in D}\sum_i \left(F^{mkt}(0,T_i) - G_0 e^{rT_i + A(T_i) - B(T_i)\delta_0}\right)^2 \tag{3.22}
$$

where D is a six dimensional domain for Θ[14].

In the same framework of the calibration performed in the previous section, we obtain: $\hat{\sigma}_G^{tri} = 0.5814$, $\hat{\rho}_{G\delta} = 0.9261$, $\hat{\delta}_0 = 0.0971$, $\hat{\bar{\delta}} = -0.0597$, $\hat{\alpha} = 0.0735$ and $\hat{\sigma}_\delta = 0.6968$. The residual mean squared pricing error is equal to 2.49. Considering that this calibration features now six parameters and that the variance of the squared residual pricing errors is equal to 0.0431, the three information criteria for this model are equal to: -1.97 (Akaike IC), -0.25 (Schwarz Bayesian IC), -2.08 (Hannan-Quinn IC).

As it appears from these measures, the stochastic convenience yield model outperforms the deterministic convenience yield one even when accounting for the increased number of parameters. This fact can be also visualised graphically in Figure 3.2, where we plotted the futures market prices alongside the forward curves obtained from the estimated values of δ - namely, $\hat{\delta}$, resulting from (3.20) - and of the set of parameters $\hat{\Theta}$ - obtained after solving (3.22).

Indeed, this model is able to capture the variability of the time-varying convenience yield, which, over a one year time horizon, is expected to even change sign, moving

[14]In particular we set $D = ((0,2),(-1,1),(-1,1),(-1,1),(0,50),(0,2))$. Since (3.22) is high-dimensional, when solving it we draw uniformly from D many different initial guesses Θ_0 in order to reach the global minimum and not one of the many local minima.

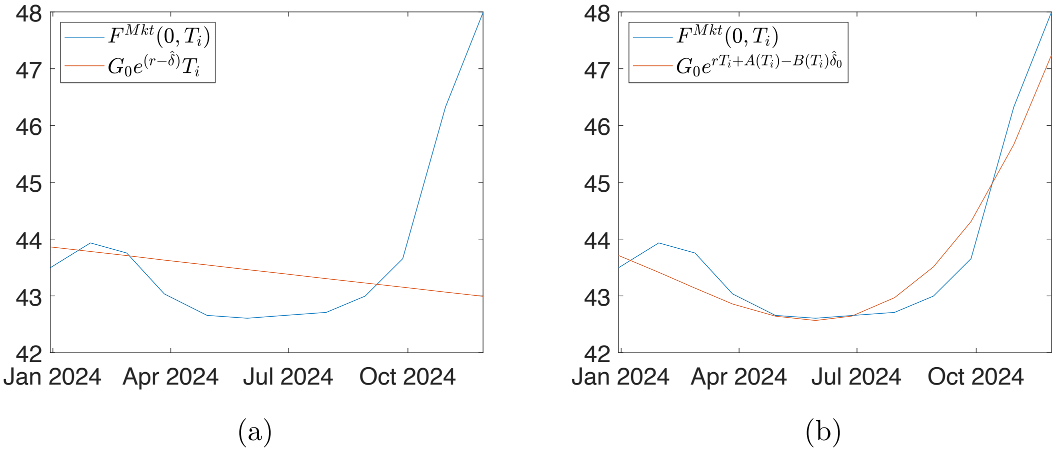

Fig. 3.2 The Figure displays futures market prices against the forward curve obtained as a function of the convenience yield in the bivariate (panel 3.2a) and in the trivariate model (panel 3.2b with the values of $del\hat{t}a$ and $\hat{\delta}_t$ resulting from the minimisation problems in (3.20) and (3.22), respectively.

from a positive δ_0 towards a negative $\bar{\delta}$. This behaviour depends of course on the seasonality of the natural gas market. This calibration exercise is carried out at the beginning of December, when the demand for natural gas is at its peak. This is clearly an advantage for the holders of the physical commodity and it translates into a positive convenience yield. Moving forward towards the next spring and summer, the demand for natural gas will probably slow down, making storage costs overcome the benefits of a physical possession of the commodity. This situation will lower the convenience yield making it negative. Moreover, it is interesting to notice how the hypothesis made at the end of Subsection 3.3.4 about $\sigma_G^{tri} < \sigma_G^{bi}$ is verified in the data.

The nature of the convenience yield of natural gas does not impact the estimation of σ_E, for which we use again the square of the sample variance of r_t^E. As for the remaining parameters of the trivariate model, ρ_{GE} and $\rho_{E\delta}$, there is no formal way to retrieve them without bringing in derivatives written on both G and E. Therefore, we keep using the sample correlation between r_t^G and r_t^E for ρ_{GE} and we claim that

$\rho_{E\delta}$ is slightly smaller than ρ_{GE} since the correlation between E and δ is most likely channelled through G.

Table 3.3 collects the parameters that we are going to use for our numerical experiments. Market parameters are a simple rounding of the ones obtained through the calibrations described above while operational parameters are adapted from Tsekrekos et al. (2012).

Table 3.3 The Table summarises the benchmark parameters of the numerical exercises of Section 3.4.

Notation	Value	Description
E_0	115 EUR/MWh	Initial electricity price
σ_E	2	Volatility of the electricity price
G_0	45 EUR/MWh	Initial natural gas price
σ_G^{bi}	1.1	Volatility of the natural gas price in the bivariate model
σ_G^{tri}	0.6	Volatility of the natural gas price in the trivariate model
δ	0.05	(Deterministic) convenience yield in the bivariate model
δ_0	0.1	Initial convenience yield value in the trivariate model
σ_δ	0.7	Volatility of the convenience yield
α	0.1	Speed of mean-reversion of the conv. yield towards $\bar{\delta}$
$\bar{\delta}$	-0.05	Long-run mean level of the convenience yield
ρ_{EG}	0.4	Correlation coefficient between W^E and W^G
$\rho_{E\delta}$	0.1	Correlation coefficient between W^E and W^δ
$\rho_{G\delta}$	0.9	Correlation coefficient between W^G and W^δ
c_{11}	5 EUR/MWh	Costs related to the production of electricity
c_{00}	0 EUR/MWh	Maintenance costs paid when the turbine is off
c_{01}	150 EUR	Cost of switching-off the turbine
c_{10}	150 EUR	Cost of switching-on the turbine
η_E	0.5	Coefficient of electrical efficiency
T	1 year	Horizon
m	24	Number of monitoring dates
r	0.035	Risk-less interest rate

3.4.2 Turbines valuation

Our starting point is the computation of the value of the static and flexible turbines according to the set of parameters in Table 3.3. We report our preliminary results, rounded to the unit, in Table 3.4.

At first glance we appreciate that, for each kind of turbine, the bivariate model returns a value lower than that produced by the trivariate one. The difference is highly significant for the static turbine (36.8%), but it becomes considerably lower when flexibility comes into play, reaching a variation of about 1.3%. Furthermore, within each model we can measure the value added by flexibility as the percentage variation in the value of the flexible turbine over that of the static one. Noticeably, the value of the flexible turbine is 3.87 times that of the static one in the bivariate case and 2.60 in the trivariate scenario, thus signalling how impactful is operational flexibility as a real option.

These findings are of utmost importance. First, they suggest that neglecting the existing uncertainty over the convenience yield of gas leads to underestimate the value of the project, coherently with Tsekrekos et al. (2012), regardless the presence of embedded options. Second, and perhaps most important, they tell us that the error is larger in absence of operational flexibility. In the following we investigate how sensitive are these quantities to changes in the main model parameters by means of some comparative analyses and keeping the numerical results in Table 3.4 as benchmarks.

Table 3.4 The Table summarises the (rounded) present values of the **S**tatic/**F**lexible turbine within the **bi**variate/**tri**variate market models introduced in the previous section conditional on the turbine operating at time zero. Parameters as in Table 3.3.

$V(S_0,1)^{S/F,bi/tri}$	bi	tri
S	174’575	218’857
F	475’518	490’782

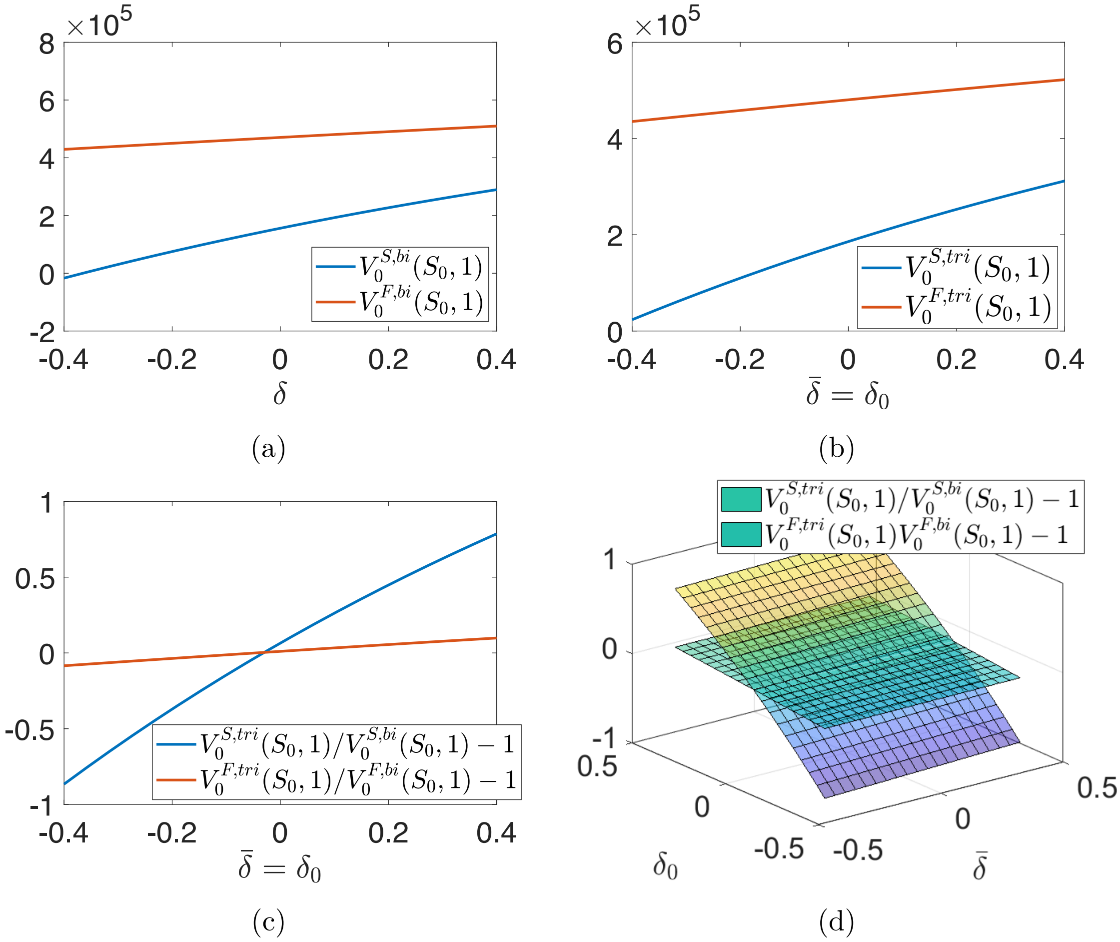

Fig. 3.3 The Figure displays the value of each turbine as a function a constant convenience yield δ (a) and of the long-run mean of the stochastic stochastic convenience yield $\bar{\delta}$ (b). Panels c and d show the impact of adopting a stochastic convenience yield rather then keeping it constant.

3.4.3 The impact of the convenience yield

We consider the sensitivity of the value of the turbines to changes in the convenience yield implied in gas prices. According to expectations, Figure 3.3 shows that the value of any turbine is substantially increasing with the level of this parameter when we keep it constant (3.3a), as well as with its equilibrium level $\bar{\delta}$ when we let it fluctuate stochastically (3.3b).

Moreover, the effect is more pronounced for the static turbine, consistently with the fact that the convenience yield enters with a negative sign in the drift of the gas price process, thus reducing its expected value, *ceteris paribus*. The natural implication is a larger expected spark spread, which also decreases the probability to switch between states as well as the value of flexibility - proved by the flexible curve being flatter than the static one. In a mirror, if the convenience yield converges to a negative level in the long-run, then the variance of the gas process is increased and flexibility has greater value. In fact, the option to switch production off-and-on is more valuable when the uncertainty over the project cash-flows is larger. Consequently, as shown in 3.3c, the use of a richer model that includes a stochastic convenience yield is increasingly beneficial with the average level of the parameter $\bar{\delta}$, as it avoids to significantly mis-estimate the value of the turbine, particularly that of the static one. Noticeably, such a conclusion holds true independently of the long-run mean value of the convenience yield being set equal with the initial one (3.3d).

3.4.4 The effect of convenience yield uncertainty

In Figure 3.4, we further look at the effect on the turbines value of the parameters driving the uncertainty over the convenience yield. Qualitatively, converging towards higher levels of $\bar{\delta}$ - unconstrained from δ_0 - positively affects the value of any turbine. The impact is observable across all the speed of mean-reversion, though being more pronounced for the highest ones (3.4a); this fact can be explained by the joint increase in the mean and reduction in the variance of the convenience yield linked to the increase in $\bar{\delta}$ and α, respectively.

Instead, altering the variance of the convenience yield process has substantially no effect on the static turbine, whilst it causes appreciable variations in the value of the flexible one, as shown in 3.4c. A lower speed of mean reversion, together with a higher level of the volatility parameter σ_δ, increases the variance of the convenience yield, suggesting higher uncertainty also over the gas price and the profit generated

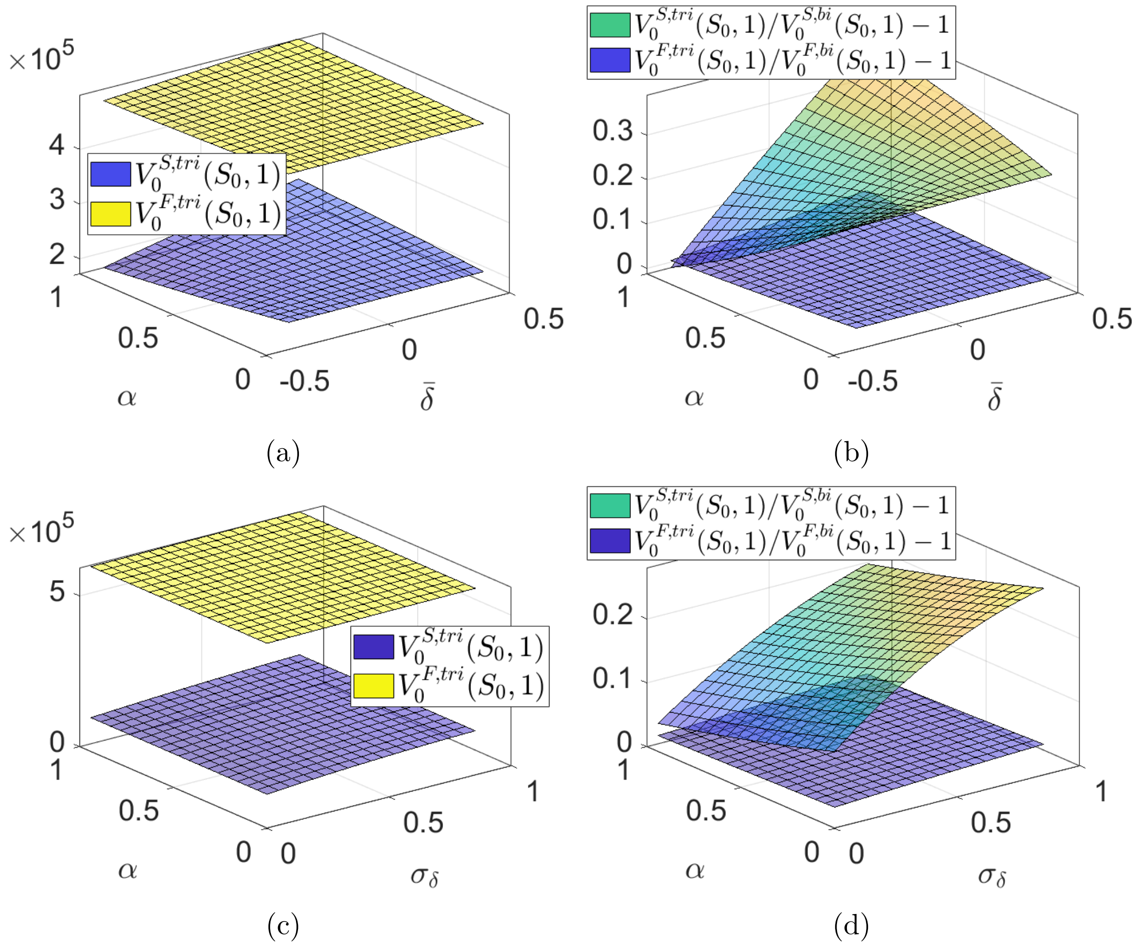

Fig. 3.4 The Figure displays the value of each turbine and the impact of including a stochastic convenience yield as functions of the speed of mean reversion α and of the long-run mean $\bar{\delta}$ (panels a and b) as well as functions of α and of the volatility parameter σ_δ (panels c and d).

by the turbine. From a theoretical perspective, operational flexibility smooths out increasing uncertainties, which, instead, have great impact on static assets. Our findings, displayed in Panels 3.4b and 3.4d, are consistent with this prescription, as we notice that the value of the flexible turbine is comparatively less sensitive to the passage from a bivariate to a trivariate model than that of the static one, for which we have that the higher the variance of the convenience yield, the larger the error committed if assuming it is constant over time.

3.4.5 The influence of main market parameters

According to the definition of spark spread introduced in (3.7) and to the value function of the turbine from (3.13), the higher the initial electricity price compared to that of gas, the higher the value of the turbine. This is easy to observe in the left panels of Figure 3.5, where the value of the flexible turbine monotonically increases with E_0 for any given value of G_0; however the effect is more pronounced for lower gas prices, as proved by the variation in the slope of the surface moving along the G_0-axis. Furthermore, there are no qualitative differences neither when moving from the bivariate (3.5a) to the trivariate (3.5c) model, nor when looking at the static turbine (for the sake of readability, the corresponding plots have been omitted). The right panels provide a valuation of flexibility for both the bivariate (3.5b) and trivariate (3.5d) model, respectively. Comparing each entry in the two matrices, we notice that the bivariate model is slightly more sensitive to operational flexibility.

Figure 3.6 shows that the value of the static turbine is insensitive to changes the volatility of electricity and gas in the bivariate case (3.6a), consistently with the closed formula for $V_0^{S,bi}(S_0, 1)$ in (3.15). Instead, flexibility is particularly valuable when the operating cash-flows are significantly uncertain, particularly because of highly volatile electricity prices and regardless the assumption over convenience yield. Despite being

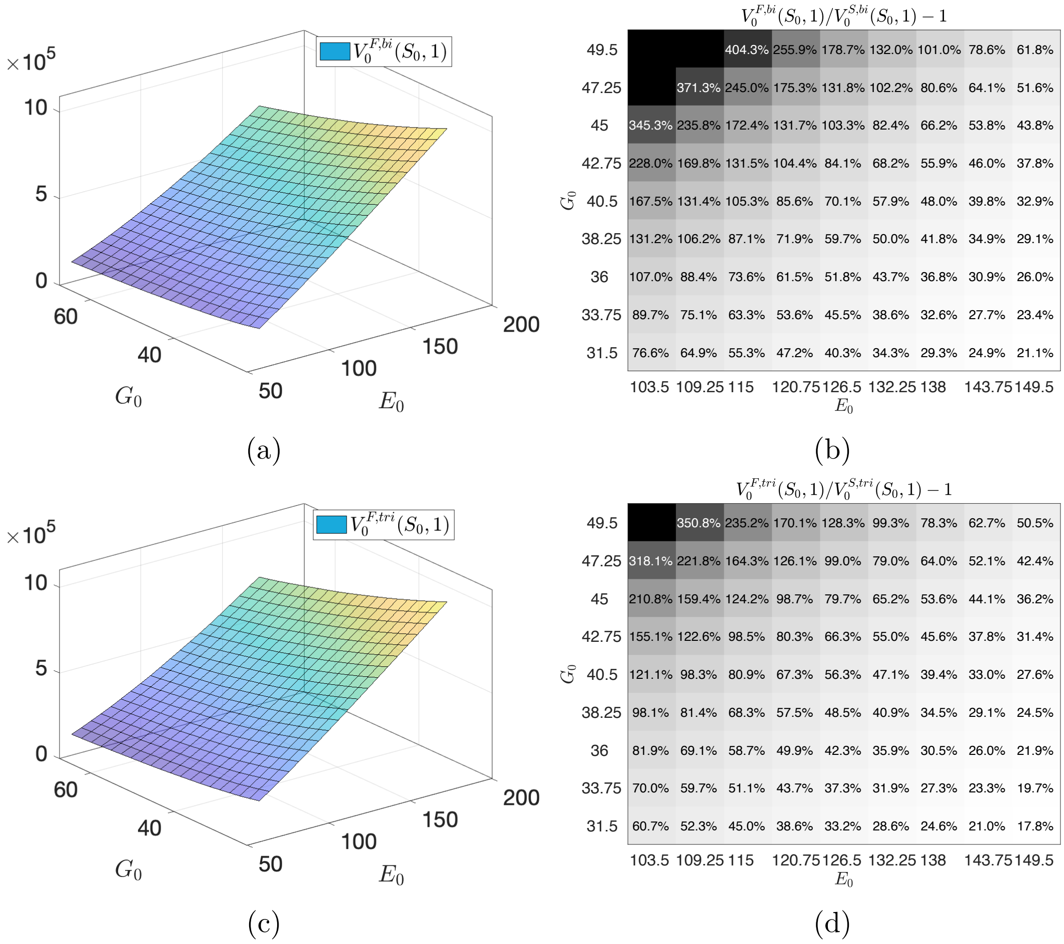

Fig. 3.5 The left-hand-side panels (a, c) show the value of the flexible turbine as a function of the initial prices for gas (G_0) and electricity (E_0). Right panels provide a numerical map of the value of flexibility as a percentage increase of the value of the flexible turbine over that of the static one. Upper panels refer to the bivariate model, whilst bottom panels derive from the trivariate one. The value of the static turbine in a and c mimics that of the flexible one, hence it has been omitted for readability. For the same reason, percentage values larger than 500% have not been reported in b and d should be thought as belonging to the black region.

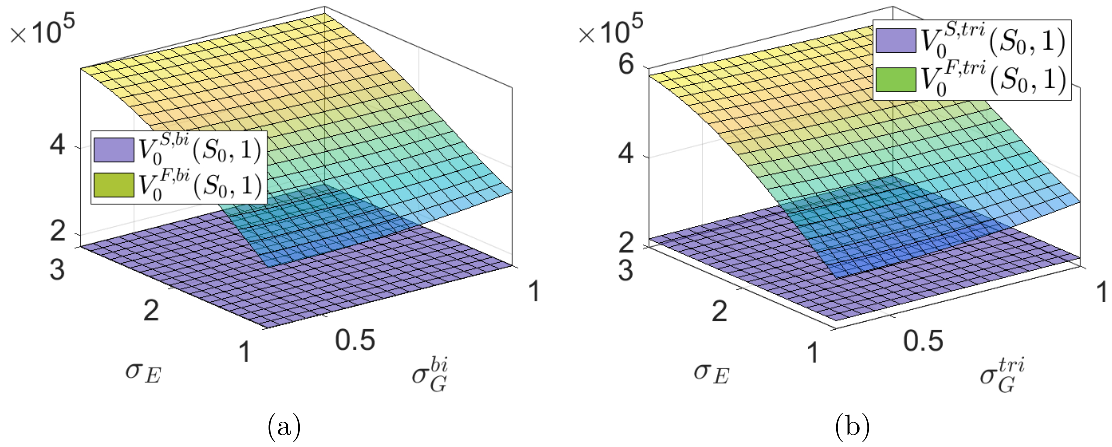

Fig. 3.6 The Figure shows the value of each turbine in the bivariate (a) and trivariate (b) model as a function of the volatility parameters of the electricity and gas prices.

qualitatively similar in the bivariate and in the trivariate models, also in this case the flexible turbine is systematically undervalued if the uncertainty in the convenience yield is neglected; the error is larger for highly volatile electricity prices, whilst it reduces for jointly low volatility parameters of electricity and gas, potentially resulting negligible for highly volatile gas prices combined with less uncertain electricity prices.

These findings highlight the importance of letting both the leading prices to be uncertain[15]: if we assumed the value of the turbine to depend only on gas prices, then we would observe only a limited variation in the value of the flexible turbine conditional on a fixed $\sigma_E = 2$; instead, the maximum variation we observe on the whole surface, accounting for the uncertainty of both gas and electricity prices, is remarkably significant.

3.4.6 The role of correlation

In the EU, the price of electricity is determined by that of the last source used to produce energy, which typically means gas (so called *merit order* principle). Hence,

[15]For example, Tsekrekos et al. (2012), which is the work closer to ours, let profits depend on the price of a single commodity and on its stochastic convenience yield only.

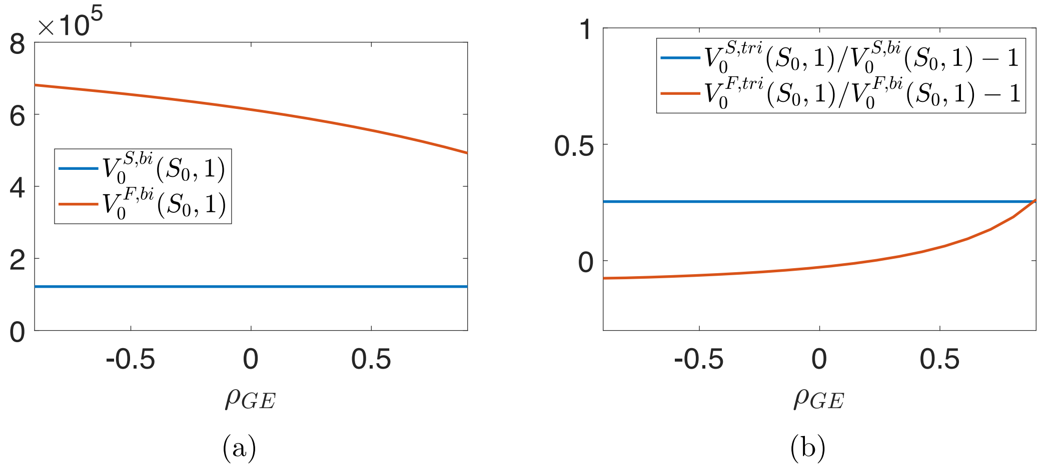

Fig. 3.7 Panel a shows the values of the turbines as functions of the correlation between the gas and electricity price processes. The impact of including a stochastic convenience yield is measured and plotted in panel b.

beside empirical evidence, there also exists a theoretical foundation to presume that positive correlation exists among the two price processes. We capture such correlation through the parameter ρ_{GE}; for the sake of completeness, we let it variate over the range $(-0.9, 0.9)$ even though the far right side of this interval is the most representative. Figure 3.7 shows that, in the bivariate model, the value of the flexible turbine monotonically decreases as the correlation gets higher. This fact could be explained by the need of switching the turbine multiple times, thus reducing cash inflows in favour of negative or null ones (3.7a). Further, we observe that, when we introduce randomness on the convenience yield, the value of the flexible turbine is increasing in the correlation between the G and E(3.7b).

Within the trivariate setting we observe the same decreasing behaviour of the flexible turbine value as ρ_{GE} enlarges, whereas the static one remains constant, as shown in Figure 3.8.

Similarly, the correlations between the main price processes and the convenience yield imply significant changes in the value of the turbine (3.8e), with $\rho_{G\delta}$ seeming to be the most important driver, compared to $\rho_{E\delta}$ (3.8c, 3.8d, 3.8e, 3.8f). Great attention

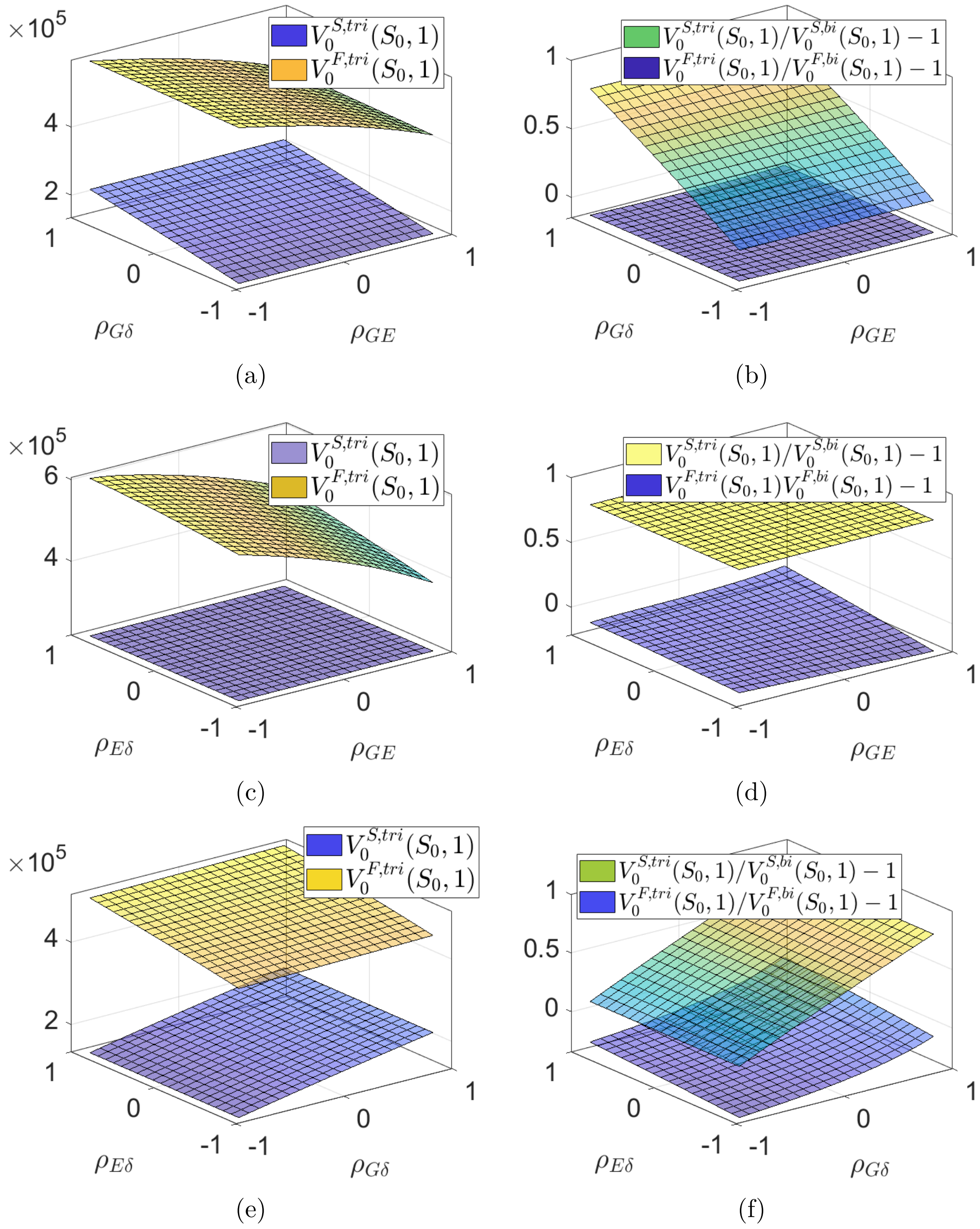

Fig. 3.8 The left-hand-side panels show the values of turbines as functions of pairs of cross-correlations between the price processes and the convenience yield. In the right panels the impact of including a stochastic convenience yield is plotted.

should be paid to the magnitude of the mis-valuation committed when considering a constant convenience yield: the value of the static turbine is mis-priced by 30% on average, with peaks up to 60% in the worst case scenarios (3.8b, 3.8f).

Finally, it is interesting to highlight that the striking relevance of the correlations is peculiar to this real option framework. If "standard" financial options - like European/American call/put options - are considered instead, the impact of the correlation between the underlying's spot price and the stochastic interest rate that drives the underlying's drift is of second order (for example, see Battauz and Rotondi, 2022).

3.4.7 The optimal switching policy

The lattices exploited for the evaluations of the turbines allow us to keep track of the strategic switching decisions made at each node and, consequently, to get the optimal "switching boundary" of the (flexible) turbine. This boundary separates the region in which it is optimal to let the turbine operate from the one in which it is optimal to suspend production. Within the bivariate (resp. trivariate) model, this boundary can be defined as the set of points (t, G, E) (resp. (t, G, δ, E)) for which the manager is indifferent between keeping the turbine in a given status or switching it to the other one.

This output is of primary relevance for the manager of the (flexible) turbine: indeed, given the current t-value of the state variables (E_t, G_t and δ_t, if considering the trivariate model), the manager can look for the corresponding point in the (t, G, E) (or (t, G, δ, E)) space and retrieve right away the optimal action she should take.

Assuming that the turbine is operating at t, the indifference condition reads

$$\Delta_t (S_t - c_{11}) = -\Delta_t c_{00} - c_{10}$$

which is equivalent to

$$G_t = \frac{E_t}{2} - \gamma_{10}$$

where γ_{10} is a constant that depends on c_{11}, c_{00} and c_{10} (considering the benchmark parameters in Table 3.3 we have $\gamma_{10} = 2.2758$). Assuming on the contrary that the turbine is suspended at t, the indifference condition reads

$$-\Delta_t c_{00} = \Delta_t (S_t - c_{11}) - c_{01}$$

which is equivalent to

$$G_t = \frac{E_t}{2} - \gamma_{01}$$

where γ_{01} depends on c_{11}, c_{00} and c_{01} ($\gamma_{01} = 2.7242$ in the benchmark scenario).

As a consequence, the optimal switching boundaries can be represented as planes in the (t, G, E) (or (t, G, δ, E)) space as we verify empirically in Figure 3.9 for the boundaries from the operating status (A) to the suspended one (S)[16].

In the case of the trivariate model, 3.9b has been obtained conditioning on the lattice's nodes for which $\delta_t = \delta_0$. Conditioning on different values of δ would deliver always the same plane as, indeed, δ_t does not enter the expressions of the planes derived above. Therefore, as far as the optimal switching decisions are concerned, the manager can ignore the current value of the convenience yield, that will impact only the evaluation of the turbine.

3.5 Conclusion

The real options literature traditionally pays attention to the stochastic behaviour of those variables that directly affect the cash-flows of investments, such as the prices of

[16] The boundaries from S to A look similar to the ones in Figure 3.9 and the related plots have been omitted for sake of brevity.

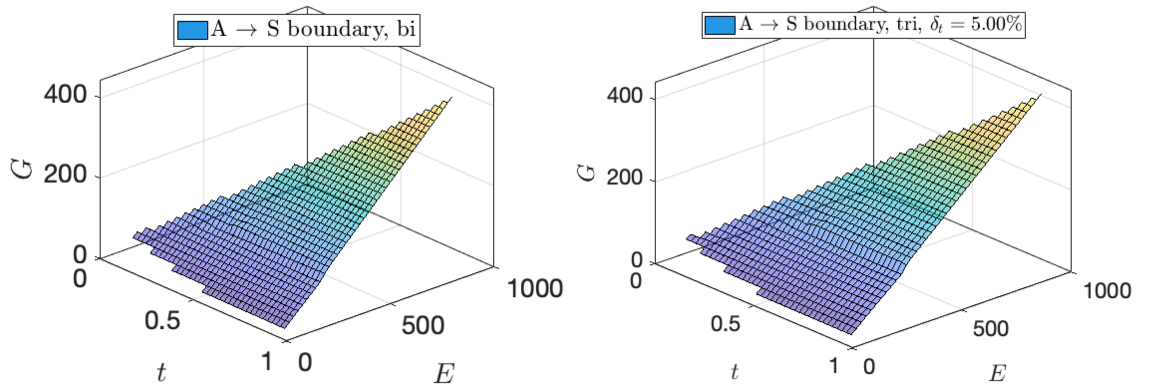

(a) (b)

Fig. 3.9 The Figure shows the optimal switching boundaries for the flexible turbine according to the bivariate (a) and trivariate (b) model conditional on $\delta_t = \delta_0$. This representation of the boundaries cover only the nodes of the bivariate/trivariate lattices and this is the reason of the triangular shape propagating from $(t_0, E_0, G_0) = (0, 115, 45)$.

output goods, of input resources, or of additional sources of profits and costs. However, there are several parameters that can affect the value of a project through a sort of second-order effect. For example, it is well established that stochastic volatility and stochastic interest interest rates are relevant value-drivers for financial derivatives contracts. On the contrary, the research on corporate financial management is still quite scarce on that.

In this paper we consider the valuation problem of a turbine for electricity generation that faces uncertain input costs and output prices and we study the effect of introducing a stochastic convenience yield in the price dynamics of the input commodity (namely, natural gas). We look upon two kinds of facilities, of which one, called static, is committed to continuous production whereas the other has the operational flexibility to be switched-off-and-on multiple times within a one year horizon.

We show that ignoring the existing uncertainty in the convenience yield process leads to systematically mis-price the value of the turbines. However, whilst the error committed in valuing the flexible plant is steadily lower than 2% and can be "safely" ignored, in the static case it raises to an average 36%, even hitting 60% if the leading price processes are strongly correlated. The effect seems to be more pronounced when the equilibrium level and the variance of the convenience yield are higher, but also when the leading price processes of the project are highly volatile. Therefore, we consider it essential that, in the absence of operational flexibility, convenience yield is included as an additional source of risk. On the contrary, operational flexibility makes it possible to mitigate the greater uncertainty that weighs on profits overall, regardless of whether it derives from a primary source, such as the commodity price, or secondary, as a drift parameter. As a result, the added value of operational flexibility is remarkably high in greatly turbulent markets.

Overall, our findings are consistent with the results of Tsekrekos et al. (2012), with respect to whom we improve by adding a further source of uncertainty. By means of this choice, we can perform a wider analysis including market parameters that are of utmost importance in practice, such as multiple mutual correlations. Additionally, we provide a detailed description of the lattice algorithm we implemented. Given the intrinsic simplicity of the intuition behind lattice algorithms, that make them suitable also for being presented to corporate boards, we believe that our contribution can help to enhance the use of accurate real options models by professionals.

Additionally, more complex models can be designed: from the market-side perspective, different or more complex dynamics can describe the relevant sources of uncertainty - for example, Gambaro and Secomandi (2021) warns about the implications of using non-Gaussian processes on operational variables and policies; focusing on plant-specific characteristics, one could account for further strategic options as well as for a different scheme of exercise conditions; overall, some constraints can be added to our optimisation problem to account for exogenous requirements, such as grid, market, or even political restrictions.

References

Abadie, L. (2015). Operating flexibility at power plants: A market valuation. *International Journal of Electrical Power & Energy Systems*, 64:41–49.

Abadie, L. and Chamorro, J. (2008). Valuing flexibility: The case of an integrated gasification combined cycle power plant. *Energy Economics*, 30(4):1850–1881.

Abadie, L. M., Chamorro, J. M., and González-Eguino, M. (2011). Optimal abandonment of EU coal-fired stations. *The Energy Journal*, 32(3):175–207.

Abadie, L. M., Chamorro, J. M., and González-Eguino, M. (2013). Valuing uncertain cash flows from investments that enhance energy efficiency,. *Journal of Environmental Management*, 116:113–124.

Abramowitz, M. and Stegun, I. (1972). *Handbook of Mathematical Functions with Formulas, Graphs and Mathematical Tables*. Dover Publ., Inc., New York.

Amin, K. I. (1993). Jump diffusion option valuation in discrete time. *The Journal of finance (New York)*, 48(5):1833–1863.

Azevedo, A., Pereira, P. J., and Rodrigues, A. (2019). Foreign direct investment with tax holidays and policy uncertainty. *International Journal of Finance & Economics*, 24(2):727–739.

Ballotta, L. and Fusai, G. (2018). Tools from stochastic analysis for mathematical finance: A gentle introduction. Working paper, available at SSRN: http://dx.doi.org/10.2139/ssrn.3183712.

Bastian-Pinto, C., Brandão, L., and Hahn, W. (2009). Flexibility as a source of value in the production of alternative fuels: The ethanol case. *Energy Economics*, 31(3):411–422.

Bastian-Pinto, C. and Brandão, L. E. (2016). The choice of mean reversion stochastic process for real option valuation.

Battauz, A. and Rotondi, F. (2022). American options and stochastic interest rates. *Computational Management Science*, 19:567–604.

Bayraktar, E. and Egami, M. (2010). On the one-dimensional optimal switching problem. *Mathematics of Operations Research*, 35(1):140–159.

Bengtsson, J. (1999). The value of manufacturing flexibility: real options in practice. *Working paper, WP 262, Department of Production economics, Linkoping Institute of Technology.*

Benth, F. E., Piccirilli, M., and Vargiolu, T. (2019). Mean-reverting additive energy forward curves in a Heath–Jarrow–Morton framework. *Mathematics and Financial Economics*, (13):543–577.

Bessembinder, Hendrik, e. a. (1995). Mean reversion in equilibrium asset prices: Evidence from the futures term structure. *Journal of Finance*, 50(1):361–75.

Bhattacharya, S. (1978). Project valuation with mean-reverting cash flow streams. *Journal of Finance*, 33(5):1317–1331.

Björk, T. (2009). *Arbitrage theory in continuous time.* Oxford Finance, 3 edition.

Black, F. (1976). Studies of stock price volatility changes. *Proceedings of the Business and Economics Section of the American Statistical Association*, page 77–181.

Black, F. and Scholes, M. (1973). The pricing of options and corporate liabilities. *Journal of Political Economy*, 81(3):637–654.

Brandão, L., E., Dyer, J., and Hahn, W. (2005). Using binomial decision trees to solve real-option valuation problems. *Decision Analysis*, 2(2):69–88.

Brandão, L. and Dyer, J. (2005). Decision analysis and real options: A discrete time approach to real option valuation. *Annals of Operations Research*, 135(1):21–39.

Brandão, L., Penedo, G., and Bastian-Pinto, C. (2013). The value of switching inputs in a biodiesel production plant. *The European Journal of Finance*, 19(7-8):674–688.

Brennan, M. and Schwartz, E. S. (1985). Evaluating natural resource investments. *The Journal of Business*, 58(2):135–57.

Brennan, M. J. and Schwartz, E. S. (1979). A continuous time approach to the pricing of bonds. *Journal of Banking & Finance*, 3(2):133–155.

Brigo, D. and Mercurio, F. (2007). *Interest rate models-theory and practice: with smile, inflation and credit.* Springer Science & Business Media.

Carmona, R. and Ludkovski, M. (2008). Pricing asset scheduling flexibility using optimal switching. *Applied Mathematical Finance*, 15:405–447.

Casassus, J. and Collin-Dufresne, P. (2005). Stochastic convenience yield implied from commodity futures and interest rates. *The Journal of Finance*, 60(5):2283–2331.

Chan, K. C., Karolyi, G. A., Longstaff, F. A., and Sanders, A. B. (1992). An empirical comparison of alternative models of the short-term interest rate. *The Journal of Finance*, 47(3):1209–1227.

Chen, D., Guo, B., and Zhou, G. (2023). Firm fundamentals and the cross-section of implied volatility shapes. *Journal of Financial Markets*, 63:100771.

Chod, J. and Zhou, J. (2014). Resource flexibility and capital structure. *Management Science*, 60(3):708–729.

Cortazar, G. and Casassus, J. (1998). Optimal timing of a mine expansion: Implementing a real options model. *The Quarterly Review of Economics and Finance*, 38(3(2)):755–769.

Cox, J. (1975). Notes on option pricing i: Constant elasticity of diffusions.

Cox, J., Ingersoll, J., and Ross, S. (1985). A theory of the term structure of interest rates. *Econometrica*, 53:385–407.

Cox, J., Ross, S., and Rubinstein, M. (1979). Option pricing: a simplified approach. *Journal of Financial Economics*, 7(3):229–263.

Dangerfield, C., Whalley, A., and Hanley N., G. C. (2018). What a difference a stochastic process makes: Epidemiological-based real options models of optimal treatment of disease. *Environ Resour Econ*, 70(3):691–711.

Davydov, D. and Linetsky, V. (2001). Pricing and hedging path-dependent options under the cev process. *Management Science*, 47(7):949–965.

Detemple, J. and Kitapbayev, Y. (2020). The value of green energy: Optimal investment in mutually exclusive projects and operating leverage. *The Review of Financial Studies*, 33(7):3307–3347.

Dias, J. C., Larguinho, M., and Braumann, C. A. (2015). Entry and exit decisions under uncertainty for a generalized class of one-dimensional diffusions.

Dias, J. C. and Nunes, J. P. V. (2011). Pricing real options under the constant elasticity of variance diffusion. *Journal of Futures Markets*, 31:230–250.

Dixit, A. (1989). Entry and exit decisions under uncertainty. *Journal of Political Economy*, 97(3):620–38.

Dixit, A. and Pindyck, R. (1994). *Investment under Uncertainty*. Princeton University Press, Princeton.

Dockendorf, J. and Paxson, D. (2013). Continuous rainbow options on commodity outputs: what is the real value of switching facilities? *The European Journal of Finance*, 19(7-8):645–673.

Dong, L., Kouvelis, P., and Wu, X. (2014). The value of operational flexibility in the presence of input and output price uncertainties with oil refining applications. *Management Science*, 60(12):2908–2926.

El Ghoul, S., Fu, Z., Guedhami, O., and Saadi, S. (2023). Firm inflexibility and the implied cost of equity. *Finance research letters*, 52:103539.

Elias, R., Wahab, M., and Fang, L. (2016). The spark spread and clean spark spread option based valuation of a power plant with multiple turbines. *Energy Economics*, 59:314–327.

Ewald, C. and Wang, W. (2010). Irreversible investment with Cox–Ingersoll–Ross type mean reversion. *Mathematical Social Sciences*, 59(3):314 – 318.

Fama, E. and French, K. (2000). Forecasting profitability and earnings. *The Journal of Business*, 73(2):161–175.

Fontes, D. B. (2008). Fixed versus flexible production systems: A real options analysis. *European Journal of Operational Research*, 188(1):169–184.

Gamba, A. and Saretto, A. (2022). Endogenous option pricing. *SSRN Electronic Journal*.

Gambaro, A. M., Kyriakou, I., and Fusai, G. (2020). General lattice methods for arithmetic asian options. *European journal of operational research*, 282(3):1185–1199.

Gambaro, A. M. and Secomandi, N. (2021). A discussion of non-gaussian price processes for energy and commodity operations. *Production and operations management*, 30(1):47–67.

Geman, H. (2005). *Commodities and commodity derivatives: modelling and pricing for agriculturals, metals, and energy*. John Wiley & Sons.

Geman, H. (2008). *Risk management in commodity markets: from shipping to agriculturals and energy*, volume 445. Wiley, Hoboken, NJ;Chichester, West Sussex, England;.

Geman, H. and Shih, Y. F. (2008). Modeling commodity prices under the cev model. *The Journal of Alternative Investments*, 11(3):65–84.

Geske, R., Subrahmanyam, A., and Zhou, Y. (2016). Capital structure effects on the prices of equity call options. *Journal of Financial Economics*, 121(2):231–253.

Gibson, R. and Schwartz, E. S. (1990). Stochastic convenience yield and the pricing of oil contingent claims. *The Journal of Finance*, 45(3):959–976.

Glensk, B. and Madlener, R. (2019). The value of enhanced flexibility of gas-fired power plants: A real options analysis. *Applied Energy*, 251.

Glover, K. and Hambusch, G. (2016). Leveraged investments and agency conflicts when cash flows are mean reverting. *Journal of Economic Dynamics and Control*, 67(C):1–21.

Goldstein, R., Ju, N., and Leland, H. (2001). An EBIT-based model of dynamic capital structure. *The Journal of Business*, 74(4):483–512.

Gonzalez-Salazar, M., Kirsten, T., and Prchlik, L. (2018). Review of the operational flexibility and emissions of gas- and coal-fired power plants in a future with growing renewables. *Renewable and Sustainable Energy Reviews*, 82(Part 1):1497–1513.

Gu, L., Hackbarth, D., and Johnson, T. (2018). Inflexibility and stock returns. *The Review of Financial Studies*, 31(1):278–321.

Guthrie, G. (2009). *Real Options in Theory and Practice*. Oxford University Press.

Gutiérrez, O. (2021). Real options and the perverse effect of interest rates on investment timing. *International Journal of Finance & Economics*, 26(3):3984–3996.

Hackbarth, D. and Johnson, T. (2015). Real options and risk dynamics. *The Review of Economic Studies*, 82(4):1449–1482.

Hackbarth, D. and Mauer, D. (2012). Optimal priority structure, capital structure, and investment. *The Review of Financial Studies*, 25(3):747–796.

Hahn, W. and Dyer, J. (2008). Discrete time modeling of mean-reverting stochastic processes for real option valuation. *European Journal of Operational Research*, 184(2):534–548.

Hahn, W. and Dyer, J. (2011). A discrete time approach for modeling two-factor mean-reverting stochastic processes. *Decision analysis*, 8(3):220–232.

Hull, J. (2018). *Options, futures and other derivatives*. Pearson, ninth edition.

Iancu, D. A., Trichakis, N., and Tsoukalas, G. (2017). Is operating flexibility harmful under debt? *Management Science*, 63(6):1730–1761.

Kaldor, N. (1939). Speculation and economic stability. *The Review of economic studies*, 7(1):1–27.

Kulatilaka, N. (1988). Valuing the flexibility of flexible manufacturing systems. *IEEE Transactions on Engineering Management*, 35(4):250–257.

Kwiatkowski, D., Phillips, P. C., Schmidt, P., and Shin, Y. (1992). Testing the null hypothesis of stationarity against the alternative of a unit root: How sure are we that economic time series have a unit root? *Journal of Econometrics*, 54(1):159–178.

Lambrecht, B. M. (2017). Real options in finance. *Journal of Banking & Finance*, 81(C):166–171.

Latini, L., Piccirilli, M., and Vargiolu, T. (2019). Mean-reverting no-arbitrage additive models for forward curves in energy markets. *Energy Economics*, (79):157–170.

Lebedev, N. N., Silverman, R. A., and Livhtenberg, D. B. (1972). *Special Functions & their Applications*. Dover Publications, Inc.

Leland, H. E. (1994). Corporate debt value, bond covenants, and optimal capital structure. *The Journal of Finance*, 49(4):1213–1252.

Li, N., Ker, A., Sam, A. G., and Aradhyula, S. (2017). Modeling regime-dependent agricultural commodity price volatilities. *Agricultural economics*, 48(6):683–691.

Li, Z., Li, Q., and Zeng, Y. (2020). Contraction flexibility, operating leverage, and financial leverage. *Journal of Management Science and Engineering*, 5(1):43–56.

Lin, T. T. (2009). The determinant of production entry and exit model on financing behavior. *European Journal of Operational Research*, 196(1):258–265.

Liu, L., Zhang, M., and Zhao, Z. (2019). The application of real option to renewable energy investment: a review. *Energy Procedia*, 158:3494–3499.

Lucia, J. J. and Schwartz, E. S. (2002). Electricity prices and power derivatives: Evidence from the nordic power exchange. *Review of derivatives research*, 5(1):5.

Lund, D. (1993). The Lognormal Diffusion Is Hardly an Equilibrium Price Process for Exhaustible Resources. *Journal of Environmental Economics and Management*, 25(3):235–241.

Mackay, P. (1999). Real flexibility and financial structure: An empirical analysis. *HKUST Business School Research Paper Series*.

Martínez, B. and Torró, H. (2023). Theory of storage implications in the european natural gas market. *Journal of Commodity Markets*, (29):100310.

Mauer, D. C. and Ott, S. H. (1995). Investment under uncertainty: The case of replacement investment decisions. *Journal of financial and quantitative analysis*, 30(4):581–605.

Mauer, D. C. and Sarkar, S. (2005). Real options, agency conflicts, and optimal capital structure. *Journal of Banking and Finance*, 29(6):1405–1428.

McDonald, R. and Siegel, D. (1986). The value of waiting to invest. *The Quarterly Journal of Economics*, 101(4):707–727.

McKean Jr., H. (1965). A free boundary problem for the heat equation arising form the problem in mathematical economics. *Industrial Management Review*, 6:32–39.

Merton, R. (1973). An intertemporal capital asset pricing model. *Econometrica*, 41(5):867–887.

Metcalf, G. and Hassett, K. (1995). Investment under alternative return assumptions comparing random walks and mean reversion. *Journal of Economic Dynamics and Control*, 19(8):1471–1488.

Mossin, J. (1968). An optimal policy for lay-up decisions. *The Swedish Journal of Economics*, 70(3):170–177.

Nelson, D. and Ramaswamy, K. (1990). Simple binomial processes as diffusion approximations in financial models. *The Review of Financial Studies*, 3(3):393–430.

Nomikos, N. and Andriosopoulos, K. (2012). Modelling energy spot prices: Empirical evidence from nymex. *Energy Economics*, 34(4):1153–1169.

Pindyck, R. S. (1990). Irreversibility, uncertainty, and investment. Number 3307 in Working Paper Series.

Pindyck, R. S. (1993). The present value model of rational commodity pricing. *The Economic journal (London)*, 103(418):511–530.

Prigent, J. (2003). *Weak convergence of financial markets*. Springer.

Reinartz, S. J. and Schmid, T. (2016). Production flexibility, product markets, and capital structure decisions. *The Review of Financial Studies*, 29(6):1501–1548.

Ritchken, P. and Wu, Q. (2020). Capacity investment, production flexibility, and capital structure. *Production and Operations Management.*

Roncoroni, A., Fusai, G., and Cummins, M. (2015). *Handbook of multi-commodity markets and products: structuring, trading and risk management.* Wiley, Chichester, England.

Rotondi, F. (2024). Seasonality and spikes in the european natural gas market. Working paper, available at SSRN: https://ssrn.com/abstract=4857299.

Said, S. E. and Dickey, D. A. (1984). Testing for unit roots in autoregressive-moving average models of unknown order. *Biometrika*, 71(3):599–607.

Samuelson, P. A. (1965). Rational theory of warrant pricing. *Industrial Management Review*, 6(2):13–39.

Sarkar, S. (2003). The effect of mean reversion on investment under uncertainty. *Journal of Economic Dynamics and Control*, 28(2):377–396.

Sarkar, S. (2014). Product–market flexibility and capital structure. *The Quarterly Review of Economics and Finance*, 54(1):111–122.

Sarkar, S. and Zapatero, F. (2003). The trade-off model with mean reverting earnings: Theory and empirical tests. *Economic Journal*, 113(490):834–860.

Schwartz, E. (1997a). The stochastic behavior of commodity prices: Implications for valuation and hedging. *Journal of Finance*, 52(3):923–973.

Schwartz, E. (1997b). The stochastic behavior of commodity prices: Implications for valuation and hedging. *Journal of Finance*, 52(3):923–973.

Schwartz, E. and Smith, J. E. (2000). Short-term variations and long-term dynamics in commodity prices. *Management Science*, 46(7):893–911.

Sharpe, W. F. (1964). Capital Asset Prices: A Theory Of Market Equilibrium Under Conditions Of Risk. *Journal of Finance*, 19(3):425–442.

Sødal, S. (1998). A simplified exposition of smooth pasting. *Economics Letters*, 58(2):217–223.

Stroock, D. and Varadhan, S. (1997). *Multidimensional diffusion processes.* Springer.

Toft, K. B. and Prucyk, B. (1997). Options on leveraged equity: Theory and empirical tests. *The Journal of Finance*, 52(3):1151–1180.

Triantis, A. J. (2000). Real options and corporate risk management. *Journal of Applied Corporate Finance*, 13:64–73.

Triantis, A. J. and Hodder, J. E. (1990). Valuing flexibility as a complex option. *The Journal of finance*, 45(2):549–565.

Trigeorgis, L. (1996). *Real Options: Managerial Flexibility and Strategy in Resource Allocation.* MIT Press, Cambridge, MA.

Tsekrekos, A. (2010). The effect of mean reversion on entry and exit decisions under uncertainty. *Journal of Economic Dynamics and Control*, 34(4):725–742.

Tsekrekos, A. (2013). Irreversible exit decisions under mean-reverting uncertainty. *Journal of Economics*, 110(1):5–23.

Tsekrekos, A., Shackleton, M. B., and Wojakowski, R. (2012). Evaluating natural resource investments under different model dynamics: Managerial insights. *European financial management*, 18(4):543–575.

Tsekrekos, A. E. and Yannacopoulos, A. N. (2016). Optimal switching decisions under stochastic volatility with fast mean reversion. *European Journal of Operational Research*, 251(1):148–157.

Tubikanec, I., Tamborrino, M., Lansky, P., and Buckwar, E. (2022). Qualitative properties of different numerical methods for the inhomogeneous geometric brownian motion. *Journal of Computational and Applied Mathematics*, 406.

Tvedt, J. (2022). Optimal entry and exit decisions under uncertainty and the impact of mean reversion. *Operations Research Forum*, 3:null.

Uhlenbeck, G. E. and Ornstein, L. S. (1930). On the theory of the brownian motion. *Phys. Rev.*, 36:823–841.

Volmer, T. (2011). A robust model of the convenience yiled in the natural gas market. *The Journal of Futures Markets*, 31(11):1011–1051.

Yash P. Gupta, S. G. (1989). Flexibility of manufacturing systems: Concepts and measurements. *European Journal of Operational Research*, 43(2):119–135.

Zhao, B. (2009). Inhomogeneous geometric brownian motions.

Čermák, M. (2017). Leverage effect and stochastic volatility in the agricultural commodity market under the cev model. *Acta Universitatis Agriculturae et Silviculturae Mendelianae Brunensis*, 65(5):1671–1678.

Appendix A

A.1 Proof of Proposition 1.3.1

We adopt a widely used approach which consists into reducing our equations of interest into a form for which the solution is known (see, for example, Tsekrekos, 2010). In particular, we refer to the general confluent differential equation, whose solution is given in the form of hypergeometric functions of the first and second kind.

Let f, h, V be twice differentiable functions of x. Consider the general confluent differential equation

$$\begin{aligned} &V'' + \left[\frac{2A}{x} + 2f' + \frac{\gamma h'}{h} - h' - \frac{h''}{h'}\right] V' + \\ &+ \left[\left(\frac{\gamma h'}{h} - h' - \frac{h''}{h'}\right)\left(\frac{A}{x} + f'\right) + \frac{A(A-1)}{x^2} + \frac{2\alpha f'}{x} + f'' + \left[f'\right]^2 - \frac{a\left[h'\right]^2}{h}\right] V \\ &= 0 \end{aligned} \tag{A.1}$$

whose solution is known to be (see Abramowitz and Stegun (1972), eqns. 13.1.36 and 13.1.37)

$$c_1 e^{-f} \Phi(\alpha, \gamma; h)\, x^{-A} + c_2 e^{-f} \Psi(\alpha, \gamma; h)\, x^{-A} \tag{A.2}$$

where

$$\Phi(\alpha,\gamma;h) := \sum_{k=0}^{\infty} \frac{(\alpha)_k x^k}{(\gamma)_k k!}, \quad |h| < \infty, \alpha \in \mathbb{C}, \gamma \in \mathbb{C} \setminus \mathbb{Z}^-$$

is a confluent hypergeometric function of the first kind and

$$\Psi(\alpha,\gamma;h) = \frac{\Gamma(1-\gamma)}{\Gamma(1+\alpha-\gamma)} \Phi(\alpha,\gamma;h) + \frac{\Gamma(\gamma-1)}{\Gamma(\alpha)} [h]^{1-\gamma} \Phi(1+\alpha-\gamma, 2-\gamma; h) \tag{A.3}$$

is a confluent hypergeometric function of the second kind.

Replace (A.3) in (A.2) to get

$$pe^{-f} \Phi(\alpha,\gamma;h) x^{-A} + qe^{-f} \Phi(1+\alpha-\gamma, 2-\gamma; h) x^{1-\gamma-A} \tag{A.4}$$

with $p = c_1 + c_2 \dfrac{\Gamma(1-\gamma)}{\Gamma(1+\alpha-\gamma)}$ and $q = c_2 \dfrac{\Gamma(\gamma-1)}{\Gamma(\alpha)}$.

IGBM, CIR and CEV with $\mu \neq 0$ and $\beta > 0$

The homogeneous part of the ordinary differential equations obtained from the IGBM, CIR and CEV (assuming $\mu \neq 0$) processes is

$$\frac{\sigma^2}{2} x^2 V'' + \kappa(\theta - x) V' - rV = 0 \qquad \text{for IGBM} \tag{A.5}$$

$$\frac{\sigma^2}{2} x V'' + \kappa(\theta - x) V' - rV = 0 \qquad \text{for CIR} \tag{A.6}$$

$$\frac{\sigma^2}{2} x^{2\beta+2} V'' + \mu x V' - rV = 0 \qquad \text{for CEV} \tag{A.7}$$

and it can be rewritten as

$$xV'' + \left[\frac{2\kappa\theta}{\sigma^2 x} - \frac{2\kappa}{\sigma^2}\right]V' - \frac{2r}{\sigma^2 x}V = 0 \qquad \text{for IGBM} \qquad (A.8)$$

$$xV'' + \left[\frac{2\kappa\theta}{\sigma^2} - \frac{2\kappa x}{\sigma^2}\right]V' - \frac{2r}{\sigma^2}V = 0 \qquad \text{for CIR} \qquad (A.9)$$

$$\frac{x}{|\beta|}V'' + \frac{2\mu\sigma}{\sigma^2|\beta|x^{2\beta}}V' - \frac{2r}{\sigma^2|\beta|x^{2\beta+1}}V = 0 \qquad \text{for CEV} \qquad (A.10)$$

Then, equations from (A.8) to (A.10) are in the form of a general confluent differential equation for some specific function h. In particular,

$$h = \begin{cases} \dfrac{2\kappa\theta}{\sigma^2 x} & \text{for IGBM} \\ \dfrac{2\kappa x}{\sigma^2} & \text{for CIR} \\ \dfrac{\mu}{|\beta|\sigma^2 x^{2\beta}} & \text{for CEV.} \end{cases}$$

In the following, we assume that $\beta > 0$; we will treat the case $\beta < 0$ separately. Set $f(x) = 0, \xi = -A$ and replace in (A.1) the proper $h(x)$ for each process to get,

for IGBM

$$V'' + \left[2 - \gamma - 2\xi + \frac{2\kappa\theta}{\sigma^2 x}\right]V' + \left[\frac{\gamma\xi - 2\xi + \xi(1+\xi)}{x} - \frac{2\kappa\theta(\alpha+\xi)}{\sigma^2 x^2}\right]V = 0; \qquad (A.11)$$

for CIR

$$V'' + \left[\gamma - 2\xi - \frac{2\kappa x}{\sigma^2}\right]V' + \left[-\frac{2(\alpha-\xi)\kappa}{\sigma^2} - \xi\frac{(\gamma-1-\xi)}{x}\right]V = 0; \qquad (A.12)$$

and for CEV

$$\frac{x}{\beta}V'' + \left[2(1-\gamma) + \frac{1-2\xi}{\beta} + \frac{\mu}{\beta\sigma^2 x^{2\beta}}\right]V' + \left[\frac{-2\xi(1-\gamma)}{x} + \frac{\xi^2}{\beta x} - 4\frac{\mu}{\beta\sigma^2 x^{2\beta+1}}\right]V = 0. \qquad (A.13)$$

For equations (A.8)-(A.10) to be equal to (A.11)-(A.13), the coefficients of V'',V' and V must be the same. Hence, a system of three equations for each process under consideration arises; we get, for IGBM

$$\begin{cases} 2-\gamma-2\xi=-\dfrac{2\kappa}{\sigma^2} \\ \gamma\xi-2\xi+\xi(1+\xi)=-\dfrac{2r}{\sigma^2} \\ -\dfrac{2\kappa\theta(\alpha+\xi)}{\sigma^2 x^2}=0, \end{cases}$$

that returns

$$\begin{aligned} \xi_{1,2} &= \frac{\sigma^2+2\kappa\pm\sqrt{(\sigma^2+2\kappa)^2+8r\sigma^2}}{2\sigma^2}; \\ \gamma_{1,2} &= 2-2\xi_{1,2}+\frac{2\kappa}{\sigma^2}; \\ \alpha_{1,2} &= -\xi_{1,2}; \end{aligned} \tag{A.14}$$

for CIR

$$\begin{cases} \gamma-2\xi=\dfrac{2\kappa\theta}{\sigma^2} \\ -\dfrac{2\alpha\kappa}{\sigma^2}+\dfrac{2\xi\kappa}{\sigma^2}=-\dfrac{2r}{\sigma^2} \\ -\gamma\xi+\xi^2+\xi=0, \end{cases}$$

that returns

$$\begin{aligned} \xi_1 &= 0; & \xi_2 &= 1-\frac{2\kappa\theta}{\sigma^2}; \\ \gamma_1 &= \frac{2\kappa\theta}{\sigma^2}; & \gamma_2 &= 2-\frac{2\kappa\theta}{\sigma^2}; \\ \alpha_1 &= \frac{r}{\kappa}; & \alpha_2 &= \frac{-2\kappa^2\theta+\sigma^2(\kappa+r)}{\sigma^2\kappa}; \end{aligned} \tag{A.15}$$

and, last, for CEV

$$\begin{cases} -\dfrac{2\xi}{\beta} - 2\gamma + \dfrac{1}{\beta} + 2 = 0 \\ \dfrac{\xi^2}{\beta x} + \dfrac{2\xi\gamma}{x} - \dfrac{2\xi}{x} = 0 \\ -\dfrac{4\alpha\mu x^{-2\beta-1}}{\sigma^2} - \dfrac{2\xi\mu x^{-2\beta-1}}{\beta\sigma^2} + \dfrac{2rx^{-2\beta-1}}{\beta\sigma^2} = 0, \end{cases} \tag{A.16}$$

which yields

$$\begin{aligned} \xi_1 &= 1; & \xi_2 &= 0; \\ \gamma_1 &= -\frac{1-2\beta}{2\beta}; & \gamma_2 &= -\frac{-2\beta-1}{2\beta}; \\ \alpha_1 &= -\frac{\mu - r}{2\beta\mu}; & \alpha_2 &= \frac{r}{2\beta\mu}. \end{aligned} \tag{A.17}$$

Then equations (A.11) to (A.13), have solutions of the form (A.4) for the appropriate set of parameters $\{\xi_1, \gamma_1, \alpha_1\}$; the second set of parameters $\{\xi_2, \gamma_2, \alpha_2\}$ enters in the solution accordingly as

$$\begin{aligned} \alpha_2 &= 1 + \alpha_1 - \gamma_1 \\ \gamma_2 &= 2 - \gamma_1 \\ \xi_2 &= 1 - \gamma_1 - \xi_1. \end{aligned}$$

CEV with $\mu \neq 0$ and $\beta < 0$

We now focus on the CEV process and, specifically, we consider the case with negative β. The proof conceptually follows the same steps from (A.10) to (A.16), but setting $f = h$ in (A.1). Then, the parameters characterising the hypergeometric functions in

(A.4) are

$$\begin{aligned}
\xi_1 &= 1; & \xi_2 &= 0; \\
\gamma_1 &= -\frac{1-2\beta}{2\beta}; & \gamma_2 &= -\frac{-2\beta-1}{2\beta}; \\
\alpha_1 &= -\frac{r-2\beta\mu}{2\beta\mu}; & \alpha_2 &= -\frac{r-2\beta\mu-\mu}{2\beta\mu}.
\end{aligned} \tag{A.18}$$

CEV with $\mu = 0$

So far, we worked under the hypothesis that $\mu \neq 0$. It is particularly simple to solve the case of CEV when $\mu = 0$ following Davydov and Linetsky (2001), who showed how to reduce equation (A.7) to a modified Bessel equation, leading to two linearly independent solutions $x^{1/2}I_\nu(z)$ and $x^{1/2}K_\nu(z)$, with $I_\nu(z), K_\nu(z)$ being modified Bessel functions, $z = \frac{\sqrt{2r}x^{-\beta}}{\sigma|\beta|}$ and $\nu = \frac{1}{2|\beta|}$. We exploit the relationships between modified Bessel and hypergeometric functions (see eqns. 9.13.14 and 9.13.15 in Lebedev et al. (1972)):

$$I_\nu(z) = \frac{(z/2)^\nu}{\Gamma(\nu+1)} e^{-z}\Phi\left(\nu+\frac{1}{2}, 2\nu+1; 2z\right) \quad |argz| < \pi \tag{A.19}$$

$$K_\nu(z) = \sqrt{\pi}(2z)^\nu e^{-z}\Psi\left(\nu+\frac{1}{2}, 2\nu+1; 2z\right) \quad |argz| < \pi \tag{A.20}$$

and the relation between hypergeometric functions of the first and second kind given in (A.3) to claim that the solution to (A.7) under $\mu = 0$ is of the form in (A.4). The proof at this point is purely algebraic and stems from substituting (A.19), (A.20) and (A.3) into the following

$$V(x) = aI_\nu(z)x^{1/2} + bK_\nu(z)x^{1/2}$$

to get

$$V(x) = \left[p\Phi(\alpha_1, \gamma_1; 2z)\, x^{\xi_1} + q\Phi(\alpha_2, \gamma_2; 2z)\, x^{\xi_2}\right]^z e^{-z}$$

where

$$\begin{aligned} \xi_1 &= 1; & \xi_2 &= 0; \\ \gamma_1 &= 2\nu + 1; & \gamma_2 &= 2 - 2\nu; \\ \alpha_1 &= \frac{1}{2} + \nu; & \alpha_2 &= \frac{1}{2} - \mu; \end{aligned} \tag{A.21}$$

with $z = \dfrac{\sqrt{2r}x^{-\beta}}{\sigma|\beta|}, \nu = \dfrac{1}{2|\beta|}$.

GBM

Last, the solution for the GBM process can be obtained from that of IGBM considering that

$$dx = \kappa(\theta - x)dt + \sigma x dW$$

converges to

$$dx = -\kappa x dt + \sigma x dW$$

that is, to a GBM with drift $-\kappa$ as $\theta \to 0$. Similarly, the ordinary differential equation

$$\frac{\sigma^2}{2} x^2 V'' + \mu x V' - rV = 0$$

can be seen as a particular case of (A.5) for $\theta \to 0$ and $\mu = -\kappa$. Consequently, it has solution of the form given by (A.4). Then, since

$$\lim_{\theta \to 0} \frac{2\kappa\theta}{\sigma^2 x} = 0 \qquad \text{and} \qquad \lim_{\chi \to 0} \Phi(\alpha, \gamma; \chi) = 1,$$

the final solution for GBM reduces to

$$
\begin{aligned}
V(x) &= p x^{\xi_1} \lim_{\theta \to 0} \Phi\left(\alpha_1, \gamma_1; \frac{2\kappa\theta}{\sigma^2 x}\right) + q x^{\xi_2} \lim_{\theta \to 0} \Phi\left(\alpha_2, \gamma_2; \frac{2\kappa\theta}{\sigma^2 x}\right) \\
&= p x^{\xi_1} + q x^{\xi_2}
\end{aligned}
$$

with

$$
\xi_{1,2} = \frac{\sigma^2 - 2\mu \pm \sqrt{(\sigma^2 - 2\mu)^2 + 8r\sigma^2}}{2\sigma^2}. \tag{A.22}
$$

□

A.2 Proof of Proposition 1.3.2

The proof follows immediately under the condition $\lim_{x \to +\infty} V_1(x) < \infty$ and accounting for the fact that $\lim_{x \to +\infty} \Phi(a, b; x) = \frac{\Gamma(b)}{\Gamma(a)} e^x x^{a-b}$ and $\lim_{x \to 0} \Phi(\alpha, \gamma; \chi) = 1$.

Moreover, to prove that only the presence of mean-reversion is discriminant in determining the particular solution $\psi(x)$, we observe that cash-flows $F(x)$ in equation (1.3) are a linear function of x. Hence, we look for a particular solution of the form $y(x) = Ax + B$, which implies $y'(x) = A$ and $y''(x) = 0$. Consequently, the form of the diffusion is irrelevant and only the expression of the drift triggers a difference to get $y(x)$. But the drift, in our models, is the same across mean-reverting and non mean-reverting processes, respectively, with at most the degenerate case of GBM. Then, for mean-reverting processes we have

$$
\begin{aligned}
\kappa(\theta - x)A - r(Ax + B) &= -(x - c) \\
\Rightarrow -A(\kappa + r)x + \kappa\theta A - rB &= -x + c
\end{aligned}
$$

from which

$$A = \frac{1}{r+\kappa}$$
$$B = \frac{\kappa\theta}{(\kappa+r)r} - \frac{c}{r}.$$

Hence,

$$\psi^{MR}(x) = \frac{x}{r+\kappa} + \frac{\kappa\theta}{(\kappa+r)r} - \frac{c}{r}$$

is the particular solution to (1.3) - and the expected present value of $(x-c)$ - when the output price follows a mean-reverting process. This expression is equivalent to eq. (15) in Bhattacharya (1978) as the time horizon is infinite.

Similarly, for non mean-reverting processes, one gets

$$\mu x A - r(Ax+B) = -(x-c)$$
$$\Rightarrow A(\mu - r)x - rB = -x + c$$

from which

$$A = \frac{1}{r-\mu}$$
$$B = -\frac{c}{r}.$$

Hence,

$$\psi^{\bar{M}R}(x) = \frac{x}{r-\mu} - \frac{c}{r}$$

is the particular solution to (1.3) - and the expected present value of $(x-c)$ - when the output price does not follow a mean-reverting process. $\square$

A.3 Value-matching conditions: flexible firm

We follow the two-steps procedure given in Dixit and Pindyck (1994) to obtain constant coefficients from value-matching conditions. To simplify the reproducibility of our analysis, we recall it here with the application to the IGBM case; the other processes follow accordingly.

First, work at suspension and resumption boundaries imposing

$$\begin{cases} V_1(x_s) & = V_0(x_s) - s_{10} \\ V_0(x_r) & = V_1(x_r) - s_{01} \end{cases}$$

which yield

$$\begin{cases} p_1 \Phi\left(\alpha_1, \gamma_1; \dfrac{2\kappa\theta}{\sigma^2 x_s}\right) x_s^{\xi_1} + (p_2 - q_2)\Phi\left(\alpha_2, \gamma_2; \dfrac{2\kappa\theta}{\sigma^2 x_s}\right) x_s^{\xi_2} & = \dfrac{f}{r} + \psi^{MR}(x_s) + s_{10} \\ p_1 \Phi\left(\alpha_1, \gamma_1; \dfrac{2\kappa\theta}{\sigma^2 x_r}\right) x_r^{\xi_1} + (p_2 - q_2)\Phi\left(\alpha_2, \gamma_2; \dfrac{2\kappa\theta}{\sigma^2 x_r}\right) x_r^{\xi_2} & = \dfrac{f}{r} + \psi^{MR}(x_r) - s_{01}. \end{cases}$$

It is immediate to notice that the above is a linear system, so it can be written as $\mathbf{A}\mathrm{x} = \mathbf{b}$, where

$$\mathbf{A} = \begin{bmatrix} \Phi\left(\alpha_1, \gamma_1; \dfrac{2\kappa\theta}{\sigma^2 x_s}\right) x_s^{\xi_1} & \Phi\left(\alpha_2, \gamma_2; \dfrac{2\kappa\theta}{\sigma^2 x_s}\right) x_s^{\xi_2} \\ \Phi\left(\alpha_1, \gamma_1; \dfrac{2\kappa\theta}{\sigma^2 x_r}\right) x_r^{\xi_1} & \Phi\left(\alpha_2, \gamma_2; \dfrac{2\kappa\theta}{\sigma^2 x_r}\right) x_r^{\xi_2} \end{bmatrix}$$

$$\mathbf{x} = \begin{bmatrix} p_1 \\ (p_2 - q_2) \end{bmatrix}$$

$$\mathbf{b} = \begin{bmatrix} \dfrac{f}{r} + \psi^{MR}(x_s) + s_{10} \\ \dfrac{f}{r} + \psi^{MR}(x_r) - s_{01} \end{bmatrix}$$

and for which the unique solution is $\mathbf{x} = \mathbf{A}^{-1}\mathbf{b}$, provided that $\mathbf{A}$ is non-singular.

Next, known p_1 and $(p_2 - q_2)$, it is easy to exploit the remaining boundary condition

$$V_0(x_a) = \eta I;$$

in fact, we have

$$p_1 \Phi\left(\alpha_1, \gamma_1; \frac{2\kappa\theta}{\sigma^2 x_a}\right) x_a^{\xi_1} + p_2 \Phi\left(\alpha_2, \gamma_2; \frac{2\kappa\theta}{\sigma^2 x_a}\right) x_a^{\xi_2} - \frac{f}{r} = \eta I$$

that returns

$$q_2 = \frac{\eta I + \frac{f}{r} - p_1 \Phi\left(\alpha_1, \gamma_1; \frac{2\kappa\theta}{\sigma^2 x_a}\right) x_a^{\xi_1} - (p_2 - q_2) \Phi\left(\alpha_2, \gamma_2; \frac{2\kappa\theta}{\sigma^2 x_a}\right) x_a^{\xi_2}}{\Phi\left(\alpha_2, \gamma_2; \frac{2\kappa\theta}{\sigma^2 x_a}\right) x_a^{\xi_2}};$$

$$p_2 = (p_2 - q_2) + q_2.$$

To extend the above procedure to any price diffusion model addressed in this work, it is sufficient to properly change the entries of $\mathbf{A}, \mathbf{x}$ and $\mathbf{b}$.

A.4 Smooth-pasting conditions: flexible firm

Mirroring the procedure in A.3, smooth-pasting conditions are first used to get the suspension and resumption boundaries x_s and x_r simultaneously, and, next, to find the abandonment barrier x_a proceeding iteratively. Again, we detail the procedure for the IGBM process only, recalling that similar considerations apply to the other models too.

Recall that smooth-pasting conditions read

$$\begin{cases} V_1'(x_s) & = V_0'(x_s) \\ V_0'(x_r) & = V_1'(x_r), \end{cases}$$

from which

$$\begin{cases} p_1\phi_1(x_s) + (p_2 - q_2)\phi_2(x_s) - \psi^{MR}(x_s) = 0 \\ p_1\phi_1(x_r) + (p_2 - q_2)\phi_2(x_r) - \psi^{MR}(x_r) = 0 \end{cases} \tag{A.23}$$

where $\phi_j(x), j = \{1,2\}$, is the first-order derivative of $\Phi\left(\alpha_j, \gamma_j, \frac{2\kappa\theta}{\sigma^2 x}\right) x^{\xi_j}$, i. e.

$$\phi_j(x) = \left[\xi_j \Phi\left(\alpha_j, \gamma_j, \frac{2\kappa\theta}{\sigma^2 x}\right) - \frac{2\alpha_j\kappa\theta}{\gamma_j\sigma^2 x}\Phi\left(\alpha_j + 1, \gamma_j + 1, \frac{2\kappa\theta}{\sigma^2 x}\right)\right] x^{\xi_j - 1}.$$

Indeed, the confluent hypergeometric function is differentiable m times[1] (Lebedev et al., 1972); furthermore, the real-valued function $h(x) = \frac{2\kappa\theta}{\sigma^2 x}$ is differentiable infinitely many times within its domain, hence, by the chain-rule:

$$\frac{d}{dx}\Phi\left(\alpha, \gamma; \frac{2\kappa\theta}{\sigma^2 x}\right) = -\frac{\alpha}{\gamma}\Phi\left(\alpha + 1, \gamma + 1; \frac{2\kappa\theta}{\sigma^2 x}\right)\frac{2\kappa\theta}{\sigma^2}x^{-2}.$$

By solving the system in (A.23) one gets the optimal suspension and resumption boundaries x_s and x_r. Next, given x_s and x_r, one proceeds iteratively to find x_a such that $V_0'(x_a) = 0$, i. e.

$$p_1\phi_1(x_a) + p_2\phi_2(x_a) = 0.$$

[1]Provided that it is defined.

Appendix B

B.1 Details on path-dependent equity valuation and option pricing

In the following, we detail the procedure that allows to assess the equity value of firms and to price financial option contracts accounting for the path-dependency due to the potential exercise of real options.

1. For a given set of model parameters, get the real options' optimal boundaries $\bar{x}_a, x_a, x_s, x_r$

2. Simulate M trajectories of the price process x for the time horizon T. Discretise the time interval $[t_0, t_{n+1}], t_0 = 0, t_{n+1} = T$, using n steps of size $\mathrm{d}t = \frac{T}{n}$

3. Assume the firm is active at t_0. Then, for all $t_k, k = 1, 2, \ldots, n+1$, and along each j-th trajectory $j = 1 =, \ldots, M$, determine the state of the firm

    I. The rigid firm is always active. Its instantaneous cash-flows are $x_{t_k}^{(j)} - c$

    II. The semi-rigid firm:

        A. is active and generates instantaneous cash-flows $x_{t_k}^{(j)} - c$ at t_k if it was active at t_{k-1} and $x_{t_k}^{(j)} > \bar{x}_a$

B. irreversibly ceases production if it was active at t_{k-1} and $x_{t_k}^{(j)} \leq \bar{x}_a$; equity-holders gets a unique cash-flow SV

C. is abandoned and has no cash-flows if abandonment occurred at t_{k-1} or before

III. The flexible firm:

A. is active and generates instantaneous cash-flows $x_{t_k}^{(j)} - c$ at t_k if it was active at t_{k-1} and $x_{t_k}^{(j)} > x_s > x_a$

B. is suspended and generates instantaneous outflows $-f$ at t_k if $x_{t_k}^{(j)} > x_a$ and

B1. it was active at t_{k-1} and $x_{t_k}^{(j)} \leq x_s$

B2. it was suspended at t_{k-1} and $x_{t_k}^{(j)} \leq x_r$

C. irreversibly stops production if it was either active or suspended at t_{k-1} and $x_{t_k}^{(j)} \leq x_a$; equity-holders gets a unique cash-flow SV

D. is abandoned and has no cash-flows if abandonment occurred at t_{k-1} or before

4. Set a maturity $T_i \leq T$. For every j-th simulated trajectory, calculate the equity value of each firm according to eqns. (2.2.1), (2.2.1) and (2.2.1) at point $x_{T_i}^{(j)}$; then compute $\hat{E}(x_{T_i}) = \frac{1}{M}\sum_{j=1}^{M} E^{(j)} x_{T_i}$ of the equity value at such horizon

5. Use equity values from the previous point as inputs to determine the payoff of a European call option and get an estimate for its price

6. Last, recover the implied volatility of the option contractfrom the Black-Scholes' formula.

Appendix C

C.1 Details of the lattice discretisations

We collect here a few technical details about the discretisations of the models defined by the systems of stochastic differential equations in (3.19) and (3.8).

C.1.1 Bivariate binomial trees

As pointed out in Hahn and Dyer (2008), the starting point of the lattice discretisation of the bivariate process (G,E) defined by (3.19) is the lattice discretisation of two generic diffusions, effectively described in Section 3.2.1 of Prigent (2003) that build on the limit theorems in Section 11.3 of Stroock and Varadhan (1997).

Let $(X,Y) := \{(X_t,Y_t)\}_{t\in[0,T]}$ be two diffusions defined by

$$\begin{cases} \mathrm{d}X_t = \mu_X \mathrm{d}t + \sigma_X \mathrm{d}W_t^X \\ \mathrm{d}Y_t = \mu_Y \mathrm{d}t + \sigma_Y \mathrm{d}W_t^Y \end{cases} \tag{C.1}$$

with some initial conditions $X_0, Y_0 \in \mathbb{R}$ and where coefficients μ_X and μ_Y might depend on t, X_t and Y_t while σ_X, σ_Y are two positive constants[1] and the instantaneous correlation between the two Brownian motions W^X and W^Y is equal to $\rho \in (-1,1)$.

Consider a uniform partition $\{i\Delta t\}_{i=0,\dots,n}$ of the time interval $[0,T]$, where $n \in \mathbb{N}$ is the number of time steps chosen and $\Delta t := \frac{T}{n}$. Then, the discrete time stochastic process $(\tilde{X}, \tilde{Y}) := \{(\tilde{X}_{t_i}, \tilde{Y}_{t_i}\}_{\{i\Delta t\}_{i=0,\dots,n}}$ with $(\tilde{X}_0, \tilde{Y}_0) = (X_0, Y_0)$ and

$$\left(\tilde{X}_{t_{i+1}}, \tilde{Y}_{t_{i+1}}\right) = \begin{cases} \left(\tilde{X}_{t_i} + \Delta X, \tilde{Y}_{t_i} + \Delta Y\right) & \text{with probability } q_{uu} \\ \left(\tilde{X}_{t_i} + \Delta X, \tilde{Y}_{t_i} - \Delta Y\right) & \text{with probability } q_{ud} \\ \left(\tilde{X}_{t_i} - \Delta X, \tilde{Y}_{t_i} + \Delta Y\right) & \text{with probability } q_{du} \\ \left(\tilde{X}_{t_i} - \Delta X, \tilde{Y}_{t_i} - \Delta Y\right) & \text{with probability } q_{dd} \end{cases}$$

where

$$\begin{aligned} \Delta X = \sigma_X \sqrt{\Delta t}, \quad \Delta Y = \sigma_Y \sqrt{\Delta t} \\ q_{uu} = \frac{\mu_X \mu_Y \Delta t + \mu_X \Delta Y + \mu_Y \Delta X + (1+\rho)\sigma_X \sigma_Y}{4\sigma_X \sigma_Y} \\ q_{ud} = \frac{-\mu_X \mu_Y \Delta t + \mu_X \Delta Y - \mu_Y \Delta X + (1-\rho)\sigma_X \sigma_Y}{4\sigma_X \sigma_Y} \\ q_{du} = \frac{-\mu_X \mu_Y \Delta t - \mu_X \Delta Y + \mu_Y \Delta X + (1-\rho)\sigma_X \sigma_Y}{4\sigma_X \sigma_Y} \\ q_{dd} = \frac{\mu_X \mu_Y \Delta t - \mu_X \Delta Y - \mu_Y \Delta X + (1+\rho)\sigma_X \sigma_Y}{4\sigma_X \sigma_Y}. \end{aligned} \tag{C.2}$$

converges in distribution to (X,Y) as the time step Δt shrinks or, equivalently, as the number of steps n grows to infinity.

Unfortunately, the bivariate process (G,E) defined by (3.19) is not of the form of (X,Y) in (C.1) as the two volatility coefficients, $\sigma_G G_t$ and $\sigma_E E_t$, are not constant but

[1] As argued in Nelson and Ramaswamy (1990), constant volatility parameters are necessary to retain computational feasibility of the resulting lattice. Time-dependent and/or state-contingent volatility parameters would result in a non-recombining tree that would still converge in distribution to the desired continuous-time process but would also feature an exponentially increasing (and thus not feasible) number of nodes.

depend on the level of the variables. To solve this issue we discretise $(\log G, \log E)$ since

$$\begin{cases} \mathrm{d}\left(\log G_t\right) = \left(r - \delta - \frac{\sigma_G^2}{2}\right)\mathrm{d}t + \sigma_G \mathrm{d}W_t^G \\ \mathrm{d}\left(\log E_t\right) = \left(r - \frac{\sigma_E^2}{2}\right)\mathrm{d}t + \sigma_E \mathrm{d}W_t^E \end{cases}$$

is precisely of the form of (X,Y) in (C.1) with $\mu_X = r - \delta - \frac{\sigma_G^2}{2}$, $\sigma_X = \sigma_G$, $\mu_Y = r - \frac{\sigma_E^2}{2}$, $\sigma_Y = \sigma_E$ and $\rho = \rho_{GE}$. Notice that since these μ_X and μ_Y are constant, the four transition probabilities in (C.2) are constant across the lattice. Finally, we build the lattice discretisation of (G,E) taking the exponential[2] of the nodes of the one for $(\log G, \log E)$ while leaving unchanged the transition probabilities.

C.1.2 Trivariate binomial trees

Generalising the scheme outlined in the previous subsection, now the starting point is the lattice discretisation of $(X,Y,Z) := \{(X_t, Y_t, Z_t)\}_{t \in [0,T]}$ defined by

$$\begin{cases} \mathrm{d}X_t = \mu_X \mathrm{d}t + \sigma_X \mathrm{d}W_t^X \\ \mathrm{d}Y_t = \mu_Y \mathrm{d}t + \sigma_Y \mathrm{d}W_t^Y \\ \mathrm{d}Z_t = \mu_Z \mathrm{d}t + \sigma_Z \mathrm{d}W_t^Z \end{cases} \tag{C.3}$$

with some initial conditions $X_0, Y_0, Z_0 \in \mathbb{R}$ and where, as before, drift coefficients $\{\mu_i\}_{i \in \{X,Y,Z\}}$ might depend on t, X_t, Y_t and Z_t while volatility coefficients $\{\sigma_i\}_{i \in \{X,Y,Z\}}$ are positive constants. Finally, the instantaneous correlations between the three Brownian motions are ρ_{XY}, ρ_{YZ} and ρ_{XZ}.

[2]Namely, inverting the functions that map (G,E) into $(\log G, \log E)$.

Given the usual uniform partition of $[0,T]$, the discrete time stochastic process $(\tilde{X},\tilde{Y},\tilde{Z}) := \{(\tilde{X}_{t_i},\tilde{Y}_{t_i},\tilde{Z}_{t_i}\}_{\{i\Delta t\}_{i=0,\dots,n}}$ with $(\tilde{X}_0,\tilde{Y}_0,\tilde{Z}_0) = (X_0,Y_0,Z_0)$ and

$$\left(\tilde{X}_{t_{i+1}},\tilde{Y}_{t_{i+1}},\tilde{Z}_{t_{i+1}}\right) = \begin{cases} \left(\tilde{X}_{t_i}+\Delta X,\tilde{Y}_{t_i}+\Delta Y,\tilde{Z}_{t_i}+\Delta Z\right) & \text{with probability } q_{uuu} \\ \left(\tilde{X}_{t_i}+\Delta X,\tilde{Y}_{t_i}+\Delta Y,\tilde{Z}_{t_i}-\Delta Z\right) & \text{with probability } q_{uud} \\ \left(\tilde{X}_{t_i}+\Delta X,\tilde{Y}_{t_i}-\Delta Y,\tilde{Z}_{t_i}+\Delta Z\right) & \text{with probability } q_{udu} \\ \left(\tilde{X}_{t_i}+\Delta X,\tilde{Y}_{t_i}-\Delta Y,\tilde{Z}_{t_i}-\Delta Z\right) & \text{with probability } q_{udd} \\ \left(\tilde{X}_{t_i}-\Delta X,\tilde{Y}_{t_i}+\Delta Y,\tilde{Z}_{t_i}+\Delta Z\right) & \text{with probability } q_{duu} \\ \left(\tilde{X}_{t_i}-\Delta X,\tilde{Y}_{t_i}+\Delta Y,\tilde{Z}_{t_i}-\Delta Z\right) & \text{with probability } q_{dud} \\ \left(\tilde{X}_{t_i}-\Delta X,\tilde{Y}_{t_i}-\Delta Y,\tilde{Z}_{t_i}+\Delta Z\right) & \text{with probability } q_{ddu} \\ \left(\tilde{X}_{t_i}-\Delta X,\tilde{Y}_{t_i}-\Delta Y,\tilde{Z}_{t_i}-\Delta Z\right) & \text{with probability } q_{ddd} \end{cases}$$

where

$$\Delta X = \sigma_X\sqrt{\Delta t}, \quad \Delta Y = \sigma_Y\sqrt{\Delta t}, \quad \Delta Z = \sigma_Z\sqrt{\Delta t}$$

$$\begin{aligned} q_{uuu} &= \tfrac{1}{8}\left(1+\rho_{XY}+\rho_{XZ}+\rho_{YZ}+\sqrt{\Delta t}\left(\tfrac{\mu_X}{\sigma_X}+\tfrac{\mu_Y}{\sigma_Y}+\tfrac{\mu_Z}{\sigma_Z}\right)\right) \\ q_{uud} &= \tfrac{1}{8}\left(1+\rho_{XY}-\rho_{XZ}-\rho_{YZ}+\sqrt{\Delta t}\left(\tfrac{\mu_X}{\sigma_X}+\tfrac{\mu_Y}{\sigma_Y}-\tfrac{\mu_Z}{\sigma_Z}\right)\right) \\ q_{udu} &= \tfrac{1}{8}\left(1-\rho_{XY}+\rho_{XZ}-\rho_{YZ}+\sqrt{\Delta t}\left(\tfrac{\mu_X}{\sigma_X}-\tfrac{\mu_Y}{\sigma_Y}+\tfrac{\mu_Z}{\sigma_Z}\right)\right) \\ q_{udd} &= \tfrac{1}{8}\left(1-\rho_{XY}-\rho_{XZ}+\rho_{YZ}+\sqrt{\Delta t}\left(\tfrac{\mu_X}{\sigma_X}-\tfrac{\mu_Y}{\sigma_Y}-\tfrac{\mu_Z}{\sigma_Z}\right)\right) \\ q_{duu} &= \tfrac{1}{8}\left(1-\rho_{XY}-\rho_{XZ}+\rho_{YZ}+\sqrt{\Delta t}\left(-\tfrac{\mu_X}{\sigma_X}+\tfrac{\mu_Y}{\sigma_Y}+\tfrac{\mu_Z}{\sigma_Z}\right)\right) \\ q_{dud} &= \tfrac{1}{8}\left(1-\rho_{XY}+\rho_{XZ}-\rho_{YZ}+\sqrt{\Delta t}\left(-\tfrac{\mu_X}{\sigma_X}+\tfrac{\mu_Y}{\sigma_Y}-\tfrac{\mu_Z}{\sigma_Z}\right)\right) \\ q_{ddu} &= \tfrac{1}{8}\left(1+\rho_{XY}-\rho_{XZ}-\rho_{YZ}+\sqrt{\Delta t}\left(-\tfrac{\mu_X}{\sigma_X}-\tfrac{\mu_Y}{\sigma_Y}+\tfrac{\mu_Z}{\sigma_Z}\right)\right) \\ q_{ddd} &= \tfrac{1}{8}\left(1+\rho_{XY}+\rho_{XZ}+\rho_{YZ}+\sqrt{\Delta t}\left(-\tfrac{\mu_X}{\sigma_X}-\tfrac{\mu_Y}{\sigma_Y}-\tfrac{\mu_Z}{\sigma_Z}\right)\right) \end{aligned} \tag{C.4}$$

converges in distribution to (X,Y,Z) as the time step Δt shrinks.

As before, it is necessary to manipulate the trivariate process (X,Y,Z) defined by (3.8) to obtain constant volatility parameters. As the convenience yield δ features already a constant volatility, we discretise $(\log G,\delta,\log E)$ which, as before, is of the form of (C.3) with $\mu_X = r - Y_t - \frac{\sigma_G^2}{2}$, $\mu_Y = \alpha\left(\bar{\delta}-Y_t\right)$, $\mu_Z = r - \frac{\sigma_Z^2}{2}$, $\sigma_X = \sigma_G$, $\sigma_Y = \sigma_\delta$,

$\sigma_Z = \sigma_E$, $\rho_{XY} = \rho_{G\delta}$, $\rho_{YZ} = \rho_{\delta E}$ and $\rho_{XZ} = \rho_{GE}$. Notice that now both μ_X and μ_Y are state contingent as they depend on the current value of Y (namely, of δ). This implies that transition probabilities in (C.4) are not constant anymore but they do change from one node of the lattice to another. Finally, taking the exponential of the first and the third variable, we map this trivariate lattice to the one of our interest for (G, δ, E).

C.2 Validation of the numerical algorithm and further details

We collect here a number of additional numerical tests for the validation of the numerical algorithm described in Subsection 3.3.6 and for the assessment of its performances in terms of accuracy and computational efficiency.

C.2.1 Static turbine

We first consider the static turbine within the bivariate market model introduced in Subsection 3.3.4. As already mentioned, in this case the turbine can be valued explicitly by expression (3.14). Setting a large number of monitoring dates (e.g., $m = 10^5$) we can get a precise estimate for the value of the continuous time problem 3.12. The evaluation of this formula with $m = 10^5$ for the benchmark parameters in Table 3.3 delivers $V(S_0, 1)^{S,bi} = 179'066$ which is only 2.51% larger than the figure in Table 3.4. Indeed, as we can see from Figure C.1, the relative errors of the values obtained by our lattice-based algorithm from the "true" value are almost negligible even after a small number of monitoring dates m.

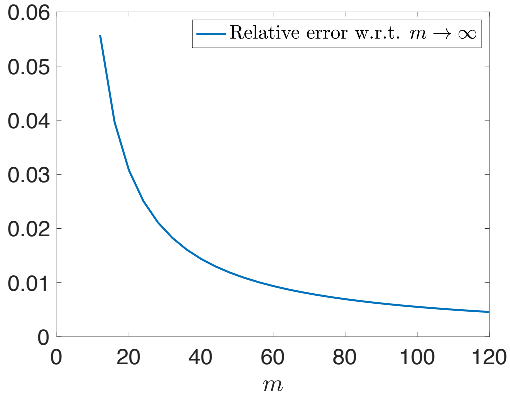

Fig. C.1 Value of the static turbine in the bivariate model computed with the proposed numerical algorithm as a function of the number of monitoring dates m with respect to the "true" value obtained with (3.14).

As mentioned in Remark 3.3.4, although sound from an economic point of view, the approximation of each integral $\int_{t_i}^{t_{i+1}} e^{-rt} X(S_t, I_t) \mathrm{d}t$ by $e^{-rt_i} \Delta t X(S_{t_i}, I_{t_i})$ might look too rough. This choice has the great advantage that when S_{t_i} is $\mathcal{F}_{t_i}$-measurable and, therefore, the computation of the value function at t_i is straightforward. Using a trapezoidal rule for the integral we would get

$$e^{-r\frac{t_{i+1}-t_i}{2}} \frac{\mathbb{E}[X(S_{t_{i+1}}, I_{t_i})|\mathcal{F}_{t_i}] + X(S_{t_i}, I_{t_i})}{2} \Delta t$$

since the decision about the status of the turbine is taken at time t_i and any t_{i+1} variable should be considered in expected value terms. If $I_{t_i} = 0$, the operating cash-flow is $-c_{00}$ and the trapezoidal rule would simply imply a slightly different discount factor ($e^{-r(t_{i+1}-t_i)/2}$ vs. e^{-rt_i}). It $I_{t_i} = 1$, then $X(S_{t_i}, I_{t_i}) = S_{t_i} - c_{11}$. Recalling that $\{S_t e^{-(r-\delta)t}\}_{t \geq 0}$ is a $\mathbb{Q}$-martingale, using the trapezoidal rule instead we would get

$$\begin{aligned}
\frac{\mathbb{E}\left[X(S_{t_{i+1}}, I_{t_i}) \middle| \mathcal{F}_{t_i}\right] + X(S_{t_i}, I_{t_i})}{2} &= \frac{\mathbb{E}\left[S_{t_{i+1}} \middle| \mathcal{F}_{t_i}\right] - c_{11} + S_{t_i} - c_{11}}{2} \\
&= \frac{S_{t_i} e^{(r-\delta)\frac{\Delta t}{2}} + S_{t_i}}{2} - c_{11},
\end{aligned}$$

but since $(r-\delta)\Delta t/2$ is rather small, the numerical difference with respect to $S_{t_i} - c_{11}$ is very limited. As an illustrative example, the benchmark value of the static turbine we would get using this correction reads 174'511, which is only 0.03% smaller than the value in Table 3.4.

As already mentioned, a closed formula for $V(S_0,1)^{S,tri}$ is not available. However, since the switching policy prescribes to let the turbine operate no matter what, the valuation problem can be tackled by standard Monte Carlo techniques. The average of the point estimates of $V(S_0,1)^{S,tri}$ and of their related 95% confidence radius (obtained out of 10 independent Monte Carlo simulations each entailing 10^5 simulated paths) are 216'245 and 902.31 respectively. The relative error of this point estimate with respect to the value in 3.4 is equal to 1.19%, which is remarkably small.

C.2.2 Limit parameters

We now consider the flexible turbine valuation problem changing a few parameters to either make it equivalent to the static one or to make the trivariate model equivalent to the bivariate one.

We first set switching costs c_{10} and c_{01} equal to 10^5 and then we value the flexible turbine within the two market models. As expected, since the switching of the turbine is now indefinitely expensive, the value of the flexible turbine collapses into the static one and we numerically verify $V(S_0,1)^{F,bi} = V(S_0,1)^{S,bi}$ and $V(S_0,1)^{F,tri} = V(S_0,1)^{S,tri}$.

Then, we consider the trivariate model with $\alpha = 0$ and $\sigma_\delta = 10^{-5}$. With this choice of parameters, the stochastic convenience yield becomes deterministic, $\delta_t \equiv \delta_0$. As expected, we numerically verify that in this case $V(S_0,1)^{S,tri} = V(S_0,1)^{S,bi}$ and $V(S_0,1)^{F,tri} = V(S_0,1)^{F,bi}$.

C.2.3 Computational efficiency

Finally, we assess the precision of our algorithm and its computational efficiency.

As already pointed out in Remark 3.3.4, the optimal value of (3.13) converges to the one of (3.12) only as $\Delta t \to 0$ or, equivalently, as $m \to +\infty$. Although we have already motivated why we are focusing on the discrete time problem rather than on the continuous time one, it is interesting to study by how much they differ. Panels (a) and (c) of Figure C.2 shows the value of the flexible turbine within the two models as a function of the number m of time steps. As we can see, the values obtained through our algorithm using different m's are converging relatively fast to the continuous time counterparts. Therefore, our restriction to the discrete time problem is not really influencing the value of the turbine even if a continuous switching is allowed.

As far as computational times are concerned, we acknowledge that lattice-based methods are usually slow and they can be hardly parallelised. However, sticking to a relatively small value of m makes the valuation feasible and does not entail a huge bias.

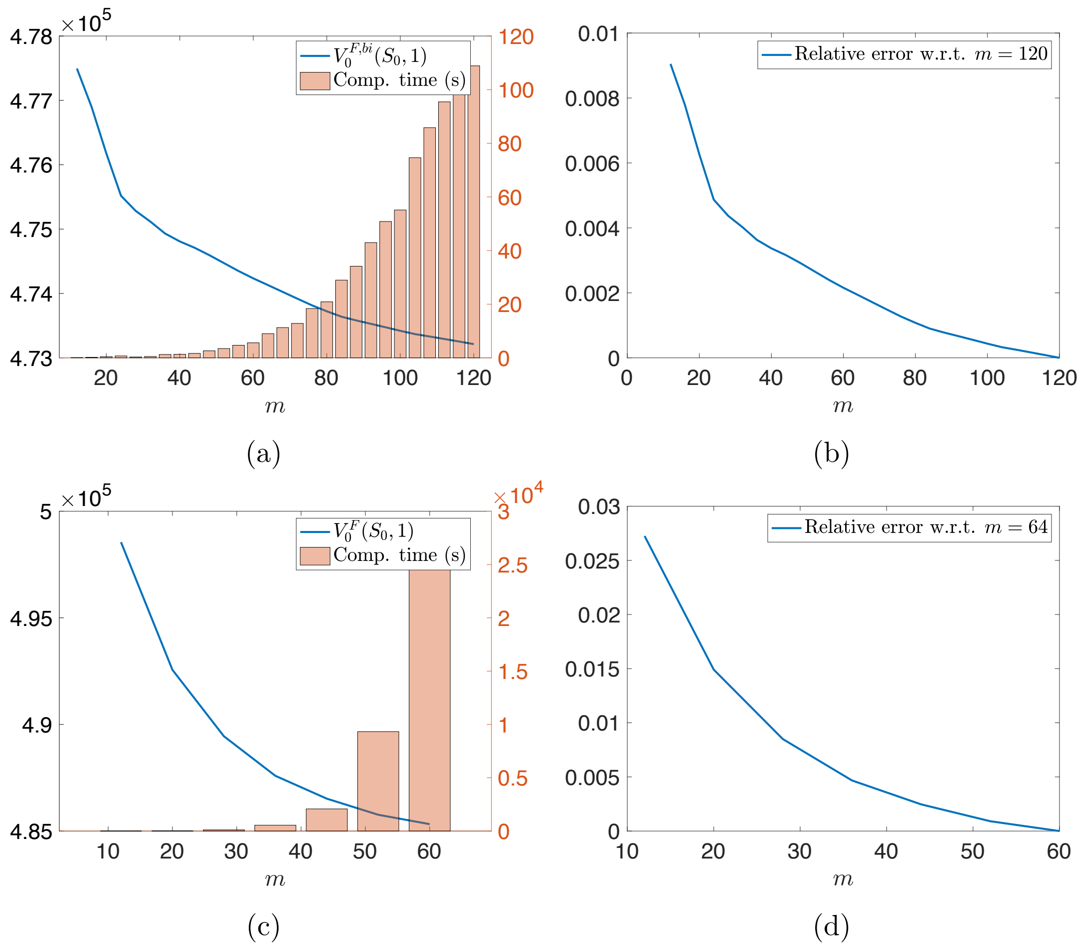

Fig. C.2 The left-hand-side panels (a, c) of the Figure show on the left axis the value of the flexible turbines across the two models as a function of the number m of steps of the uniform partition of $[0,T]$. The computational time (expressed in seconds) of our algorithm for each value of m is plotted against the right axis. The right-hand-side panels (b, d) show the relative error as a function of m of the value of the flexible turbine with respect to the value obtained setting $m = 120$ and $m = 68$.